2009

Sequence and chemostratigraphic study across the basal Eureka Quartzite unconformity in the Great Basin, Nevada: Implications for the origin of the Late Ordovician carbon isotope excursion

Apostolos Paul Kosmidis
University of Nevada Las Vegas

Repository Citation

SEQUENCE AND CHEMOSTRATIGRAPHIC STUDY ACROSS THE BASAL

EUREKA QUARTZITE UNCONFORMITY IN THE GREAT BASIN,

NEVADA: IMPLICATIONS FOR THE ORIGIN OF THE LATE

ORDOVICIAN CARBON ISOTOPE EXCURSION

by

Apostolos Paul Kosmidis
University of Nevada, Las Vegas

Bachelor of Science
Temple University
2005

A thesis submitted in partial fulfillment of
the requirements for the

Master of Science in Geoscience
Department of Geoscience
College of Science

Graduate College
University of Nevada, Las Vegas
August 2009

TABLE OF CONTENTS

ABSTRACT

Sequence and chemostratigraphic study across the basal Eureka Quartzite unconformity in the Great Basin, Nevada: implications for the origin of the Late Ordovician carbon isotope excursion

by

Apostolos Paul Kosmidis

Dr. Ganqing Jiang, Examination Committee Chair
Assistant Professor of Geoscience
University of Nevada, Las Vegas

The positive carbon isotope (δ^{13}C) excursion from the late Middle Ordovician Copenhagen Formation that underlies the Eureka Quartzite in central Nevada has been hypothesized to record a global cooling event ~10 Myr prior to the well-recognized Late Ordovician Hirnantian glaciation (~443 Ma). However, direct evidence for pre-Hirnantian continental glaciation remains scarce, raising uncertainties in the relationship between the inferred eustatic sea-level fall and the origin of the positive δ^{13}C excursion. Additionally, previous stratigraphic studies from southern Nevada and California suggest relative sea-level fall in excess of ~ 150 meters, which exceeds estimates for younger glacial periods (e.g., Hirnantian: ~45-60 m, Late Paleozoic: ~ 60-75 m, and Last Glacial Maximum: ~125 m of sea-level fall) despite the paucity of glaciogenic deposits at this time.

An integrated sequence and chemostratigraphic study across the basal Eureka Quartzite unconformity and underlying carbonate strata (Antelope Valley Limestone) indicates that the Copenhagen Formation in central Nevada was most likely deposited in a fault-controlled sedimentary basin. The absence of a comparable positive δ^{13}C

excursion in sections away from the Monitor and Copenhagen valleys suggests that the

$\delta^{13}C$ excursion reported from the Copenhagen Formation in central Nevada was likely a

localized signal formed through carbon cycling (e.g., high biologic production and

eutrophication) in a restricted, geographically limited formation that was deposited

during the period of exposure and karstification of the paleo-shelf in southern Great

Basin locations.

LIST OF FIGURES

ACKNOWLEDGMENTS

CHAPTER 1

INTRODUCTION

Studies on deep-time climate changes show a strong correspondence between

atmospheric CO_2 concentration and average global seawater temperature. Ordovician to

Neogene paleoclimate records (Royer et al., 2004; Royer, 2006) indicate that the Earth's

climate has varied between global icehouse and greenhouse conditions corresponding

with times of low (< 500 ppm) and high (> 1000 ppm) pCO_2 concentrations. An

intriguing interval in Earth history is the Late Ordovician time (Mohawk Stage; ~454 to

~443 Ma) when widespread glacial conditions existed in mid-latitude Gondwana despite

atmospheric CO_2 levels 10-18 times higher than the present (Berner 1994; Kump et al.,

1999; Berner and Kothavala, 2003). In the stratigraphic record this glaciation is

represented by physical evidence, such as glacially-striated pavements, tillites and glacial

diamictites (Hughes, 1981; Frakes et al., 1992; Crowley and Baum, 1995; Crowell,

1999), which are closely associated with unconformities in carbonate strata believed to

have developed during the ensuing eustatic sea-level fall (Marshall and Middleton, 1990;

Brenchley et al., 1994; Brenchley et al., 1997; Berry et al., 2002). Correlation of these

unconformities globally has placed the initiation of the climatic shift at the terminal

Ordovician Hirnantian Stage, approximately 442 Ma, and suggests a short-duration event

that lasted 0.5 to 2 million years (Brenchley et al., 1997).

In addition to physical sedimentary evidence, proxy data in the form of positive

carbon isotope excursions in sedimentary rocks also supports a strong correlation

between fluctuations of pCO_2 and changes in the Earth's climate at the end of the

Ordovician period. The transfer and removal of carbon from one reservoir to another

often leaves traces in the sedimentary record reflecting biologic, chemical, and physical processes, and can be studied employing chemostratigraphic and sequence stratigraphic principles. In the case of the Hirnantian Stage positive $\delta^{13}C$ excursion, a widely accepted mechanism regarding the origin is glacially-induced de-stratification of the water column resulting in nutrient enrichment and higher rates of bio-production in Earth's oceans. This proliferation of biologic production results in an increase in the rate of sedimentary burial (sequestration) of isotopically light (^{12}C-enriched) organic carbon leading to a positive shift in $\delta^{13}C$ values of contemporaneous marine carbonates (Knoll et al., 1986; Kaufman and Knoll, 1995; Weissert et al., 1998; Kump & Arthur, 1999).

Recently a positive $\delta^{13}C$ excursion with maximum values up to +3‰ was documented from late Middle Ordovician (Chatfieldian Stage, ~454 - 443 Ma) strata of the Great Basin, approximately 10 My earlier than the Hirnantian glaciation (Saltzman and Young, 2005; Fig. 1A). In the stratigraphic record this $\delta^{13}C$ excursion was obtained from the upper member (informally designated as "Member C") of the Copenhagen Formation in central Nevada, and occurs stratigraphically below the Eureka Quartzite. Coupled with additional proxy data such as phosphorite deposits which indicate continental margin upwelling during this time (Pope and Read, 1997, 1998; Pope and Steffen, 2003), it has been hypothesized that the primary processes responsible for the formation and deposition of this excursion were identical to those active during the Hirnantian glaciation. This is supported indirectly by the presence of ^{13}C-enriched strata worldwide, varying in age throughout Middle to Late Ordovician time (Hatch et al., 1987; Bergström, 1995; Ainsaar et al., 1999, 2004; Ludvigson et al., 1996, 2004; Patzkowsky et al., 1997; Young et al., 2005; Tobin et al., 2005), and implies a global-

scale cooling event. However, unlike the younger Hirnantian Glacial epoch for which

there is much documented physical evidence, the paucity of glaciogenic deposits during

the late Middle Ordovician period across Gondwana (Hamoumi, 1999) argues against a

glacio-eustatic origin for this isotopic excursion.

This problem becomes more apparent when the late Middle Ordovician stratigraphic

record in southern Nevada and California is considered (Fig. 1B). In these southern

Great Basin locations the Eureka Quartzite is in direct contact with the Pogonip Group,

with the majority of the Copenhagen Formation missing (~ 140 meters thick; Ross, 1964,

1967; Ross and Shaw, 1970). The absence of the Copenhagen Formation in southern

Nevada can have two interpretations: 1) erosion of this unit occurred during regression

prior to Eureka Quartzite deposition, resulting in a juxtaposition of carbonate strata of the

Antelope Valley Limestone and siliciclastic strata of the Eureka Quartzite; and 2) the

Copenhagen Formation is a local unit with limited geographic extent. The first

interpretation would require a major sea-level fall (> 140 m) in order to erode the entire

Copenhagen Formation in southern Nevada, exceeding the magnitude of sea-level change

during the Last Glacial Maximum (~120 m) and the Hirnantian glaciation (~45-60 m) and

would result in a prominent unconformity containing significant erosional relief across

the study area in addition to definitive glaciogenic deposits worldwide. Alternatively, the

second interpretation implies that the Copenhagen Formation is a localized facies

deposited in a tectonically controlled basin and the geochemical signal obtained from this

unit may not be representative of the global average ocean isotopic composition.

Therefore, determining the origin and paleoenvironmental setting of the Copenhagen

Formation would elucidate the significance of the positive $\delta^{13}C$ excursion as a proxy for glaciation and initiation of the climatic transition in the late Middle Ordovician.

In order to test the two alternative interpretations on the origin of the positive carbon isotope excursion and its connection to glaciation, two hypothetical depositional models are proposed. Each model outlines the expected sedimentologic and chemostratigraphic patterns, assuming that glacioeustasy would result in a shoaling deposition and formation of a major sequence boundary post-dating the positive excursion.

Model 1: This model features deposition of the Copenhagen Formation uniformly across the paleo-shelf. The Copenhagen Formation was subaerially exposed and eroded during the subsequent sea-level fall. This interpretation requires that the Copenhagen Formation to be a regressive unit which was deposited during the sea-level fall. In this case, the positive carbon isotope excursion in the upper Member "C" should correspond to the global cooling, polar ice sheet expansion, and high rates of biologic production and organic matter burial (Fig. 2). Sedimentologic evidence should indicate a shallowing-upward trend in its type location and the presence of a sharp, erosional contact between the Eureka Quartzite (EQ) and Copenhagen Formation. Accordingly, studied locations outside of the Monitor-Antelope Valley area should also exhibit erosional relief at the unconformity, corresponding to the amount of sea-level fall necessary to erode the thickness of this unit. Chemostratigraphic evidence should corroborate these observations by the presence of a negative isotopic shift at the EQ-Copenhagen contact due to diagenetic modification by ^{12}C-enriched meteoric fluids during sub-aerial exposure following sea-level fall, or a reproducible positive $\delta^{13}C$ excursion in strata that did not experience significant alteration. Additionally, a conformable contact between the

4

Antelope Valley Limestone and the Copenhagen Formation is expected as deposition shifts gradually from the Antelope Valley Limestone into the Copenhagen Formation.

Model 2:   In this scenario the Copenhagen Formation is deposited over a limited geographic extent within a restricted circulation environment, and undergoes a facies change across the shelf (Fig. 3) at Lone Mountain and southern sections in the Pahranagat and Arrow Canyon Ranges, and White River Narrows. Time equivalent units of the Copenhagen Formation outside of the Monitor-Antelope Valley area should be the mixed siliciclastic-dolomitic units first described by Kirk (1933) as the transitional lithology between the pure carbonate strata of the Antelope Valley Limestone and the siliciclastic Eureka Quartzite at Lone Mountain or the basal Eureka Quartzite unconformity itself.

Validation of this model would require sedimentologic evidence to indicate disparate depositional trends across the paleo-shelf in the type section of the Copenhagen Formation and in sections outside the Monitor-Antelope Valley region. In the Monitor-Antelope valley area, a gradual transition between the Antelope Valley Limestone and the Copenhagen Formation is expected, while outside of this region a shoaling-upward trend towards the top of the Antelope Valley Limestone should be observed, along with the development of paleokarst features indicative of exposure and erosion below the Eureka Quartzite. This interpretation should also be supported isotopically by the absence of an associated $\delta^{13}C$ excursion outside the Monitor-Antelope Valley area and the background $\delta^{13}C$ values may differ due to the local environmental effects on isotope values. Also expected is the potential diagenetic alteration of isotope values associated with subaerial exposure at the unconformity between the Eureka Quartzite and the Antelope Valley Limestone.

In this thesis, I present the data that support the second interpretation, which invokes local carbon cycling as the primary cause of the positive carbon isotope excursion in the Great Basin. Paleoenvironmental reconstruction of the five studied localities indicates a shallowing-upward trend in the Antelope Valley Limestone and a deepening-upward trend in the Copenhagen Formation. However, the effects of local carbon cycling cannot be separated from global effects of glacio-eustasy and increased organic carbon burial because the presence of a major sequence boundary below the Eureka Quartzite implies a net base-level fall. Whether this base level fall was caused by glacioeustatic sea-level fall or regional tectonic uplift requires further investigation in broader areas. Nonetheless, the disparate depositional environments indicated by the Copenhagen Formation and Antelope Valley Limestone argue against a uniform deposition of the Copenhagen Formation across the paleo-shelf.

CHAPTER 2

GEOLOGIC BACKGROUND

<u>Tectonic Setting</u>

Paleozoic strata of western North America record deposition along a passive

continental margin following a complex episode of rifting beginning in the Latest

Proterozoic (Bond et al., 1985). Cambrian to Late Devonian strata form a westward-

thickening wedge of shallow-water carbonates with minor amounts of siliciclastic

sediments. These carbonate-rich strata overlie older terrigenous units derived from the

ancient craton during the rift stage (Finney et al., 2000; Dickinson, 2004). Comparison of

subsidence rates derived from Cambrian to Ordovician strata from southwestern United

States to Canada, and model-driven inferences of thermal decay constants of thinned

lithosphere indicated a good fit between subsidence and the exponential decay curves,

supporting a thermal decay mechanism as the primary driver of crustal subsidence during

the early Paleozoic (Stewart and Suczek, 1977; Manspeizer and Cousminer, 1988).

Quantitative analyses of these strata suggest that post-rift thermo-tectonic subsidence of

the passive continental margin did not begin until 525-515 Ma (Bond et al., 1983; Armin

and Mayer 1983; Bond & Kominz 1984; Levy and Christie-Blick, 1991), and lasted

approximately 55-65 million years. This estimate reflects the revision of the base of the

Cambrian from 570 Ma to 541 Ma, and places the onset of thermal subsidence within

Early Cambrian time (Dickinson, 2006).

This conservative time frame proposed for rift-to-drift transition and thermal

lithospheric contraction suggests that eustasy was the dominant control on sedimentation

in an exponentially-subsiding basin well before deposition during Ordovician time (Bond

and Kominz, 1988). Deposition occurred along the length of the continental margin nearly uninterrupted until the inception of the late Devonian-Mississippian Antler Orogeny, which marked the transition from passive to accretionary margin at the western edge of the Laurentian paleocontinent. Earliest evidence for tectonic destruction of the passive margin by overthrust oceanic allochthons exists along the Roberts Mountains Thrust belt, where miogeoclinal strata of Ordovician and Cambrian age are emplaced above younger Silurian and Devonian platform carbonates (Finney et al., 2000).

More recent tectonic displacement of Ordovician strata occurred during the Permian-Triassic Sonoma Orogeny, although no tectonic episode had more influence on the current position of Ordovician rocks than Cenozoic extension (Dickinson, 2004). Present-day exposures of Middle Ordovician carbonate rocks occur throughout Nevada in north-to-south trending mountain ranges as far west as the Toquima Range, separated by longitudinal extensional valleys.

The effects of local tectonism should not be overlooked on the regional and local expression of sequences within the stratigraphic record. Tectonic activity during the Ordovician has been demonstrated by several researchers (Webb, 1958; Ketner, 1977, 1986; Cotkin, 1989), although no definitive evidence has been put forth, partially due to the lack of preserved strata indicative of extension or contraction. Nonetheless, indirect evidence such as intrusive rocks of Middle to Late Ordovician age support the notion that local tectonism could have had a significant impact on depositional patterns during the Ordovician (Cotkin, 1992). Thus, it is possible, as Ketner (1977) suggested, that offshore tectonic elements could have been active and influenced sedimentation to the east well before thrusting initiated in the latest Devonian to Mississippian time.

8

<center>Ordovician Paleogeography of Laurentia</center>

The Middle to Late Ordovician strata of this study were deposited in a broad

carbonate platform situated 5° to 20° south of the paleo-equator, with an area ~500 km in

length and up to 200 km wide. Despite the immense paleogeographic extent of this

carbonate shelf, estimates of paleodepth do not exceed ~75 meters at the slope-shelf

margin (Ross, Jr., 1977), which can be approximated by the 0.706 line of $^{87}Sr/^{86}Sr$. The

orientation of this marker also roughly correlates to the hinge point of the subsiding

basin, and can be used to infer shallow versus deeper parts of the basin along a shoreline

to slope transect. The orientation of the continental margin during Ordovician time has

been estimated as striking towards northeast-southwest (Fig. 4), which is supported by

sedimentologic evidence of deep-water deposits at northwestern sections and exposure

and erosion at more southern locations (Zimmerman and Cooper, 1999; Cooper and

Keller, 2001).

Palinspastic restoration of Ordovician strata in the Great Basin is not attempted in this

study due to the lack of published data for the mountain ranges from which measured

sections were documented. Additionally, previous studies (Parsons, 1996) have

demonstrated that sedimentologic evidence does not necessarily support the inferred

position of studied locations with respect to location within the paleo-basin.

<center>Ordovician Biostratigraphy of the Great Basin</center>

Biostratigraphic data serve as the basis for the sequence stratigraphic analysis in this

study. The data sets are the results of work that began in the 1960's (Webb, 1958; Byers

et al., 1961; Langenheim et al., 1962; Ross et al., 1964, 1967, 1970; Chamberlin, 1975;

Ross and Shaw 1972; Ethington and Schumacher, 1969; Fortey and Droser, 1999; Li and

<center>9</center>

Droser, 1999; Finney and Ethington, 2000). In the Great Basin the stratigraphic units of interest span the Middle Ordovician Whiterockian and Late Ordovician Mohawkian Series of North America. Comparable chronostratigraphic units have been recognized in eastern United States (Fisher, 1957; Finney et al., 1999; Kapp and Stearn, 1975), Great Britain (Fortey et al., 1991, 1995), Baltoscandia (Bergström, 1995; Brenchley et al., 2003) and serve as the basis for the correlation of eustatic events and isotopic excursions at regional and global scales (Fig. 5). The approximate time spanned by the Whiterockian and Mohawkian Series is ~464-443 Ma, which were mainly determined by distinct conodont, brachiopod, graptolite, and coral fossil zones (Ross et al., 1991) and later confirmed by isotopic stratigraphy. The relevant units of this study in Nevada are the upper member of the Antelope Valley Limestone, the Copenhagen Formation and the Eureka Quartzite, which have been dated according to the appearance of fossil zones across the basin.

The Whiterockian Series, a chronostratigraphic unit of global significance, is well-constrained by four different phyla and permits correlation from basin to platform environments across the globe (Table 1; Ross et al., 1989). The type section of the Whiterockian Series is found in Whiterock Canyon, southern Monitor Range, central Nevada, and was proposed by Ross et al., (1991). Division of this series is based on the presence of three distinct faunal zones and two subzones, and its base is defined by the first occurrence of the *Isograptus victoriae* graptolite fauna in basin and slope settings, and the *Orthidiella sp.* brachiopod zone in shallow shelf environments. The upper boundary of the Whiterockian Series is defined by the appearance of the *Baltoniodus gerdae* conodont Subzone. However, this boundary is ambiguous in the Great Basin due

to the absence of sufficient fossils across the lithologic change of the Antelope Valley Limestone and Eureka Quartzite.

The Late Ordovician Mohawkian Series is not as well-defined in the Great Basin as the older Whiterockian Series, mostly due to the paucity of preserved fossils within the Eureka Quartzite. Nonetheless, the appearance of new faunal assemblages following the Sauk-Tippecanoe regression in the mid-continent and eastern United States (Fisher, 1957) provide enough evidence to correlate this chronostratigraphic unit to the well-defined Late Ordovician British Series, most notably the Caradocian Series. Globally, the basal boundaries of the North American Mohawkian and British Caradocian Series coincide at the first appearance of the *Baltoniodus gerdae* conodont subzone, but differ at their upper boundaries, with the Caradocian representing another ~4 my of deposition (Barnes, 1992). In the study area this stratigraphic interval is either obscured by Eureka Quartzite debris or eroded prior to, and during deposition of the Eureka Quartzite.

Strata of the Great Basin that comprise the Whiterockian and Mohawkian Series are divided into three major units, including 1) carbonate-dominated strata of the Antelope Valley Limestone and this unit's southern Nevada equivalent, (i.e., the unnamed upper Pogonip Group units); 2) interbedded fine-grained siliciclastic and carbonate strata of the Copenhagen Formation; and 3) the conspicuous siliciclastic Eureka Quartzite. From the Eureka District to southern Nevada, the Copenhagen Formation between the Antelope Valley Limestone and Eureka Quartzite varies in thickness from up to ~180 meters at Martin's Ridge to less than 30 meters approximately 20 km southward at Hot Creek Canyon. At Meiklejohn Peak in southern Nevada, a transitional unit that is ~10 m thick between the Antelope Valley Limestone and Eureka Quartzite was ascribed to the

Copenhagen Formation (Webb, 1958; Ross et al., 1977), but in most other sections such as the Arrow Canyon Range, this unit is either absent or has a minor thickness of less than 5 m. This variation in thickness and the presence of an unconformity below the EQ in southern Nevada has led some researchers to believe that the Copenhagen Formation is time equivalent to the lower part of the Eureka Quartzite in some areas of the Great Basin (Cooper, 1956). This discrepancy could not be easily reconciled because of poor biostratigraphic control across the stratigraphic units and potential erosion at the base of the Eureka Quartzite. A definitive relationship between the Copenhagen Formation and lower Eureka Quartzite members has not yet been elucidated, and underlies the impetus for this study.

The oldest strata involved in this study belong to the Antelope Valley Limestone, which overlies the Early Ordovician Ninemile Formation at most locations in Nevada, and represent the majority of Middle Ordovician deposition in the Great Basin. This formation was first defined by Nolan et al. (1956) in the vicinity of Eureka, Nevada as the limestone units deposited between the siliciclastic Ninemile Formation and Eureka Quartzite. In southern Nevada further subdivision of the Pogonip Group by Byers et al. (1961) created three members within the Antelope Valley Limestone (AVL), named the Paiute Ridge, Ranger Mountains, and Aysees Peak Members. These members are laterally persistent in a north-south trend, but lose their expression to the west and east, where they transition into fine-grained mudstone and siltstone of the basin deposits to the west, and proximal siliciclastic deposits to the east. In the southern Great Basin these members are equivalent to Units Opc-Opf (1962) of Langenheim et al. in Arrow Canyon, but only the correlation of Byers et al. (1961) Aysees Peak Member and Unit Opf is

currently documented in the published record (Ross et al., 1989; Kaya and Friedman, 1997). Because the oldest strata described in this study are of the upper Aysees Peak member, the upper Pogonip Group units will also be referred to as the Antelope Valley Limestone (AVL). During field work the upper Aysees Peak member was easily distinguishable across the field area by the presence of the "*Girvanella* algal shoals" (Fig. 6), which marks the upper extent of the middle Aysees Peak Member.

The stratigraphic unit of greatest interest is the Copenhagen Formation, first described by Kirk (1933) as the "brownish-weathering sandy dolomite" above the AVL and beneath the Eureka Quartzite at Lone Mountain, central Nevada. Further work since that time has determined the presence of three members, spanning approximately 140 meters from the top of the AVL to the base of the Eureka Quartzite in Copenhagen Canyon of Antelope Valley, approximately 18 km south of Lone Mountain (Cooper, 1956). The oldest member of the Copenhagen Formation is composed of brown lithic arenite, resting conformably on Antelope Valley Limestone (Ross and Shaw, 1972). This basal sandstone member transitions gradually into thin-bedded limestone and dark-colored argillaceous limestone units of the middle and upper members, respectively. The three members are informally designated A, B, and C, and will be referred to as such in this thesis. Correlation of these members across the shelf is hampered by lack of outcrops and the great variability of the thickness of this unit over short geographic distance. This variation has led many researchers to believe that this unit has either been eroded along the shelf prior to EQ deposition (Webb, 1958; Miller, 1977; Cooper and Keller, 2001), or deposited in a restricted basin (Finney and Ethington, 2000). Member C is of particular importance to this thesis, as it includes the stratigraphic interval from which the positive

carbon isotope excursion was documented, and interpreted as a period of glaciation and sea-level fall (Fig. 1A; Saltzman, 2005).

Above the Copenhagen Formation, the Eureka Quartzite spread across the shelf and inundated carbonate production until deposition of the Late Ordovician Ely Springs Dolomite. In the type section at Lone Mountain three members can be recognized within the Eureka Quartzite. Description of these members and correlation to the south indicates the persistence of all members, and recognition of a fourth, youngest member (Webb, 1958) in the Grant Range, central Nevada. The thickness of this unit varies predictably in sections north of the Pahranagat Range where it attains its maximum, but thins consistently from this location toward the south until it disappears conspicuously south of Las Vegas. At the west flank of Arrow Canyon it has a thickness of ~30 meters but three recognizable members are still present and they are correlatable with those from the Pahranagat Range and the White River Narrows locations in the north.

Correlation of these units across the Great Basin indicates a complex relationship between lithologic and biochronologic boundaries of Ordovician subdivisions, and suggests a diachronous deposition for the Antelope Valley, Copenhagen and Eureka Quartzite Formations (Ross et al., 1989). In general, existing data suggest that the siliciclastic Eureka Quartzite is oldest in central Nevada and is progressively younger toward the south-southeast.

Sequence Stratigraphic Concepts and Controls

Sequence stratigraphy is a methodology that was initially used to interpret the ordered arrangement of strata in seismic reflection profiles by subdividing sedimentary packages into units that correspond to deposition during the different phases of base-level rise or

14

fall (Vail et al., 1977; Posamentier et al, 1988; Van Wagoner et al., 1988). Unlike lithostratigraphy which divides strata solely on their lithological similarities, sequence stratigraphy emphasizes the stratal geometry and their bounding surfaces that have been implicitly linked to "relative" sea-level changes. The primary controls on "relative" sea-level change can be tectonic, eustatic, or fluctuations in sediment supply. Since its inception and subsequent modification, this approach has been applied to the outcrop scale by identifying meter-scale sedimentary cycles and their vertical stacking patterns to infer the position of stratigraphic discontinuities and the migration of depositional environments relative to coastal lines and/or continental shelf margins. Sequence boundaries, defined as unconformities in shallow-water environments and their correlative conformities in deep-water environments, have been used to package the stratigraphic units into depositional sequences that have chronostratigraphic meaning in intra- and inter-basinal correlations (Vail et al., 1977; Haq et al., 1987; Posamentier et al., 1988; Sarg 1988). Identification of key surfaces (sequence boundaries) in the rock record involves lithologic, biostratigraphic and chemostratigraphic data, and a well-defined sequence stratigraphic framework can be used to investigate the influence of local tectonism and global eustasy on sediment accumulation in sedimentary basins as old as the Proterozoic (Christie-Blick et al., 1988).

The main element of sequence stratigraphy is a sequence, first described in the work of Sloss (1963) as a "stratigraphic unit[s]… traceable over major areas of continent and bounded by unconformities of interregional scope". This definition of a sequence has been modified in subsequent sequence stratigraphic models as "a relatively conformable succession of genetically related strata… bounded at its top and base by unconformities

and their correlative conformities" (Vail et al., 1977). Sequence boundaries separate a sequence from the one below or above it, and typically exist as unconformities at the landward edge of a basin, to correlative conformities in deep-water parts of basins.

Parasequences form the basic units of sequence stratigraphy, and their arrangement and expression determine the architectural elements of depositional systems tracts. A parasequence is defined as a relatively conformable succession of genetically related beds or bed-sets that exhibit an upward-shoaling or deepening trend of lithofacies deposited in lateral continuity across a basin. The upper and lower contacts reflect an abrupt shift in facies usually with deeper-water facies overlying shallow-water deposits. Parasequences can exhibit progradational, retrogradational, or aggradational stacking patterns according to the position of facies in relation to the parasequence below and above (Fig. 7).

The vertical stacking patterns of parasequences are used to infer systems tracts, which comprise the major architectural subdivisions of a depositional sequence. Systems tracts (Fig. 8; Brown and Fisher, 1977) comprise a distinct assemblage of depositional systems that are active during different phases of sea-level fluctuations. In theory systems tracts occur in an ordered arrangement along the dip direction, and are enveloped by key surfaces that record maximum and minimum positions of sea-level. Much of the disagreement in sequence stratigraphy stems from the variety of defined systems tracts and their nomenclature, and by which surfaces sequences are bounded. An excellent review of the competing models and their differences and similarities is given in Catuneanu (2002) and Catuneanu et al. (2009). However, because defining the systems tracts requires information on spatial geometric organization of sedimentary units that is commonly unavailable in separated outcrops, outcrop sequence stratigraphy focuses on

16

identifying the key surfaces and stacking patterns rather than packing the stratigraphic units into systems tracts. Within the context of a sequence stratigraphic study the main focus of this thesis is to identify the position of the major sequence boundary related to the isotopic excursion.

Sequence boundaries have received the most attention in the literature due to their chronostratigraphic value and utility as intra-basinal correlation surfaces (Catuneanu et al., 1988; Miall, 1991). Their expression can be conformable along the dip direction towards the basin. In the up-dip direction sequence boundaries are unconformable surfaces formed during times of base-level fall that eliminates the accommodation space for sediment accumulation. They are expressed as exposure and/or erosional surfaces, and in some cases manifested by paleosols and locally by incised-valley fills (Rankey and Bechtel, 1998). Ideally, exposure and erosion created by base-level fall would leave identical dissolution features and stratigraphic truncation along the sequence boundaries, yet examples from ancient carbonate platforms (e.g., Montanez and Osleger, 1996; Osleger and Montanez, 1996; Jiang et al., 2002) indicated that, at a particular outcrop location, the expression of sequence boundaries would be very subtle. In such cases, changes in stratigraphic stacking patterns would be very useful to locate the potential sequence boundaries and lateral tracing of surfaces in closely spaced sections is important to reveal the small-scale stratigraphic truncation and/or erosion at the sequence boundary.

In this study, efforts for interpreting the sequence boundaries have been made in looking for one or more of the following lines of evidence indicative of subaerial degradation (Jiang et al., 2002): 1) local stratigraphic truncations underneath the sequence boundary demonstrable by comparing closely-spaced sections; 2) paleokarstic

17

depressions with visible relief; 3) subaerial dissolution and weathering products (breccias and calcrete) filling vertical fissures, dikes, cavities, and shallow depressions in underlying carbonate rocks; and 4) small-scale evidence for subaerial exposure at an erosion surface.

CHAPTER 3

METHODOLOGY

<u>Sequence Stratigraphy and Chemostratigraphy</u>

An integrated sequence and chemostratigraphic approach was employed in this thesis
to determine the plausibility of a possible proxy record of glaciation in Ordovician strata
of the Great Basin. Isotope stratigraphy has made major advances since the pioneering
works of Friedman and Hall (1963), O'Neil and Epstein (1966), Veizer and Hoefs (1976),
and others, enabling stratigraphic correlation as well as investigation of geochemical
processes through time. Coupled with advances in sedimentologic studies within a
sequence stratigraphic context, this dual approach has proven successful in deciphering
the relationship between sedimentary and biogeochemical processes and the secular
variations in the carbon isotope record. In this study, isotopic data are used to: (1) trace
the extent of the positive δ^{13}C excursion to the north and south of the Antelope Valley,
and (2) document the potential isotope variations resulting from subaerial exposure and
meteoric diagenesis along the sequence boundary.

Sequence stratigraphic study in outcrops focused on the upper ~100 m of the Aysees
Peak Member and the Eureka Quartzite and included bed-by-bed measurement of
stratigraphic sections aimed at understanding the depositional environments of facies,
their stacking patterns, and exposure/erosional features along sequence boundaries.
Meter-scale carbonate cycles and their stacking patterns were used to determine the
temporal evolution of the carbonate platform before the deposition of the Eureka
Quartzite and to locate potential stratigraphic truncation at the unconformity below the
Eureka Quartzite.

Six localities were investigated across Nevada in an approximate north-south transect from the Arrow Canyon Range in the south to the northern edge of Lone Mountain in central Nevada. Four of those locations provided sedimentologic and stratigraphic data, and were complemented with chemostratigraphic data obtained from three of the six sections (Fig. 9). The sampling interval in these sections varied between 1 to 1.5 meters, in an effort to choose micritic versus coarse or re-crystallized lithology.

Thin-sections created from samples collected at these four localities were used to classify carbonate lithologies, and interpret sedimentary textures according to methods outlined in Scholle and Scholle-Ulmer (2003), Tucker (1988) and Tucker and Wright (1990). Petrography was used to support a list of widely-accepted criteria to define stratigraphic surfaces in carbonate sediments (Handford and Loucks, 2001) which was then used to identify the position of the sequence boundary across the study area. Sequence boundary recognition and correlation were conducted by field observations documenting erosional relief and lithological changes across the key surfaces. A total of 128 samples were collected and analyzed for $\delta^{13}C$ and $\delta^{18}O$ values to determine the extent of the positive carbon isotope excursion, and possible diagenetic overprinting during exposure at the sequence boundary.

The $\delta^{13}C$–$\delta^{18}O$ pattern and their regional consistency were used to determine the degree of diagenetic alternation. Although such criteria may not be definitive, numerous studies suggest that fine-grained carbonates such as micritic limestone or micritic matrix of packstone and wackestone preserve $\delta^{13}C$ values close to their primary seawater composition (e.g., Ripperdan et al., 1992; Saltzman et al., 1998; Kump et al., 1999; Saltzman et al., 2000; Joachimski et al., 2002; Railsback et al., 2003; Saltzman and

20

Young, 2005; Shields et al., 2005; Dilliard et al., 2007; Theiling et al., 2007). This

inference has been confirmed by the similarity of features between micrite-based and

brachiopod-based $\delta^{13}C$ curves; the latter has been considered as the most stable mineral

phase during diagenesis because brachiopod shells are precipitated as low-Mg calcite

from seawater – the only metastable mineral phase in natural carbonates (Azmy et al.,

1998; Mii et al., 1999; Saltzman, 2002). Oxygen isotopes ($\delta^{18}O$) are vulnerable to

diagenetic alteration because oxygen is a major component in meteoric and formation

fluids.

Isotope analysis was conducted at the Las Vegas Isotope Science Lab. Samples were

cut, polished, and drilled using the FOREDOM micro-drill apparatus, and the powder

analyzed using the ThermoElectron Delta V Stable Isotope Ratio Mass Spectrometer

coupled to a Kiel IV automated carbonate preparation device. Isotopic results are

reported in the standard δ-notation as per mil (‰) deviations from Vienna-Pee Dee

belemnite (V-PDB) and the data are given in Appendix 1.

CHAPTER 4

DATA AND RESULTS

Stratigraphic Analysis

Fourteen lithofacies have been identified from the sections in Arrow Canyon,

Pahranagat Range, White River Narrows, Hot Creek Canyon, Martin's Ridge (in

Copenhagen Canyon) and Lone Mountain, covering stratigraphic intervals including the

upper member of the Antelope Valley Limestone, Copenhagen Formation and the Eureka

Quartzite. These lithofacies and their vertical arrangement allow the identification of

carbonate cycles and critical exposure/erosional surfaces in a sequence stratigraphic

framework. Key features of lithofacies are summarized in Table 2 and their

paleodepositional interpretations are given in Figure 10.

Correlation of sections across the study area was based on the unconformity at the

basal Eureka Quartzite and the readily-identifiable marker bed composed of "*Girvanella*"

oncolitic and oolitic grainstones in the middle member of the Antelope Valley Limestone.

Litho- and biostratigraphic studies of this marker bed indicated that it belongs to the

Anomalorthis and *Palliseria* biozones (Kaya and Friedman, 1997) and can be used as a

marker for regional stratigraphic correlation across the Basin and Ranges Province (Ross,

Jr. 1964; Ross, Jr. et al., 1989).

Facies Associations

The fourteen lithofacies identified from the upper Aysees Peak member of the

Antelope Valley Limestone, Copenhagen Formation, and Eureka Quartzite can be

grouped into five facies associations according to their depositional environments (Fig.

11), including (1) foreshore to shoreface siliciclastics, (2) shallow-marine carbonate-

siliciclastics, (3) restricted subtidal shale and carbonates, (4) peritidal carbonates, and (5) oncolitic-oolitic sand shoals.

Facies Association 1: Foreshore-shoreface siliciclastics (Lithofacies I and II)

The foreshore-shoreface siliciclastic facies association is composed of two main facies: cross-bedded quartz arenite and bioturbated lithic arenite (lithofacies I and II, Figs. 12 and 13; Table 2). These two facies comprise the Eureka Quartzite and alternate at uneven thickness. Locally, intervals of intensely bioturbated fine-grained sandstones and parallel-laminated siltstone and dolowackestone are also present.

The lower 4 to 15 m of the Eureka Quartzite is composed predominantly of bioturbated lithic arenite (lithofacies I; Figs. 12C and 13A) that contain trough and planar cross stratifications. Locally, 5 to 10 cm thick ripple cross-laminated siltstone and fine-grained sandstone layers are present between silica-cemented fine sandstone beds. Burrows characteristic of the *Skolithos* ichnofacies are common in addition to vermiform, silt and fine sand-infilled irregular burrows (Fig. 13D). At the top of this lithofacies, there is a 0.5 to 1.0 m thick sandy dolostone interval containing oncoids of 0.5 to 1 cm in size, separating this lithofacies from the overlying quartz arenite-dominated facies.

Lithofacies II characterizes the upper part of the Eureka Quartzite. This lithofacies is composed of coarse- to medium-grained quartz arenite with low-angle planar and trough cross stratifications and parallel laminations, and less commonly, ripple cross-laminated siltstone layers (Fig. 12B, D). Trough cross-stratification is prevalent in the lower portion of this subdivision, but becomes relatively sparse toward the top. Burrows are common. In the lower part, most of the burrows are *Skolithos*, but *Calianassa*-type (Fig. 13C, F) ichnofacies are observed to increase up - section. A parallel-laminated siltstone

23

to fine sandstone interval up to 5-10 m thick is present in the upper part of the sections, containing flat to rounded, columnar features interpreted as stromatolites (Fig. 13B, E; Druschke et al., *in press*). In the topmost part of the Eureka Quartzite, a herringbone cross-stratified, ripple cross-laminated dolomitic quartz arenite and parallel-laminated sandy dolomite interval makes the transition to the overlying Hanson Creek Limestone-Ely Springs Dolomite. This transitional unit varies in thickness from less than 2 m in sections of the Lone Mountain, Pahranagat Range and White River Narrows to about 10 m in the Arrow Canyon Range section.

Lithofacies I and II are interpreted as deposited from the upper shoreface to foreshore environments (Fig. 14). The presence of trough and planar cross bedding indicates high-energy conditions where subaqueous sand dunes migrated to form cross bedding. The abundance of vertical burrows (*Skolithos*) is consistent with resting traces in high-energy upper shoreface environments. Herringbone cross stratification may have been formed in tidal channels, suggesting that in the uppermost part of lithofacies II the shoreface may have evolved into a barrier-island system, consistent with the thickness change of the interval across the sections. Locally present fine-grained sandstone and siltstone with *Calianassa*-type ichnofacies may have been deposited from relatively low-energy environments protected by large sand dunes. Lithic fragments in lithofacies I may record a more proximal terrestrial source during the early transgression following the basal Eureka Quartzite unconformity, while the quartz arenite of lithofacies II records deposition from compositionally mature coastal environments during the latter stage of transgression and highstand.

Facies Association 2: Tidal flat mixed carbonate- siliciclastics (Lithofacies III, VI)

This facies association consists of alternating dolomitic siltstone and lime mudstone (lithofacies III; Fig. 15) and fenestral silty dolostone (lithofacies IV) and occurs as a transitional unit between the Antelope Valley Limestone and Eureka Quartzite. This unit was first recognized by Nolan et al. (1956) at Lone Mountain and this study found its presence in most sections outside of the Antelope Valley-Monitor Valley region, with a thickness change from 5 to 16 meters.

Thinly bedded (5-10 cm thick) dolomitic siltstone and lime mudstone are moderately bioturbated and in some cases, layer-parallel muddy drapes in siltstone layers form flaser bedding. Less commonly, thin (1-2 cm thick) fenestral silty dolostone is present as interbeds between dolomitic siltstone and lime mudstone.

This facies association is interpreted as having formed in a tidal flat environment. Carbonate mud was brought into the intertidal to supratidal areas by waves and tides, where microbial mats may have colonized. Decomposition of microbial mats created layer-parallel cavities that were filled in with calcite, forming fenestral structures (Fig. 15E).

Facies Association 3: Restricted subtidal shale and carbonates (Lithofacies V and VI)

The restricted subtidal facies association is composed of two lithofacies: shale and argillaceous limestone (lithofacies V; Fig. 16D) and lime mudstone/wackestone (lithofacies VI; Fig. 16A, B, C). These facies constitute the classic Copenhagen Formation in the Antelope Valley and Monitor Valley areas and are not present outside of this region. In the Hot Creek Range to the south of Monitor Valley observance of these lithofacies indicates the presence of all three members of the Copenhagen Formation,

suggesting a thinning trend of the entire formation, consistent with the local geographic extent of this unit.

The shale and argillaceous limestone (lithofacies IV) alternates with lime mudstone and wackestone (lithofacies V). In general, the ratio of shale to argillaceous limestone increases up-section. Millimeter-thick parallel laminations are common in shales and argillaceous limestones. Lime mudstone and wackestone beds are relatively thicker (5-15 cm) than the shaley beds and are often intensively bioturbated. Fossil fragments and abundant well-preserved body fossils of brachiopods, bryozoans, and gastropods are observed in lime mudstone and wackestone beds.

These lithofacies are interpreted as having formed in a low energy, deep subtidal environments, possibly in a restricted embayment (sensu Rees, 1986). The presence of parallel laminations and the lack of packstones and grainstones and other shallow-water sedimentary features such as fenestrae, cross beds, and desiccation cracks suggest deposition from suspension below the fair-weather wave base. Bioclastic fragments were possibly brought into the depositional sites by storms or washed out into depositional sites from coeval shallow-water environments. The increase of parallel-laminated shales up-section suggests an overall deepening upward trend during deposition of the Copenhagen Formation (Fig. 17).

Facies Association 4: Peritidal carbonates (Lithofacies VII, VIII, IX, X, XI, and XII)

The peritidal carbonate facies association forms the upper Antler Valley Limestone in the study areas. It include lithofacies VII (peloidal wackestone), VIII (mudcracked lime mudstone), IX (bioclastic packstone and grainstone), X (intraclastic conglomerate), XI (bioturbated/nodular mudstone), and XII (bioturbated/nodular wackestone; Figs. 18, 19,

20, and 21). These facies commonly form 3 to 10 meter thick, shallowing-upward cycles (Fig. 22) bounded by exposure surfaces expressed by fenestral structures, mudcracks, and dissolution cavities and depressions filled with sandstone/siltstone and conglomerates.

The peloidal wackestone lithofacies (VI) occurs as 0.3 to 1.5 meter thick units that show thin (1-3 cm) wavy or flat bedding. Compositionally this facies contains visible peloids and subordinate bioclasts including brachiopod and bryozoan fragments. In many cases the tops of this lithofacies exhibit dissolution cavities and brecciation, locally infilled with poorly-sorted deposits consisting of rounded carbonate clasts in a silty to sandy matrix (Fig. 18A, B, C). Vertical thin burrows approximately 3 to 5 millimeters are common, particularly towards the top of the units. This facies is interpreted to have deposited from the upper intertidal to supratidal environments on the basis of dissolution cavities and brecciation.

Mudcracked lime mudstone (VIII) occurs as 10 to 20 cm thick, yellowish to light gray units that are commonly found at the top of the meter-scale cycles (18D). These units often exhibit abrupt thickness change due to erosion by overlying coarser-grained facies (e.g., intraclastic grainstone and packstone) and in many cases are completely eroded; in such instances the presence of mudcracked lime mudstone facies is inferred from rounded centimeter-wide clasts incorporated within the overlying lithofacies. Less commonly, fenestral fabrics are present, along with partial dolomitization at the top. Mudcracks, when present, are filled with siltstone and curve upward around the edges, suggesting microbial encrustation (Fig. E). Trace and body fossils are rare, except for a few small gastropods occurring as millimeter-thick grainstone lenses, and sparse

bioturbation (Fig. 18F). The presence of mudcracks and fenestrae indicates that this facies was deposited in supratidal environments with subaerial exposure.

Bioclastic packstone and grainstone (IX; Fig. 19) forms 5-25 cm thick beds that commonly show erosional bases. Occasionally ripple cross laminations and planar cross beds are present. Bioclasts include brachiopods, crinoids and gastropods. This facies is interpreted as having formed in a subtidal environment above the fair-weather wave base, but have also been observed within lithofacies XI and XII, here interpreted as storm-generated deposits below fair-weather wave base.

Intraclastic conglomerates (X) are conspicuous in the studied sections (Fig. 20A, B, C, D). They appear as 20 to 35 cm thick beds that typically overlie mudcracked lime mudstone (VIII; Fig. 20E) or peloidal wackestone (VI). This facies is commonly present at the base of the meter-scale cycles with erosional bases. Intraclasts are composed of laminated lime mudstone and wackestone (Fig. 20F). Additional grains include brachiopod and gastropod fragments and subordinate quartz. This facies is interpreted as deposited from shallow subtidal environments above fair-weather wave base.

Bioturbated mudstone and wackestone lithofacies (XI and XII; Fig. 21) make up the majority of each cycle in the Pahranagat Range and White River sections, but are less abundant in cycles of the Lone Mountain and Arrow Canyon Range sections, where cycles are generally composed of coarser-grained facies (lithofacies VI and IX). These facies are thinly bedded (1-4 cm) and laterally persistent. Parallel and wavy dolomitized laminations are present but are often disrupted by *Calianassa*-type burrows (Fig. 21A, C). Occasionally thin (< 10 cm), lenticular bioclastic grainstone layers or lenses with

erosional bases are present within these facies. They are interpreted as deposition from lower intertidal to protected, low-energy lagoonal environments.

Facies Association 5: Oncolitic-oolitic sand shoals (Lithofacies XII, XIII)

This facies association is composed of two lithofacies: oolitic grainstone (XII) and oncolitic packstone (XIII; Fig. 6). They are present in the middle Upper Antelope Valley Limestone and form 5 to 10 m thick units that show up to 3 m relief (Fig. 6A). Oolitic grainstones form 10-30 cm thick beds and contain planar cross bedding. Laterally this facies can be transitional to oncolitic packstones, which also contain a significant amount of ooids. Oncoids form lenticular units up to several meters thick, serving as one of the most distinctive markers easily recognizable across the study area. These facies are interpreted as deposits from shallow, high-energy oncolitic-oolitic sand shoals.

Chemostratigraphic Data

Carbon isotope analysis of upper Antelope Valley Limestone beds were initially undertaken to document the extent of the positive $\delta^{13}C$ excursion in sections outside Antelope Valley, which was to be used for stratigraphic correlation of the upper Copenhagen Formation elsewhere. Paired carbon and oxygen isotopes are also used to investigate the potential diagenetic alteration of carbonate strata below sequence boundaries, where meteoric fluids may have been pervasive due to prolonged subaerial exposure, karstification and erosion. Isotope profiles obtained from the four sections in Arrow Canyon, Pahranagat Range, Hot Creek Range, and Lone Mountain are shown in Figures 23 and 24, where the data of the Monitor Valley section are from Saltzman (2005). Paired oxygen and carbon isotope curves have been used previously to evaluate the effects of meteoric diagenesis in carbonate strata of modern environments (Allan and

Matthews, 1982), and successfully applied to deposits of Miocene (Goldstein et al.,

1990), Cretaceous (Moldovanyi and Lohmann, 1984; Joachimski, 1994; Immenhauser et

al., 1999) and Ordovician age (Railsback et al, 2003; Thieling et al., 2007). In particular,

Railsback et al. (2003) and Thieling et al. (2007) have demonstrated the utility of isotopic

excursions in the identification of sequence boundaries where other obvious exposure

criteria are absent, or difficult to interpret from the sedimentary record.

Isotope profiles obtained from the four sections in Arrow Canyon, Pahranagat, and

Hot Creek Ranges, and Lone Mountain show substantial variability compared to those

from the Monitor-Antelope Valley composite section of Saltzman (2005). In Lone

Mountain (Figs. 23A and 24A), isotope measurements cover the uppermost 30 m of the

Antelope Valley Limestone. In the lower 15 m, δ^{13}C values are slightly positive (+0.5–

1.2 ‰). The upper 15 m has δ^{13}C values mostly from -0.5‰ to -2.3‰ and reach

minimum values of -3‰ to -5‰ in the uppermost part close to the basal Eureka

unconformity. The up to +3‰ positive δ^{13}C excursion seen in the Copenhagen Formation

(Fig. 23B) is missing in the Lone Mountain. Oxygen isotopes of the Lone Mountain

section are mostly from -4‰ to -6‰, with a few reaching -7.5‰ immediately below the

basal Eureka unconformity (Fig. 24A). No systematic covariation exists between δ^{13}C

and δ^{18}O (R^2 = 0.3369) if all the samples are considered, but in the uppermost 3 m of the

Antelope Valley Limestone (the transitional unit; Facies Association 2 in Table 2) right

below the Eureka Quartzite, samples that produced the most negative δ^{13}C values do have

the lowest δ^{18}O values.

The δ^{13}C and δ^{18}O trends from the Hot Creek Range (Figs. 23C and 24C) are similar

to those of the Lone Mountain section, but the absolute values differ. Most of the δ^{13}C

values in this section are negative, varying from -0.5‰ to -1.5‰, but close to the basal Eureka Quartzite unconformity, a few $\delta^{13}C$ values are as low as -4.5‰. These low $\delta^{13}C$ values are associated lower $\delta^{18}O$, suggesting diagenetic modification (e.g., Kaufman and Knoll, 1995). Again, the positive $\delta^{13}C$ excursion reported from the Copenhagen Formation (Saltzman, 2005) is not present here below the Eureka Quartzite. Most of the $\delta^{18}O$ values of this section are -4–6‰, but lower values down to -11.8‰ are found close to the basal Eureka Quartzite unconformity.

In the Pahranagat Range section isotope measurements cover the uppermost 61 m of the Antelope Valley Limestone below the Eureka Quartzite (Figs. 23D and 24D). When compared to the other sections, $\delta^{13}C$ values in this section show larger variations from about -1‰ to -4‰, with two intervals (10-21 m and 42-50 m, respectively), displaying a negative shift with a minimum value down to -4.5‰. Carbon isotope values become less negative (-0.7–1.6‰) in the transitional unit (facies association 2, table 3) between the Antelope Valley Limestone and Eureka Quartzite, but no positive excursion is observed. In the lower 50 m of the measured section, $\delta^{18}O$ values are quite stable, from -6‰ to -8‰, but a positive shift from -7‰ to -2‰ is found right below the basal Eureka Quartzite unconformity (Fig. 24D). This type of oxygen isotope shift is similar to those found at prolonged exposure surfaces where localized evaporation may have led to high $\delta^{18}O$ values that were partially preserved through the later stage of diagenesis (Railsback et al., 2003; Thieling et al., 2007).

The isotope profiles from the Arrow Canyon section (Figs. 23E and 24E) differ from the other sections. In the 67 m section below the Eureka Quartzite, $\delta^{13}C$ values vary from -2‰ to -4.5‰ in the lower 41 m, but shift to near 0‰ in the upper 16 m approaching the

31

Antler Valley/Eureka contact. Although the $\delta^{13}C$ values shift from more negative to less negative values, this change seems to be consistent with that of the Monitor Valley section (Fig. 23B), the absolute $\delta^{13}C$ values are different. The $\delta^{18}O$ values do not co-vary with $\delta^{13}C$, showing a positive shift from -8‰ to -2‰ at the interval from 30 to 40 m of the section where $\delta^{13}C$ values are stable (around -2‰).

In summary, none of the sections outside of the Monitor Valley section contain a positive $\delta^{13}C$ excursion reported from the Copenhagen Formation (Saltzman, 2005), where the lithological contents are also different. In addition, the $\delta^{13}C$ and $\delta^{18}O$ trends and absolute values vary from one section to another, suggesting that either localized, facies-dependent isotope variation or diagenetic alterations below a regional unconformity.

CHAPTER 5

DISCUSSION

The positive carbon isotope excursion from the late Middle Ordovician Copenhagen

Formation that underlies the Eureka Quartzite in central Nevada (Fig. 23B; Saltzman,

2005) has been hypothesized to record the initiation of the Late Ordovician climatic

transition ~10 Myr prior to the well-recognized Hirnantian glacial epoch (~443 Ma). A

particular question is whether this positive $\delta^{13}C$ excursion is a record of increased organic

carbon burial associated with a glacio-eustatic sea-level fall (Saltzman, 2005), or a facies-

dependent variation of local carbon cycling processes superimposed on the global carbon

cycle signal. Although positive isotope excursions of similar magnitude have been

documented elsewhere in epeiric and continental margin carbonate strata of the late

Middle Ordovician age (Hatch et al., 1987; Ludvigson et al., 1996; Patzkowsky et al.,

1997; Simo et al., 2003), the synchrony of these excursions still needs to be confirmed

(Fig. 5). In contrast, local carbon cycling processes have been shown to influence secular

variations (Panchuk et al., 2006) in $\delta^{13}C$, particularly during times of sea-level change

and basin restriction. During the Whiterockian Series the majority of the North American

continent was experiencing a major depositional hiatus with the exception of western

Laurentia, suggesting a period of sea-level instability, increased silicate and carbonate

exposure and weathering, and variable circulation and exchange of marginal seas with the

open ocean, which could potentially lead to development of restricted basins where local

carbon cycling could overprint the secular $\delta^{13}C$ variations of the global ocean. Therefore,

determining the geographic extent of the positive carbon isotope excursion in the Great

Basin and depositional trends across the paleo-shelf is critical for evaluating the origin of the $\delta^{13}C$ excursion documented from the Copenhagen Formation.

The absence of the positive $\delta^{13}C$ excursion below the Eureka Quartzite outside of the Copenhagen and Monitor Valley (Figs. 23 and 24) invokes two alternative interpretations: (1) the Copenhagen Formation, along with the positive $\delta^{13}C$ excursion, existed across the carbonate shelf but was later eroded during development of the basal Eureka Quartzite unconformity, leaving only a localized lithologic unit and isotope record (such as those documented from the Monitor Valley); and (2) the Copenhagen Formation and associated $\delta^{13}C$ excursion were deposited in a restricted basin where carbon cycling processes were influenced by local fault-controlled differential subsidence, which preserved the isotopic record of sea-level fall. Using the sedimentological and stratigraphic results, these interpretations are evaluated below.

If the Copenhagen Formation was deposited as a uniform stratigraphic unit but was eroded during development of the basal Eureka Quartzite unconformity, sedimentologically one would expect to see (1) a similar shallowing-upward trend from the upper Antler Valley limestone to the Copenhagen across the sections and (2) similar $\delta^{13}C$ values between the transitional facies (Facies association 2; Table 3) in measured sections (Lone Mountain, Pahranagat Range, White River Narrows and Arrow Canyon Range) and the basal Copenhagen Formation.

These expectations, however, are not satisfied with the sedimentological observations and isotope data. Sedimentologic evidence in the Monitor-Antelope Valley region (Fig. 25) indicate that the Copenhagen Formation was deposited in a restricted deep subtidal environment and the upward increase of thinly-laminated shales suggests a deepening-

upward trend. In contrast, the peritidal carbonate facies and the tidal flat carbonate and

siliciclastic (Facies associations 2 and 3) outside the Monitor-Antelope Valley region

show an overall upward-shallowing trend towards the basal Eureka Quartzite. In concert

with this discrepancy in depositional trends, chemostratigraphic data also do not support

a glacio-eustatic origin for the positive carbon isotope excursion. The absolute δ^{13}C

values from the transitional unit below the Eureka Quartzite in Lone Mountain,

Pahranagat Range, White River Narrows and Arrow Canyon Range sections vary from

one section to another, in contrast to the exclusively negative δ^{13}C values (-1.35–2.7‰)

of the lower Copenhagen Formation in the Monitor-Antelope Valley region (Saltzman,

2005). Because of the large variations in δ^{13}C below the Eureka Quartzite and the unique

δ^{18}O patterns that in most cases indicate either homogenization of δ^{18}O (e.g., Fig. 24C) or

covariation between δ^{13}C and δ^{18}O immediately below an unconformity, it is more likely

that the isotope values below the Eureka Quartzite have been significantly modified by

meteoric diagenetic alterations (Allan and Matthews, 1982). In addition, the magnitude of

a glacio-eustatic sea-level fall required to remove the Copenhagen Formation, which is >

140 m thick in the Monitor Valley (Saltzman, 2005), should exceed this amount. This

magnitude of sea-level fall is larger than that of the Hirnantian glaciation (~45 to 80 m;

Crowley and Baum, 1991; Brenchley et al. 2005) and the Last Glacial Maximum (~125

m; Denton and Hughes, 1981). Considering the widespread glacial deposits of Hirnantian

and early Holocene ages, the paucity of documented Chatfield Stage glacial deposits

globally argues against a > 140 m glacio-eustatic sea-level fall that is even larger than

Hirnantian and early Holocene, especially when considering that only a few meters of

35

erosional relief were documented at the Eureka Quartzite-Antelope Valley Limestone contact (Fig. 26).

An alternate scenario for the origin of the positive carbon isotope excursion and Copenhagen Formation requires deposition in a restricted geographic environment, much different than the typical shelf to ramp carbonate sequences representative of the upper Antelope Valley Limestone. Such environments have been shown to have significant isotopic departure from the average ocean seawater values. In the modern Florida Bay areas, the $\delta^{13}C$ values from the restricted lagoon is up to 4‰ lower than those from the carbonate platform margins (Patterson and Walter, 1994). A statistic of the global isotope trends of the last 10 million years show large isotope variations particularly from areas where circulation was sluggish (Swart, 2008). Isotope analyses from the modern lakes show up to 2.5‰ increase in $\delta^{13}C$ during the summer seasons, due to the increase of biological production and eutrophication (Hollander and McKenzie, 1991) and the limited size of the dissolved inorganic carbon (DIC) pool in a confined lake basin. Large variations up to 5‰ to 10‰ in $\delta^{13}C$ from restricted basins have also been documented from the Paleozoic and Precambrian carbonate platforms. For example, up to 4.5‰ variation in $\delta^{13}C$ was documented from the Late Ordovician Mohawkian Sea of eastern Laurentia (Panchuk et al., 2006) and up to 10‰ differences in $\delta^{13}C$ are found in the Ediacaran Doushantuo basin (Jiang et al., 2007; 2008). It is thus possible that the positive $\delta^{13}C$ excursion of the Copenhagen Formation in Monitor-Antelope Valley was derived from local carbon cycling in a restricted basin where high biological production and eutrophication led to ^{13}C-enrichment in local water bodies away from open ocean circulation.

36

The most pertinent line of evidence supporting the localized extent of the

Copenhagen Formation is the contrasting depositional environments implied by

sedimentologic evidence from the studied sections. Four sections (Fig. 25) are

characterized by shallow-water peritidal sequences represented by Facies Association 4

below the Eureka Quartzite and change dramatically in the Monitor-Antelope Valley area

into the deeper-water environment of Facies Association 3 comprising the Copenhagen

Formation. Such a lithologic change implies a distinct difference in depositional

environments over a relatively limited geographic area, and would not occur if

Copenhagen Formation deposition across the basin was uniform prior to any subsequent

erosion by the Eureka Quartzite unconformity. Additional stratigraphic evidence includes

the observation of the three informal members of the Copenhagen Formation (Cooper

1956) in the Hot Creek Range at much thinner intervals, implying a facies change across

sections rather than a prominent stratigraphic erosion/truncation at the end of the

Copenhagen Formation, as would be expected if the Copenhagen Formation was

deposited uniformly below the Eureka Quartzite.

In addition to the disparate paleoenvironmental interpretation inferred from the

lithologic record, the evolving depositional trends below the Eureka Quartzite also

support a restricted depositional setting for the Copenhagen Formation. Facies analysis

of the upper Antelope Valley Limestone in studied locations implies an upward

shallowing trend inferred from an increase of subaerially exposed lithofacies toward the

Eureka Quartzite. Conversely, the composition of the Copenhagen Formation exhibits a

gradual increase of fine-grained siliciclastic, organic-rich facies and coincident decrease

of limestone strata upward, and is here interpreted as either an increase of detrital input

into the basin resulting in a decrease of carbonate production, or a change in depositional environments resulting from differential subsidence across the basin. The Copenhagen Formation represents deep-water deposits, but it overlies shallow-water carbonate facies and is overlain by the Eureka Quartzite. This phenomenon suggests an abrupt increase in accommodation space at the beginning of the Copenhagen deposition, possibly derived from syndepositional faults.

The presence of a sequence boundary above the Copenhagen Formation, but a conformable lower contact with the Antelope Valley Limestone also suggests that this unit is not time-equivalent to the lower Eureka Quartzite. Instead, it was more likely to have deposited prior to the transgression that deposited the Eureka Quartzite. Although this observation does not exclude either of the localized deposition or glacio-eustatic interpretations for the origin of the Copenhagen Formation, when considered in the context of depositional trends across the platform, it seems more plausible that the sequence boundary above the Copenhagen Formation in Antler-Monitor Valley region should coincide with subaerial exposure at the top of the Antelope Valley Limestone in other sections.

During the late Middle Ordovician period it is believed that the Earth's climatic change initiated the geochemical perturbations that could have been a pre-cursor to the well-established but short-lived Hirnantian glacial epoch. Positive $\delta^{13}C$ excursions documented prior to the glaciation could represent an earlier episode of glaciation, or a prolonged, cooling trend highlighted by local excursions in $\delta^{13}C$ prior to the Hirnantian glacial epoch. If our sedimentologic analysis is correct the $\delta^{13}C$ excursion in the

Copenhagen Formation could represent a localized proxy record of glacio-eustasy across

the paleo-shelf that was not exposed or eroded as a result of fault-controlled subsidence.

CHAPTER 6

SUMMARY

Sedimentologic analysis of strata directly below the Eureka Quartzite indicates a geographically limited depositional extent of the Copenhagen Formation. This interpretation is supported by several lines of evidence including: 1) a shallowing-upward trend in studied sections of the Pahranagat Range, White River Narrows, Arrow Canyon Range, and at Lone Mountain; 2) progressively deeper depositional environments comprising the middle and upper Members B and C of the Copenhagen Formation, as other sections experienced exposure and erosion, and; 3) contrasting depositional environments between the Monitor-Antelope Valley area and locations to the north and south. This interpretation is strengthened by the presence of a sequence boundary above the Copenhagen Formation and Antelope Valley Limestone across the study area, indicating both units were deposited concurrently and prior to the transgressive Eureka Quartzite. The gradual thinning of members of the Copenhagen Formation in the Hot Creek Range just south of the Monitor-Antelope Valley area, rather than attaining a uniform thickness also suggests a facies change across the paleo-shelf. Transition of facies from shallow-to-deep water environments is explained by an inferred listric fault located between the Lone Mountain and Copenhagen Canyon sections consistent with a localized deepening trend as the footwall subsided throughout deposition of the Copenhagen Formation. Isotopic analysis of the upper Antelope Valley Limestone suggests the presence of an exposure surface above both the Copenhagen Formation and Antelope Valley Limestone. Coupled with the magnitude of documented erosional relief of approximately 6 meters at the sequence boundary, it is likely the two stratigraphic

units are regressive, with the Copenhagen Formation being deposited in a fault-controlled

basin during exposure of the upper Antelope Valley Limestone southward and at Lone

Mountain.

FIGURES
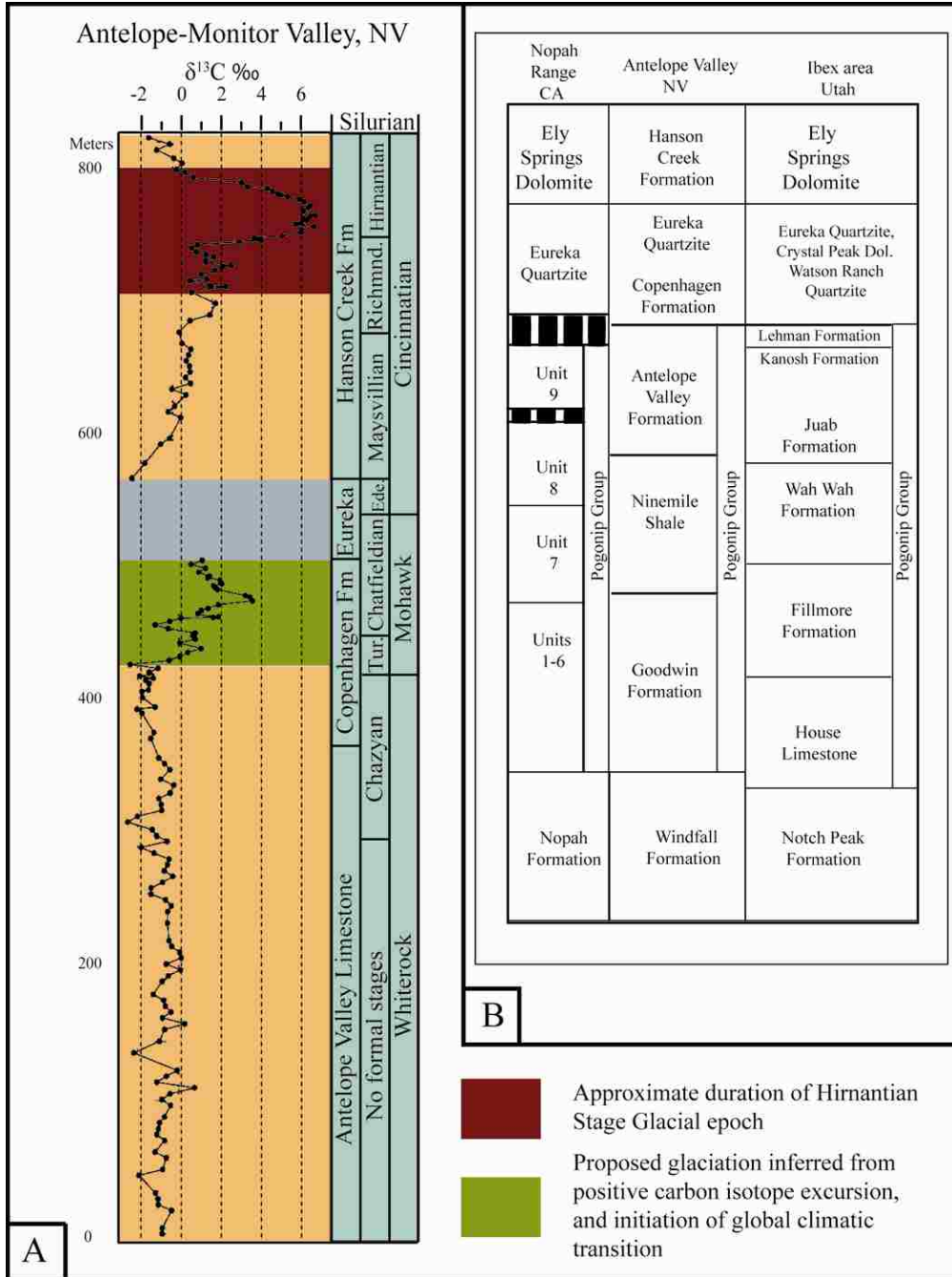
Figure 1. Isotopic excursions and stratigraphy of Late Ordovician strata. **A**. Carbon isotope excursions and inferred climatic variation during the Middle and Late Ordovician period. The positive excursion occurring in the Hirnantian Stage is preceded by a similar, yet smaller isotope enrichment in the Chatfield Stage, suggesting a climatic transition from greenhouse-to-icehouse conditions approximately 10 million years earlier. **B**. Stratigraphic correlation of key units in the southwestern United States. The absence of the Copenhagen Formation outside of Antelope Valley, NV raises doubt about the origin and extent of the isotopic excursion.
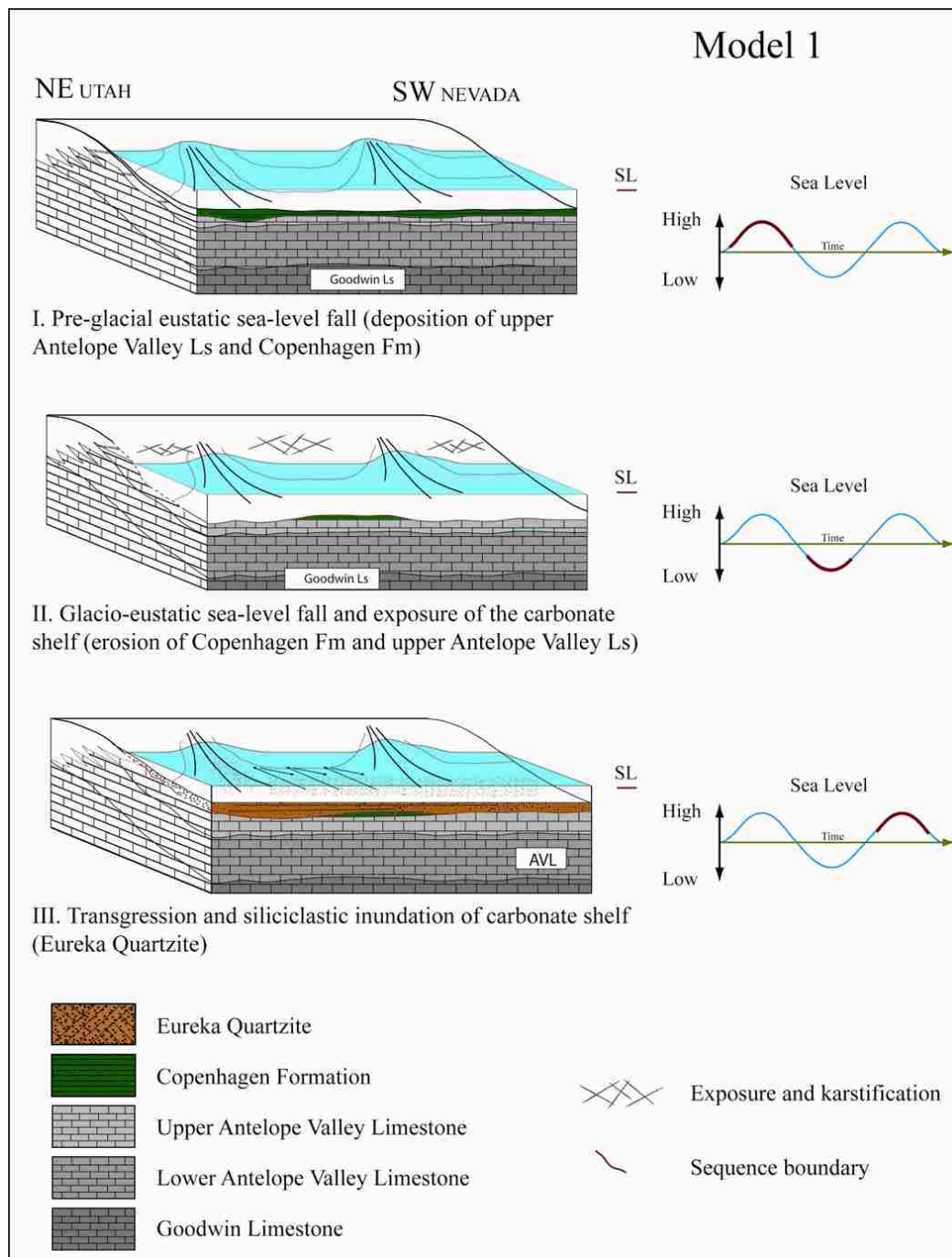
Figure 2. Hypothetical Model 1. This model depicts uniform deposition of the Copenhagen Formation across the paleo-shelf. This interpretation attributes the absence of the Copenhagen Formation to base-level fall and subsequent erosion, and karstification of the underlying Antelope Valley Limestone at the sequence boundary below the Eureka Quartzite.
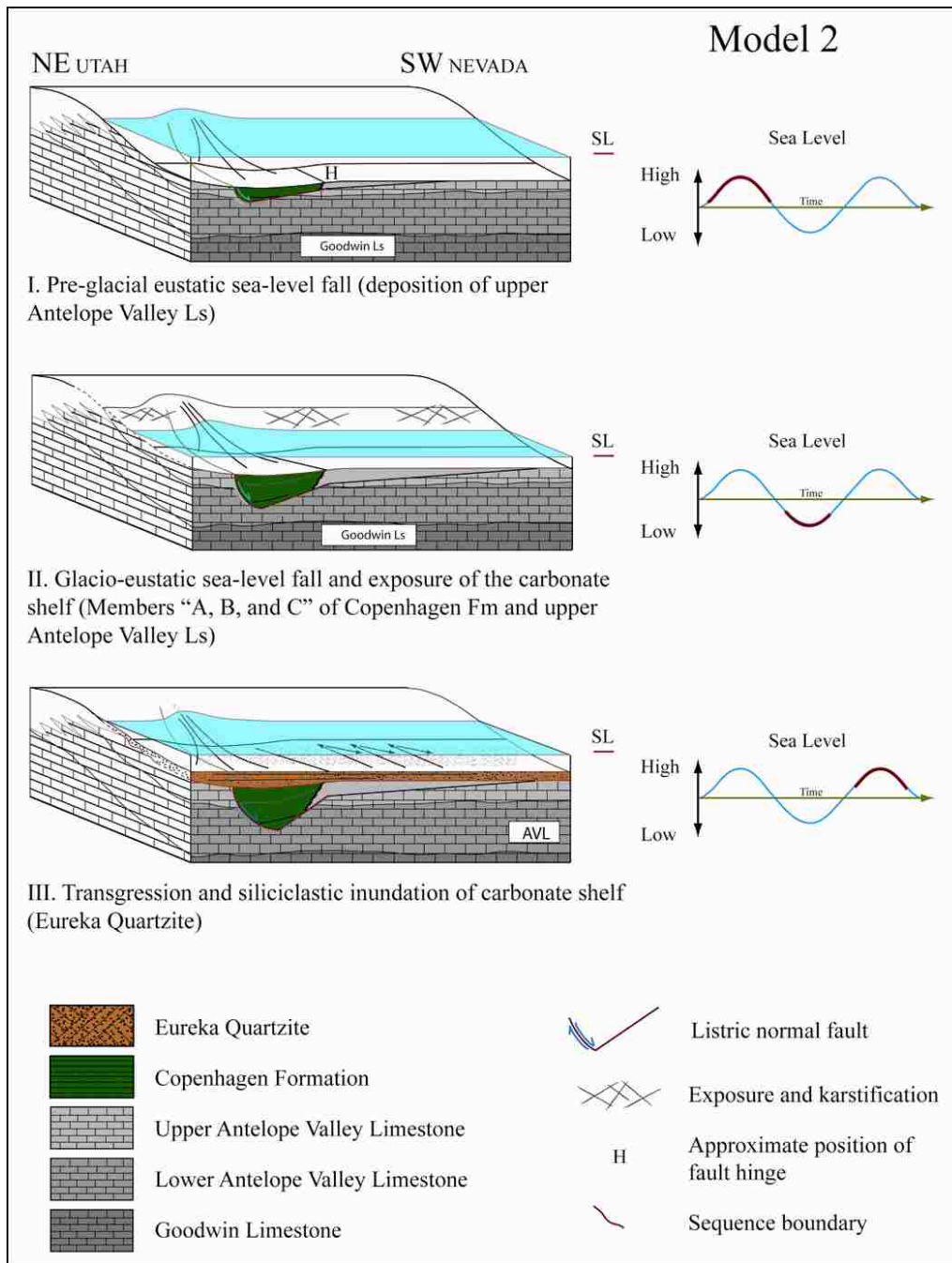
Figure 3. Hypothetical Model 2. This model depicts fault-controlled deposition of the Copenhagen Formation across the paleo-shelf. This interpretation implies the Copenhagen Formation was deposited in a fault-bounded basin coinciding with base-level fall, culminating at the sequence boundary below the Eureka Quartzite.
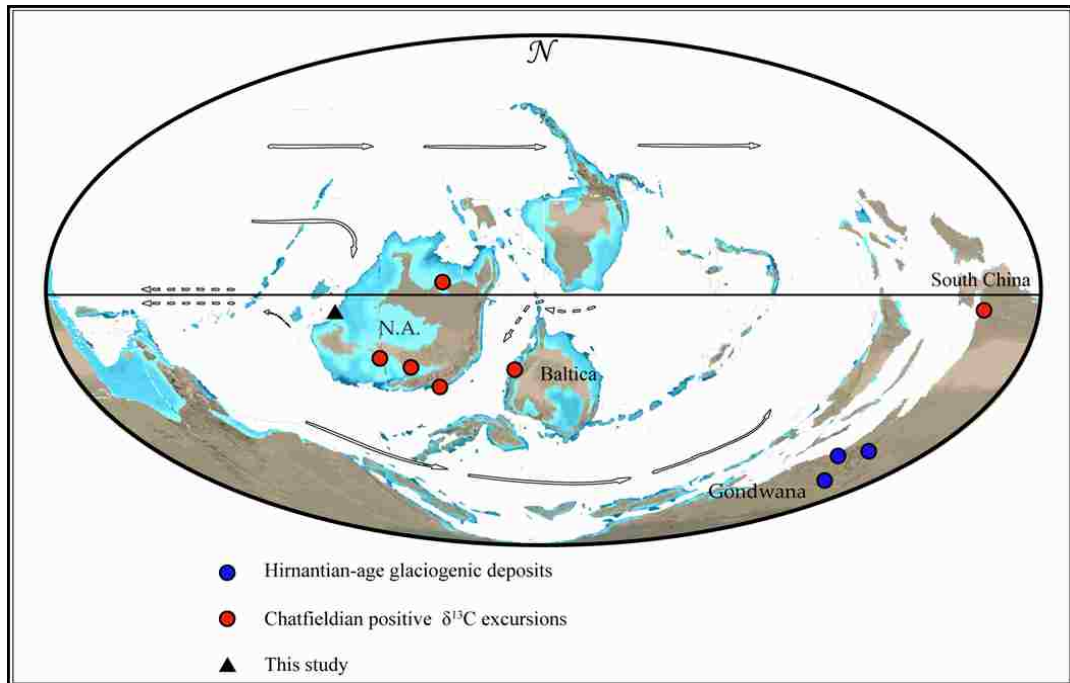
Figure 4. Paleogeographic reconstruction of land masses during the Middle Ordovician period. Isotopic excursions in literature are documented from shallow-marine carbonate strata, within 10-15° of the inferred paleogeographic equator. Figure modified from R. Blakey's paleogeographic globes.

SERIES			STAGES		AGE	LITHOSTRATIGRAPHY		
GLOBAL	BRITISH	N. AMER.	N. AM.	BRITISH	M.Y.	Western NA	Iowa/Missouri	Eastern App.
ORDOVICIAN LATE / MIDDLE	ASHGILL	CINCINNATI.	MAYVILLE EDEN.	Hirnantian / Rawtheyan / Cautleyan / Pusgillian / Streffordian	443.7	ELY SPRINGS DOLOMITE / EUREKA QUARTZITE	Guttenberg Limestone	Cincinnatian Shaley Carbonates
	CARADOC	MOHAWK.	CHATFIELD.	Cheneyan / Burrellian / Aurelucian		ANTELOPE VALLEY LIMESTONE	Specht's Ferry Formation / Quimby's Mill Formation	Lexington Limestone / Tyrone Limestone
	LLAN-VIRN	WHITEROCK.	CHAZY.	Llandelian / Aberiddian	460.9			
	ARENIG		Undefined	Fennian				
		IBEX			471.8			

Figure 5. Correlation of North American and British Stages and Series, and corresponding stratigraphic units in North America. Lithostratigraphic units correspond to deposition during the Copenhagen Formation.
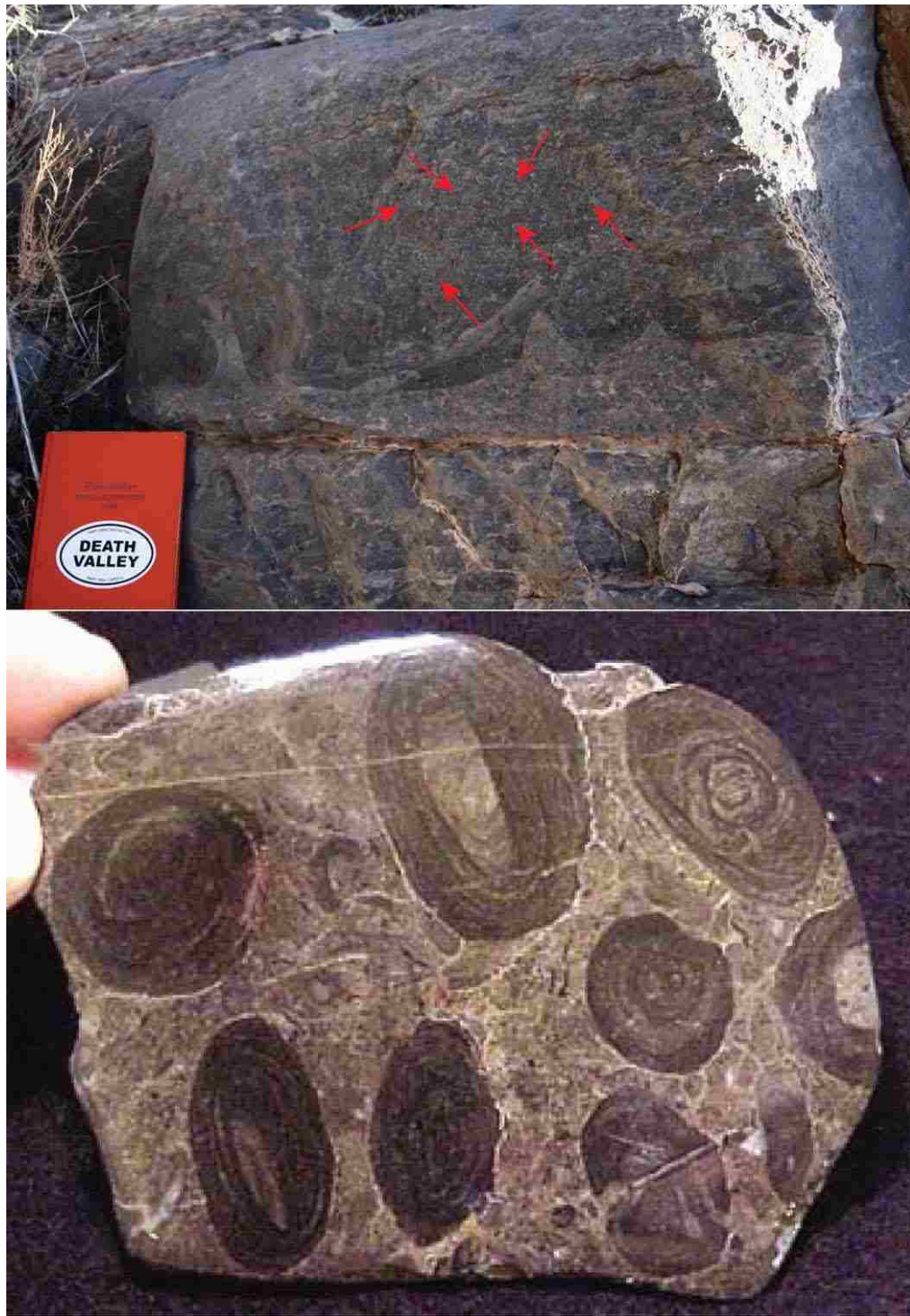
Figure 6. *Girvanella*-algae preserved in carbonate strata of the Great Basin. This diagnostic stratigraphic unit was used to correlate sections across the field area, and demarcated the oldest studied member of the Antelope Valley Limestone.
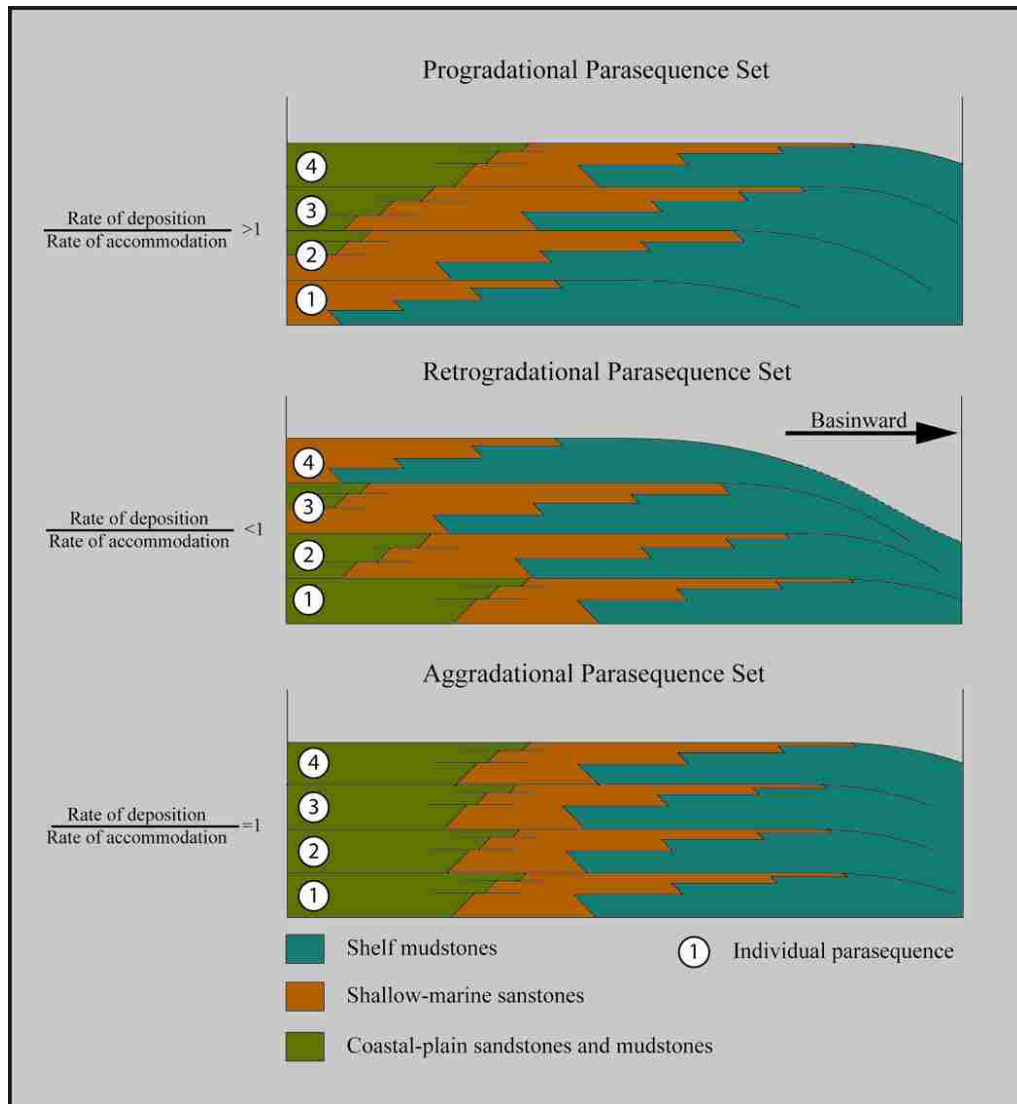
Figure 7. Parasequence set stacking patterns. The vertical variation of parasequence sets enables evaluation of base level fluctuation and sedimentation rates relative to the strandline. Modified from Van Wagoner et al., 1988.
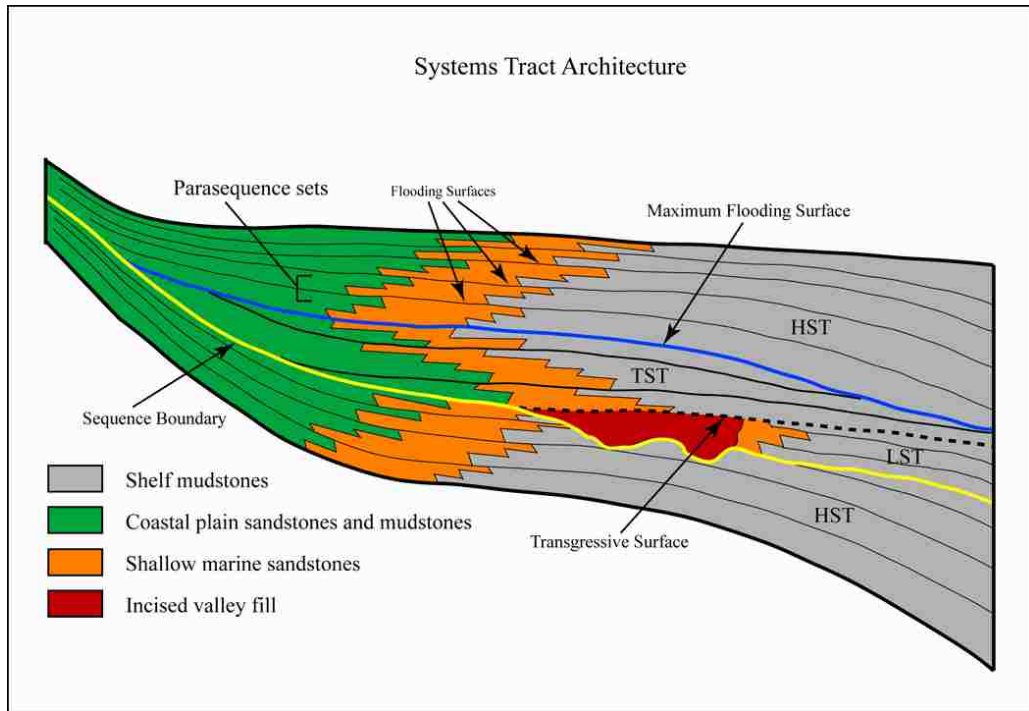
Figure 8. Systems tract architecture. Depositional sequence hierarchy comprising one transgressive-regressive cycle. Modified from Van Wagoner et al., 1990.
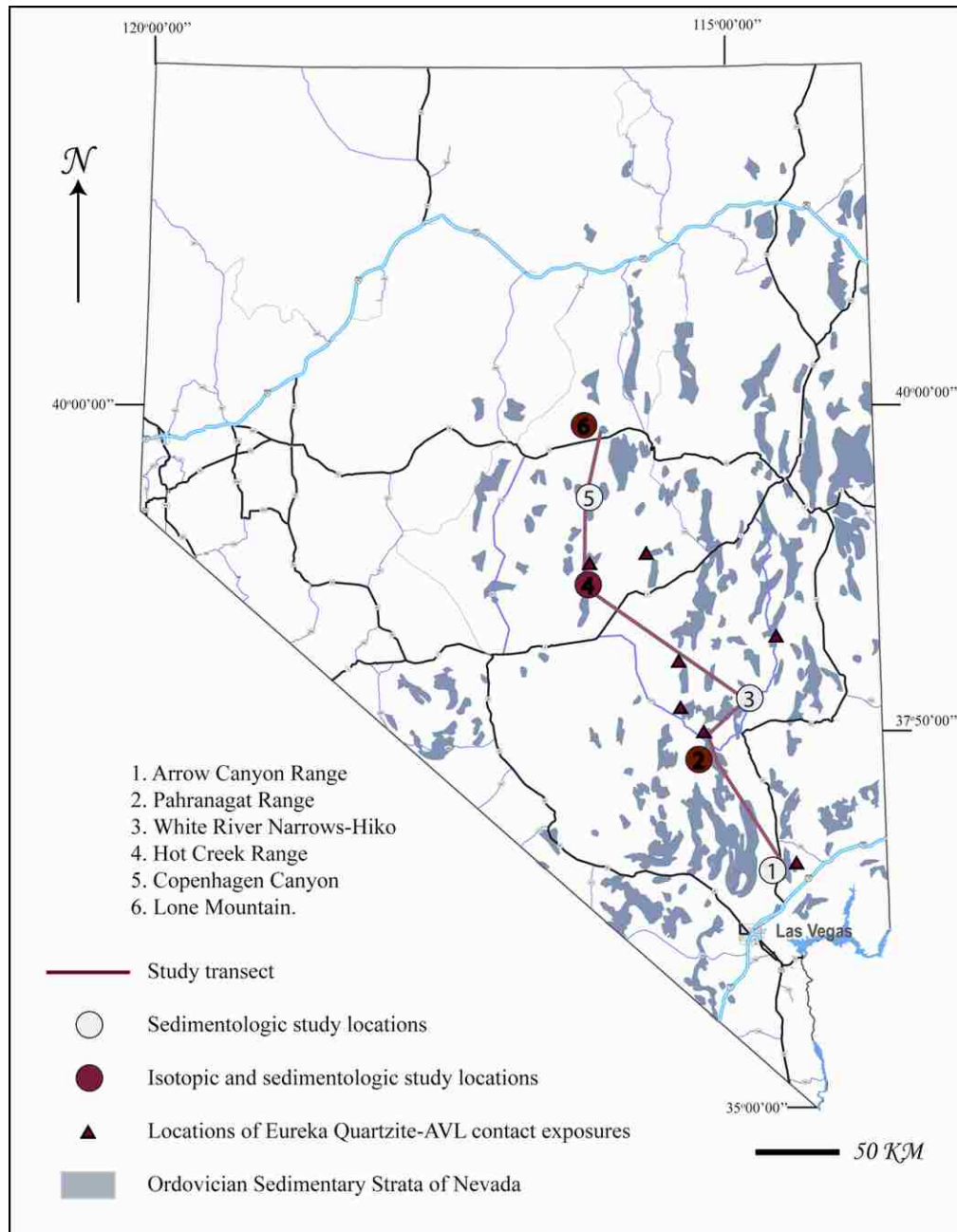
Figure 9. Site location map of studied sections in Nevada.

50
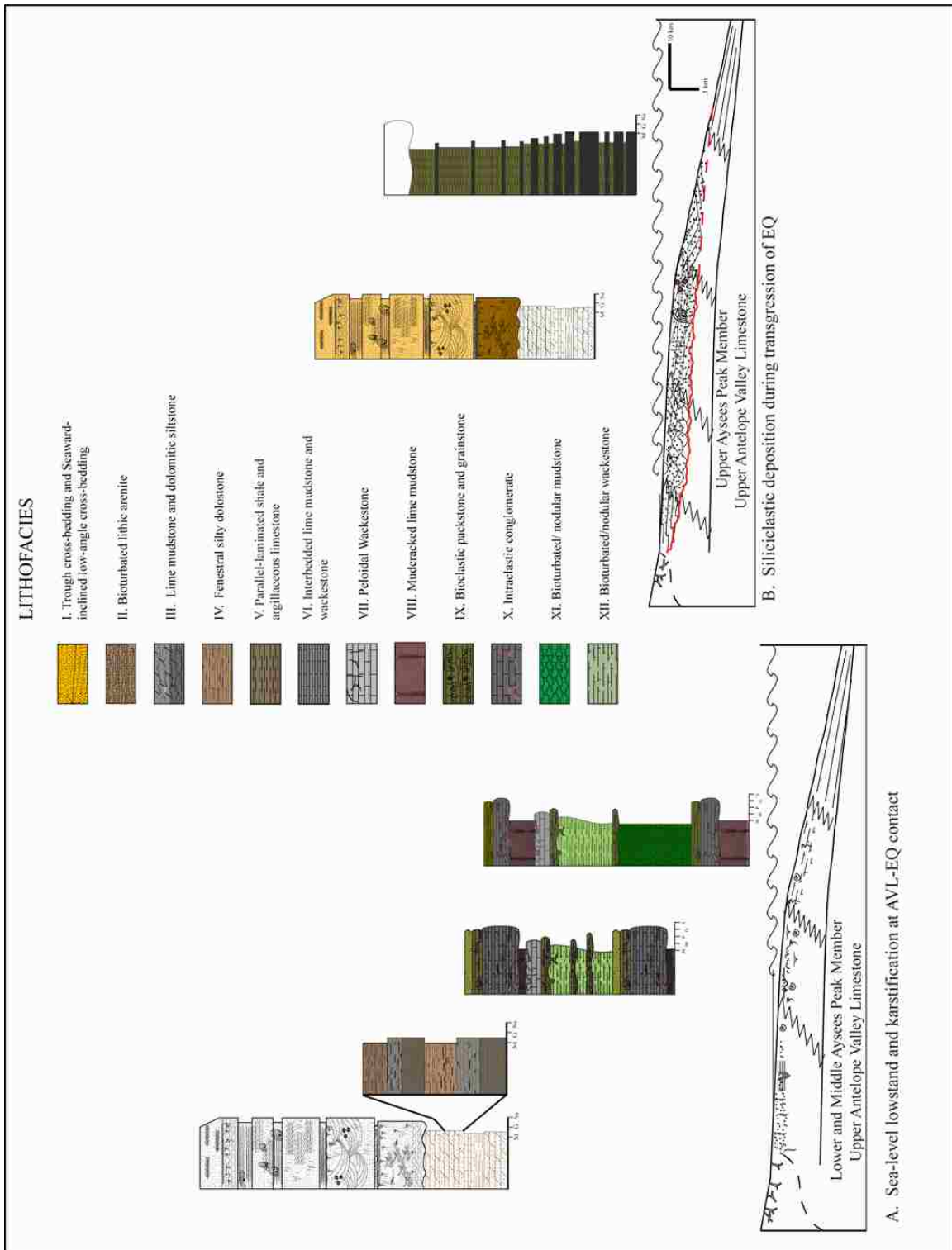
Figure 10. Paleoenvironmental reconstruction of sequences. Lithofacies of the upper Antelope Valley Limestone, Copenhagen Formation and Eureka Quartzite. Reconstructed depositional environments and their relative position on a shoreline to basin transect inferred from vertical facies variation.
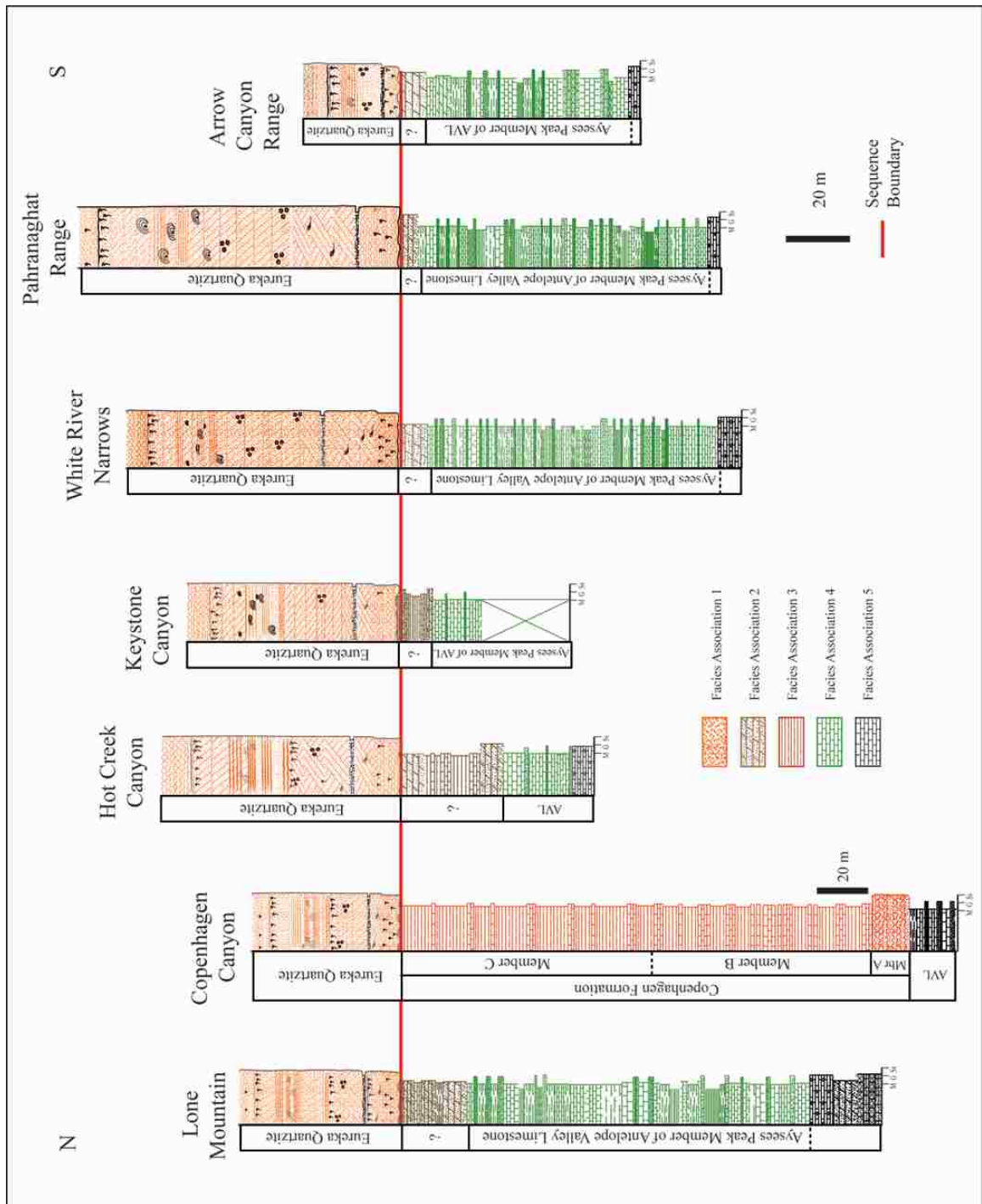
Figure 11. Lithostratigraphic correlation of facies across study area showing position of sequence boundary and *Girvanella*-rich member of the Antelope Valley Limestone.

52
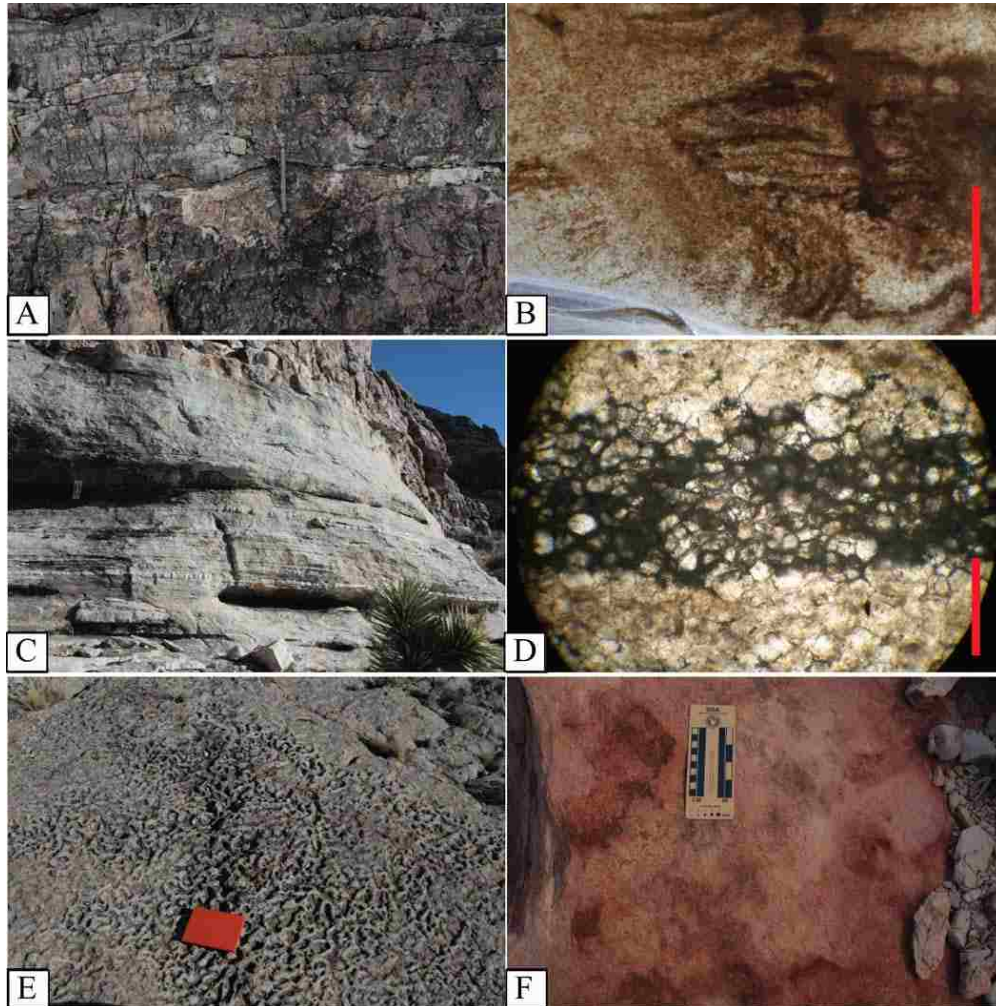
Figure 12. Lithofacies comprising Facies Association 1. **A.** Bioturbated lithic arenite lithofacies of the lower Eureka Quartzite. **B**. Vermiform mud and silt-infilled burrows disrupting bedding surfaces in lithic arenite lithofacies of the lower Eureka Quartzite. Scale bar is 1.2 cm. **C.** Silt and fine sand comprising algal laminated interval in upper Eureka Quartzite. **D.** Thin-section depicting laminated silt and fine sand representing alternating algae-growth and sedimentation. Scale bar is 1mm. **E, F.** *Calianassa*-type burrows representing low-energy deposition within upper Eureka Quartzite.
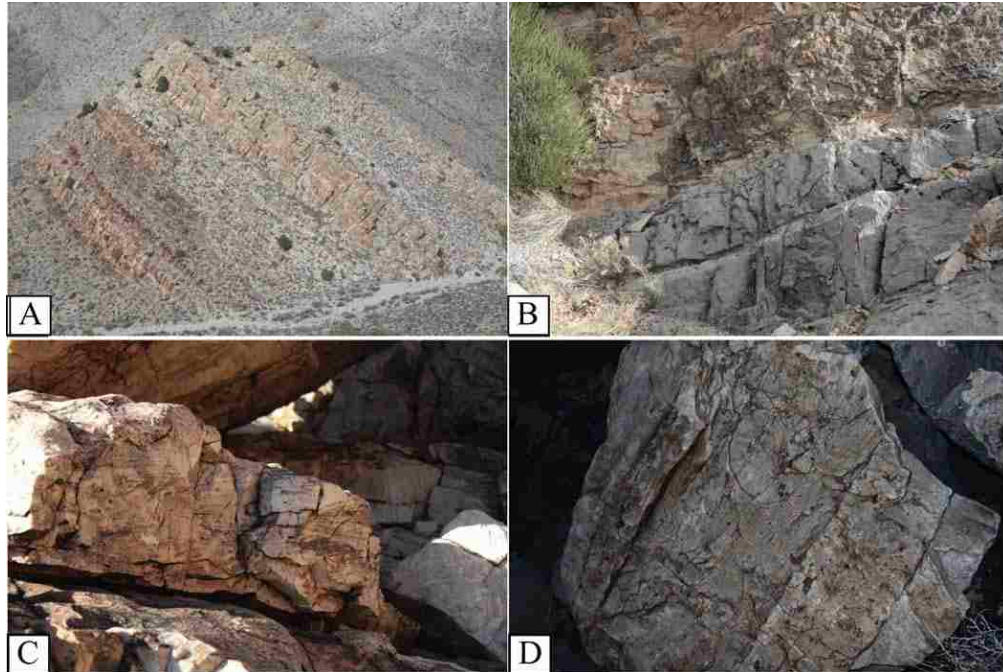
Figure 13. Field photographs of Facies Association 1. **A**. Eureka Quartzite exposed at Pahranagat Range showing upper and lower lithofacies. EQ is 88 meters thick. **B**. Contact of lower bioturbated lithic arenite lithofacies and transitional siliciclastic-carbonate lithofacies. **C, D**. Upper lithofacies consisting of well-sorted, silica-cemented quartz arenite.
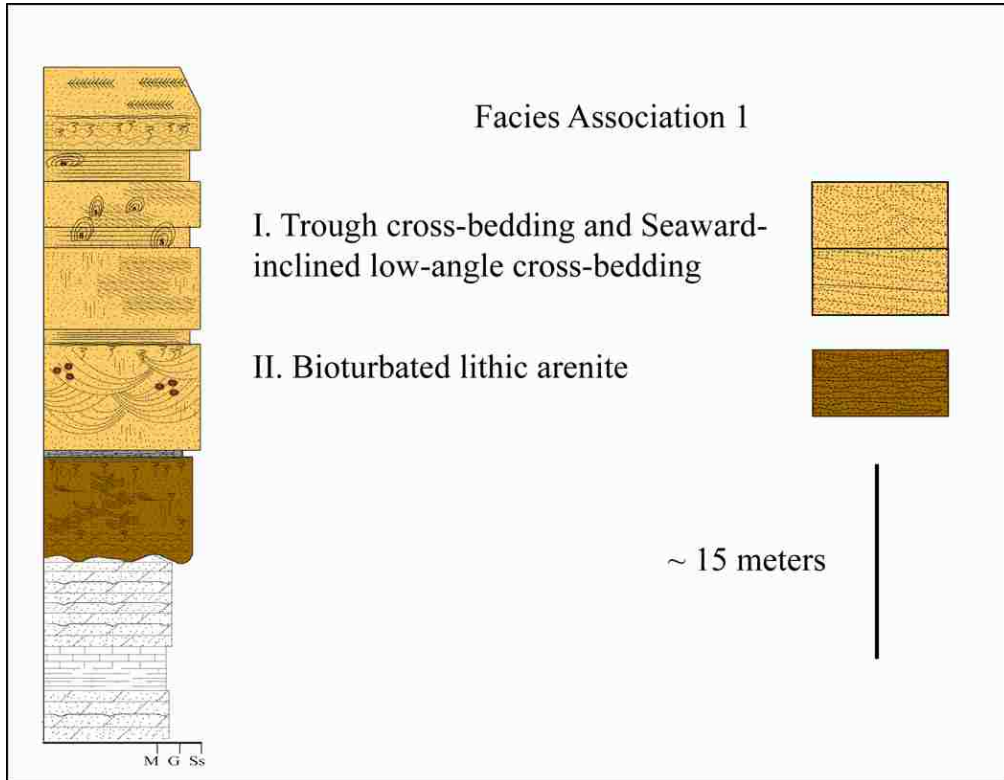
Figure 14. Interpretation of Facies Association 1. Lithofacies comprising the Eureka Quartzite and upper Copenhagen Formation age-equivalent strata outside of the Monitor-Antelope Valley region.
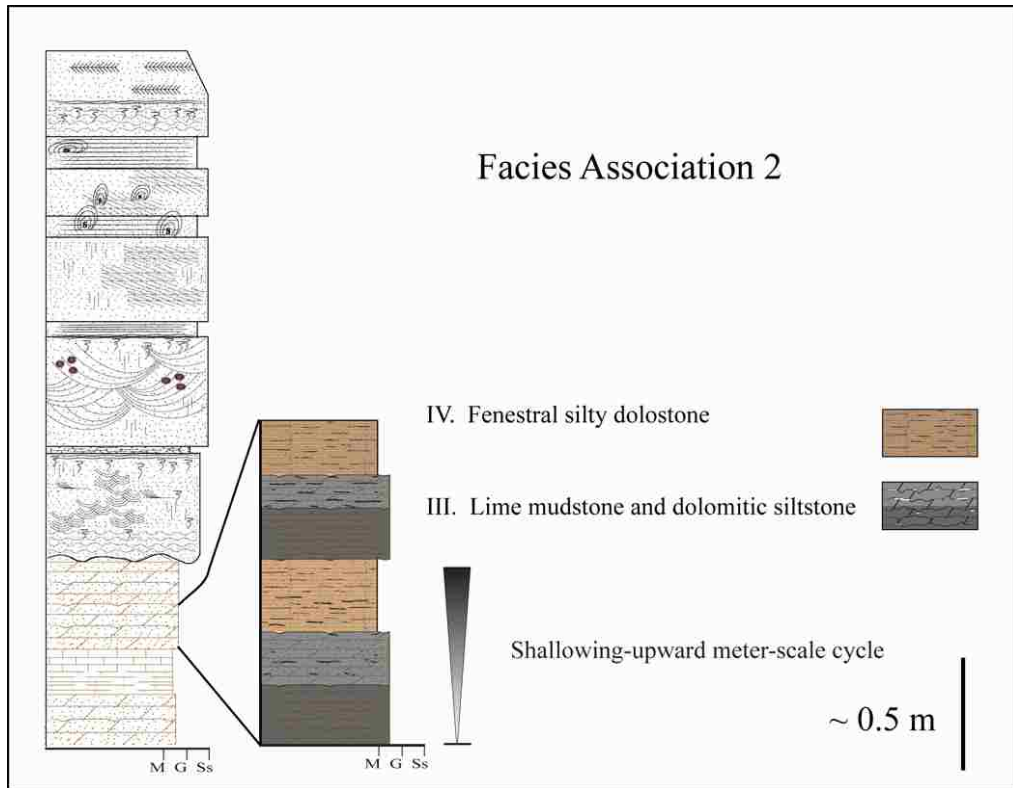
Figure 15. Interpretation of Facies Association 2. Lithofacies comprise the transitional interval between the pure carbonate cycles of the Upper Antelope Valley Limestone and the silica-rich Eureka Quartzite.
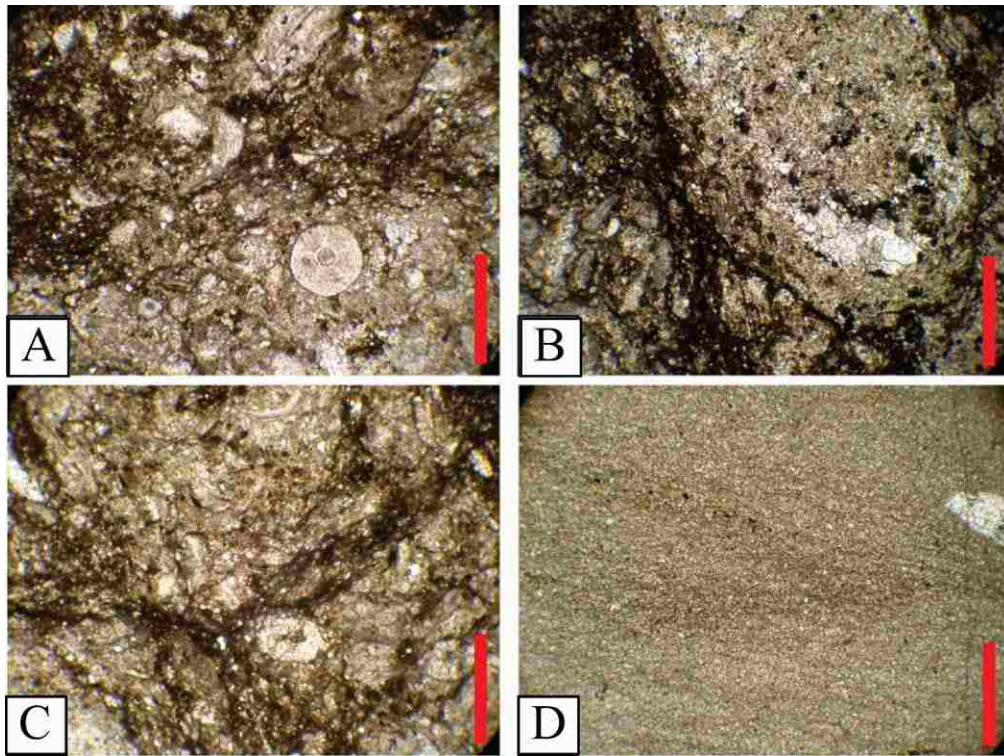
Figure 16. Thin-section photographs of Facies Association 3. **A, C.** Lime mudstone and wackestone lithofacies comprising middle to upper Copenhagen Formation. **B.** Burrows commonly exhibit lower amount of mud and silt than surrounding matrix. **D.** Parallel-laminated shale and mudstone of the upper Copenhagen Formation.
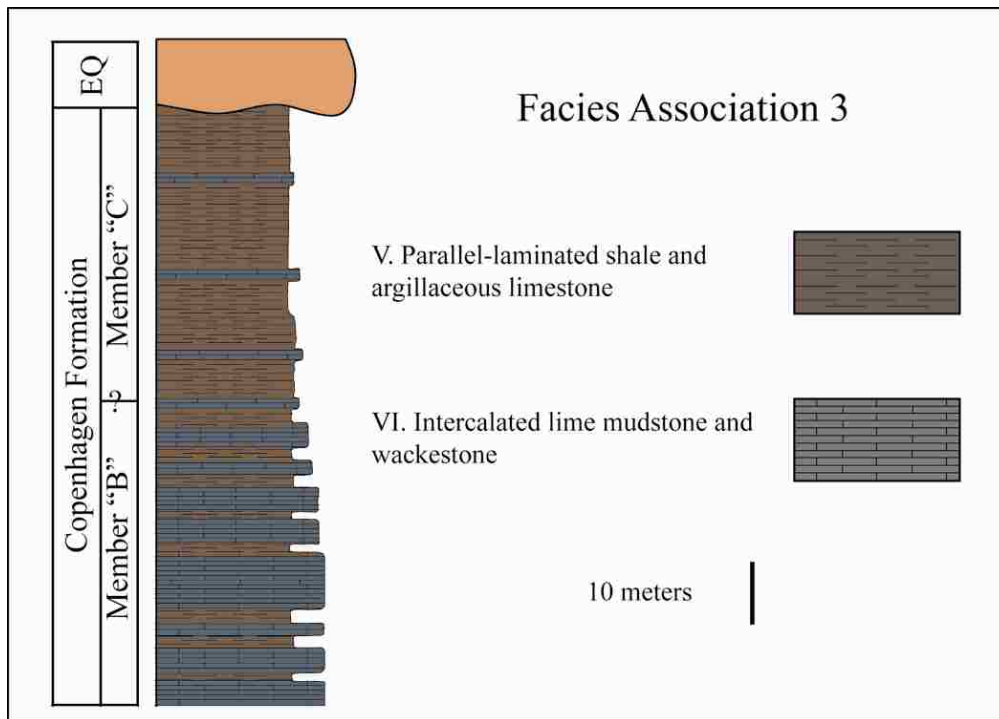
Figure 17. Interpretation of Facies Association 3. Lithofacies comprising upper members "B and C" of Copenhagen Formation in the Monitor-Antelope Valley area, and unconformable contact with the overlying Eureka Quartzite.
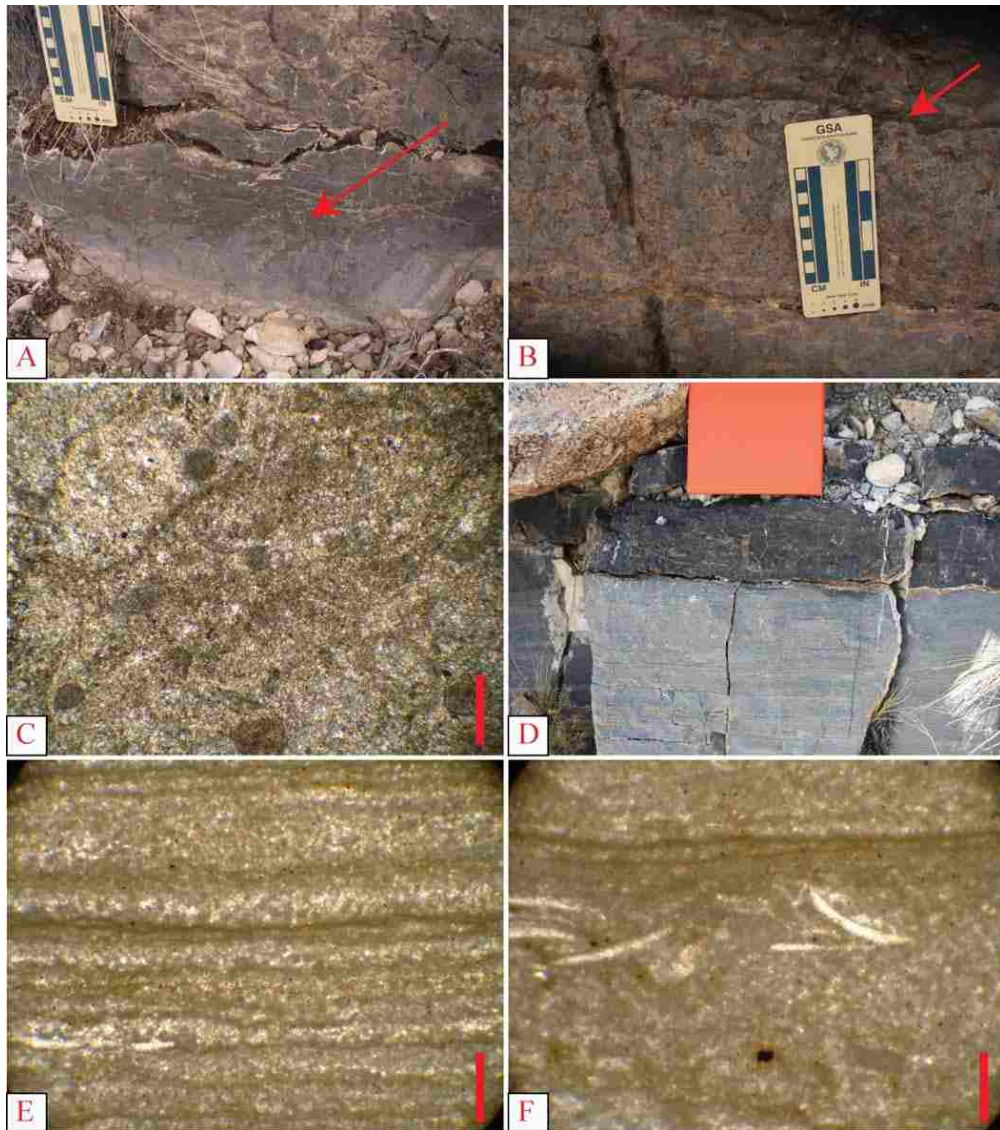
Figure 18. Field and thin-section photographs of Facies Association 4. **A, B.** Peloidal wackestone lithofacies exhibiting irregular upper contact with Intraclast conglomerate lithofacies. **C**. Thin-section of peloidal wackestone. **D**. Mudcracked lime mudstone and intraclast conglomerate contact. **E,F**. Mudcracked lime mudstone thin-sections. Scale bar is 1.2 mm.
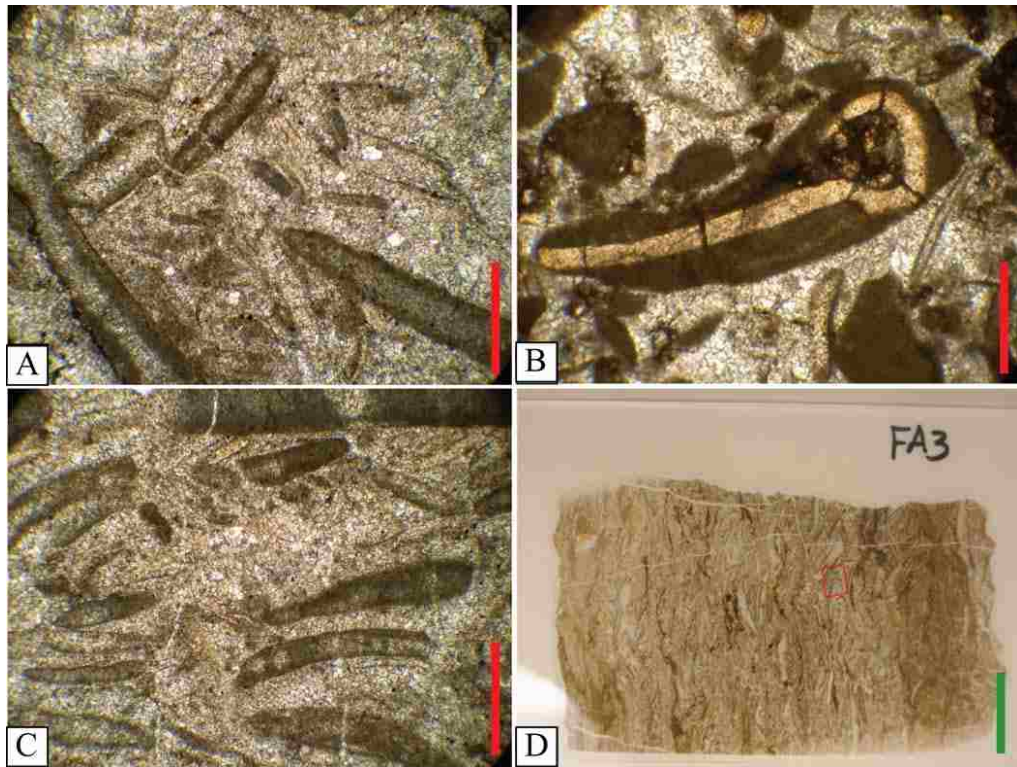
Figure 19. Bioclastic packstone and wackestone lithofacies. Scale bar is 1.2 mm in **A,B,C**, and 1.4 cm in **D**.
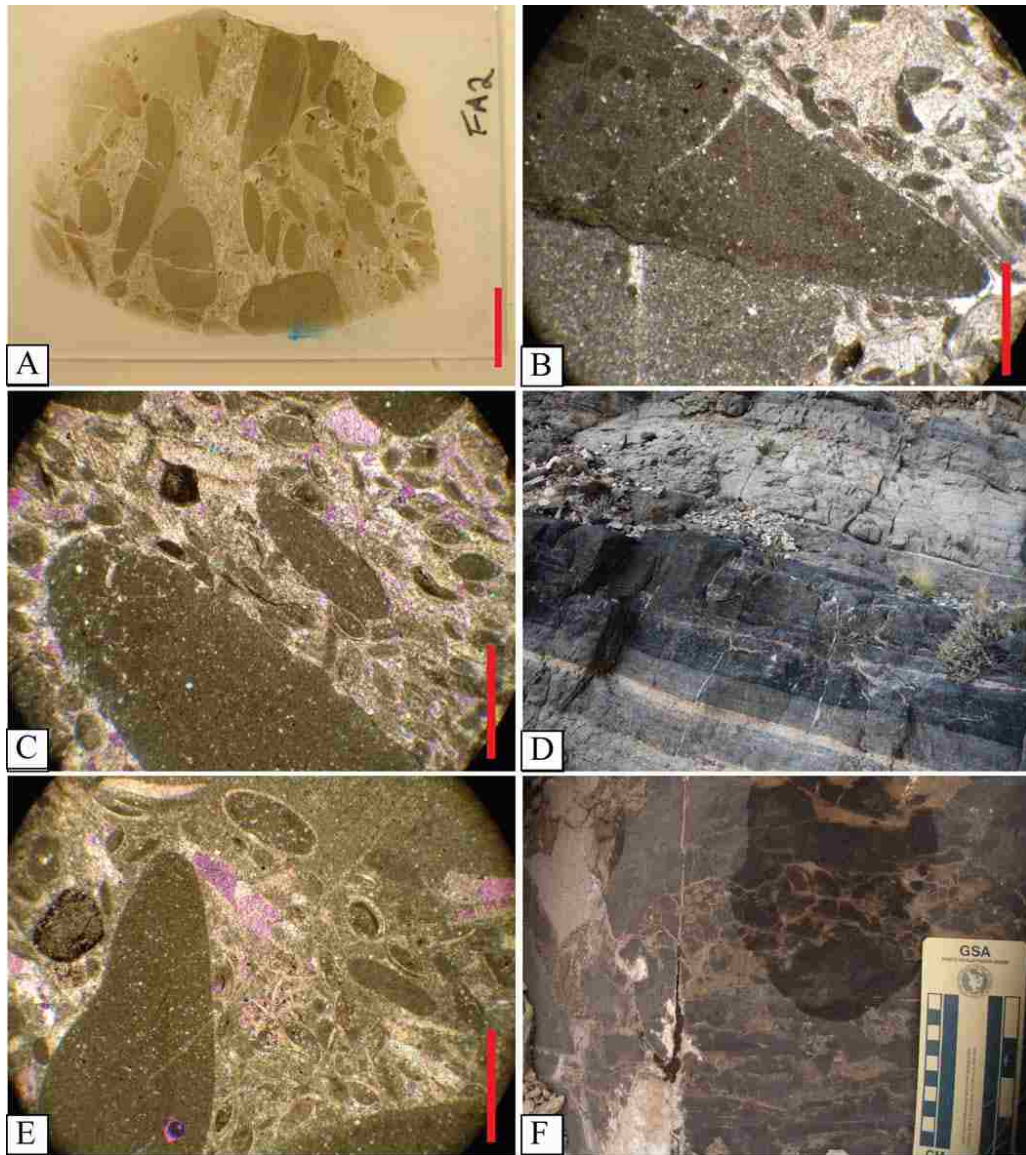
Figure 20. Intraclast conglomerate lithofacies. **A**. Thin-section of representative sample. **B, C, E**. Thin-sections of laminated clasts within a packstone to grainstone matrix. **D**. Field exposures of intraclast facies overlying intertidal limestone facies in Arrow Canyon Range. **F**. Brecciated interval in Intraclast facies in the Pahranagat Range.
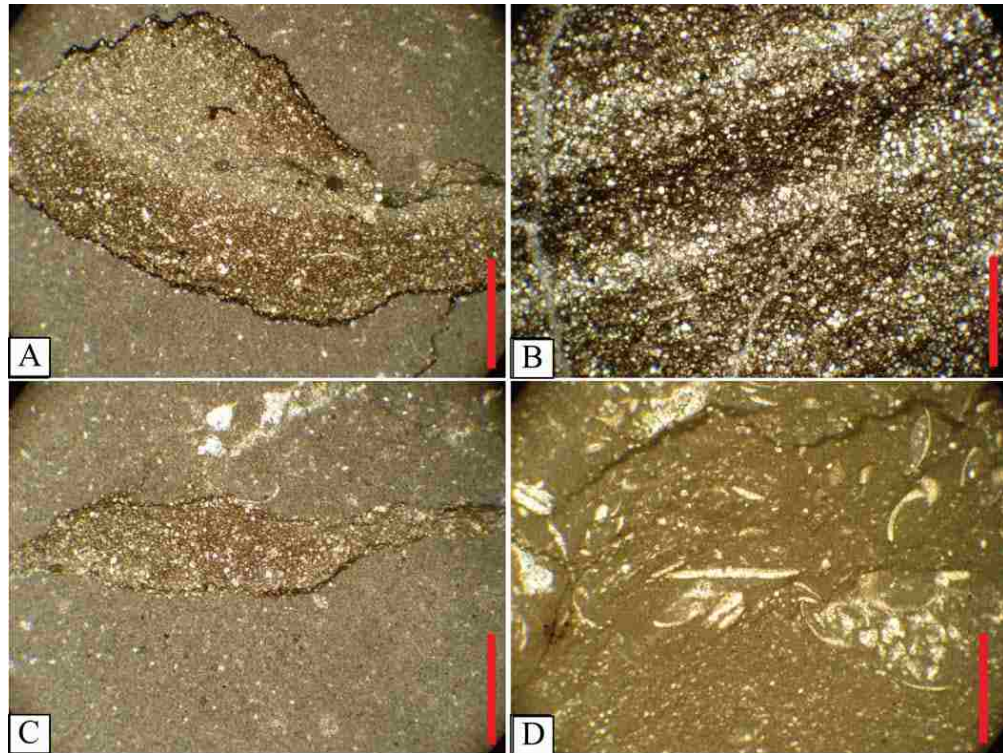
Figure 21. Thin-section photographs of Copenhagen Formation lithofacies. Bioturbated mudstone and wackestone lithofacies. **A, C, D**. Thin-sections show dolomitized silty laminae, with close-up of laminae in **C**. Scale bar is 1.2 mm in **A, C**, and **D**; 2mm in **B**.
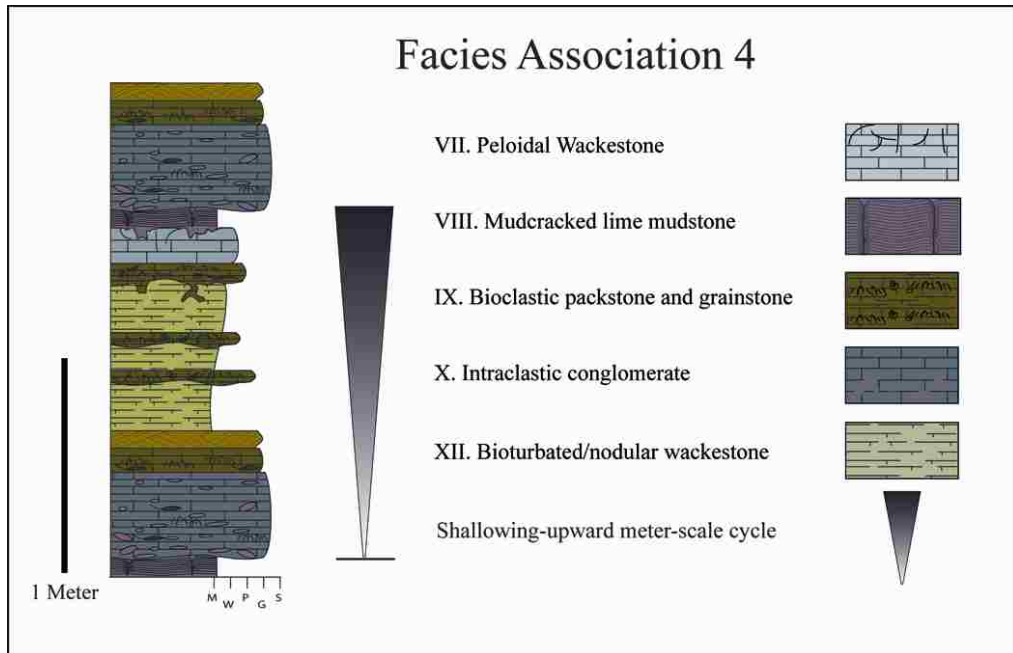
Figure 22. Lithofacies comprising peritidal carbonate cycles of Facies Association 4. Idealized cycles are commonly not observed in outcrop; reconstructed vertical arrangement is based on stratal order of several documented cycles from White River Narrows and Pahranagat Range sections. Arrow Canyon cycles contain coarser clastic carbonate lithology, thinner cycles, and less lithologic variation.
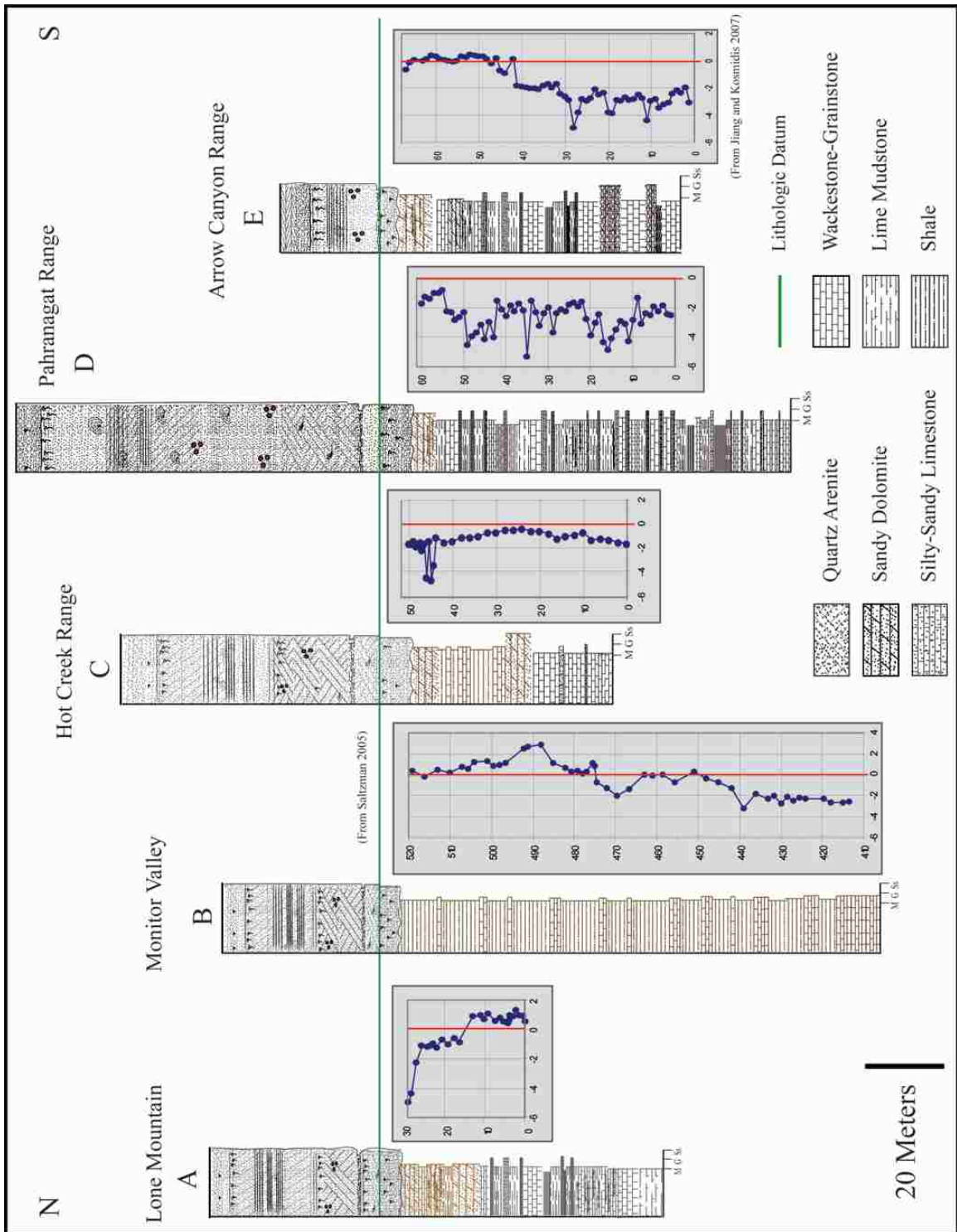
Figure 23. Carbon isotope chemostratigraphy of upper Antelope Valley Limestone. Green line represents most consistent lithologic datum throughout studied sections.
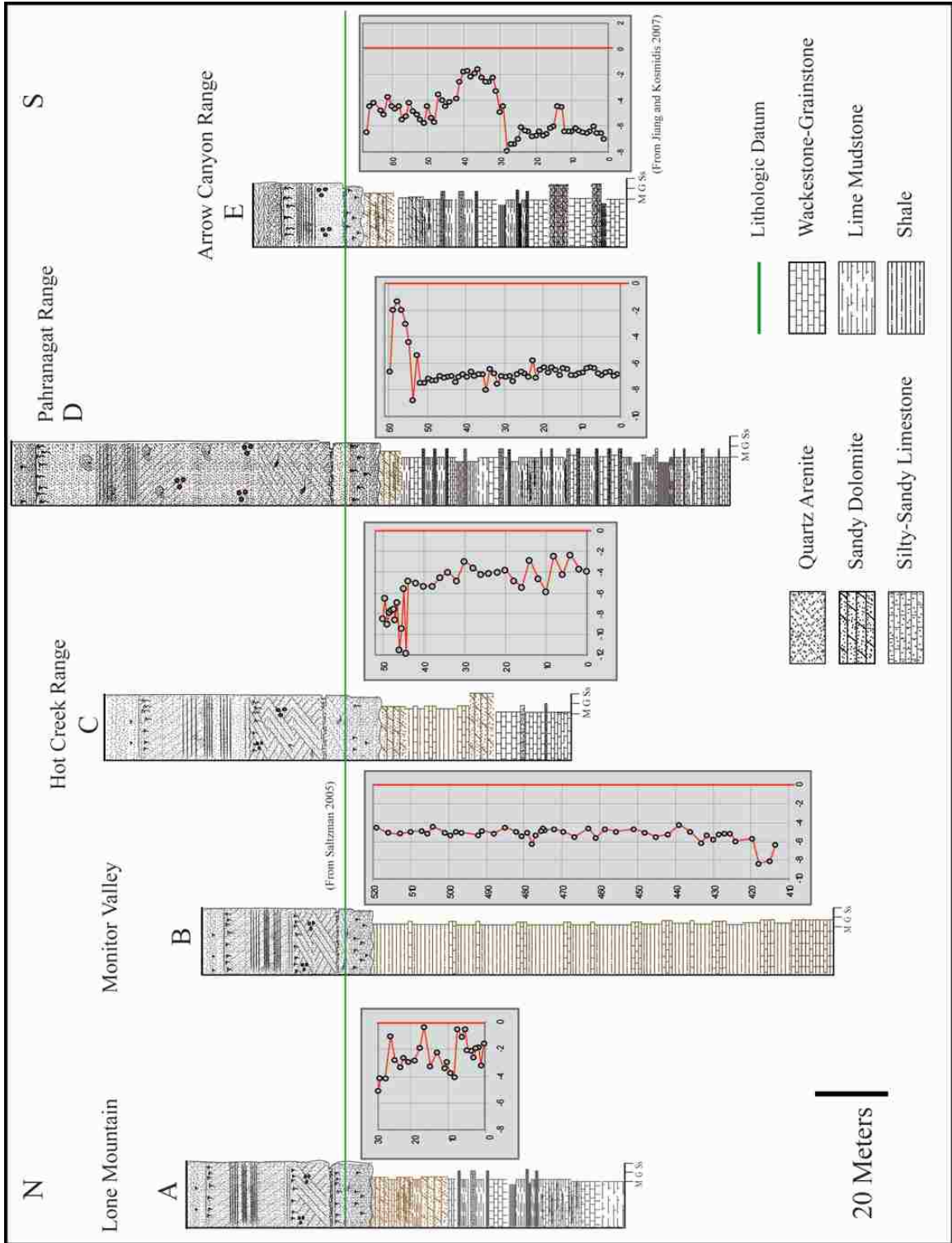
Figure 24. Oxygen isotope chemostratigraphy of upper Antelope Valley Limestone. Green line represents most consistent lithologic datum throughout studied sections.
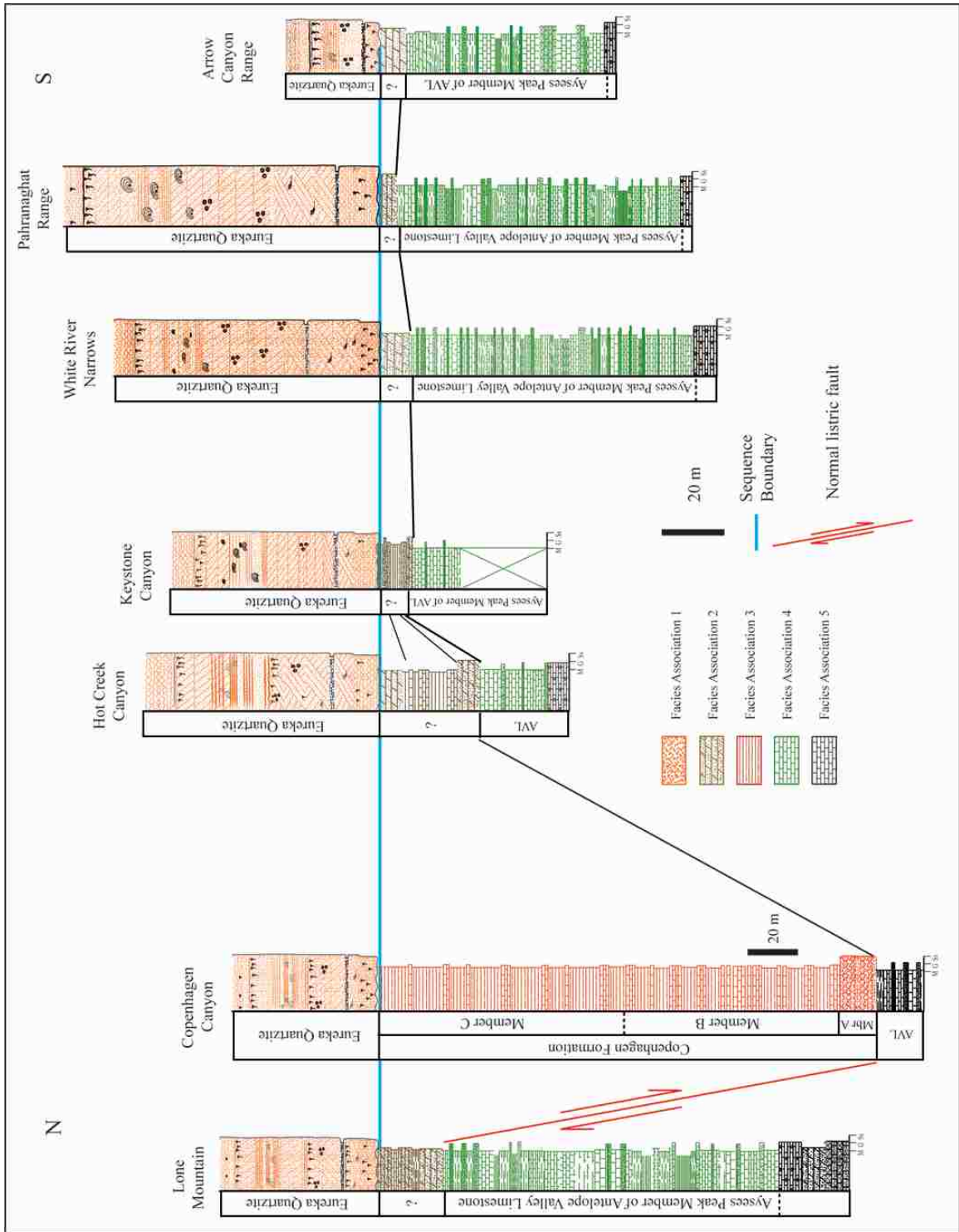
Figure 25. Sequence stratigraphic and chemostratigraphic results. The presence of a listric fault between the Lone Mountain and Copenhagen Canyon sections is inferred from the abrupt change in lithofacies between these two locations, and the gradual change and thinning of traceable lithofacies southward.
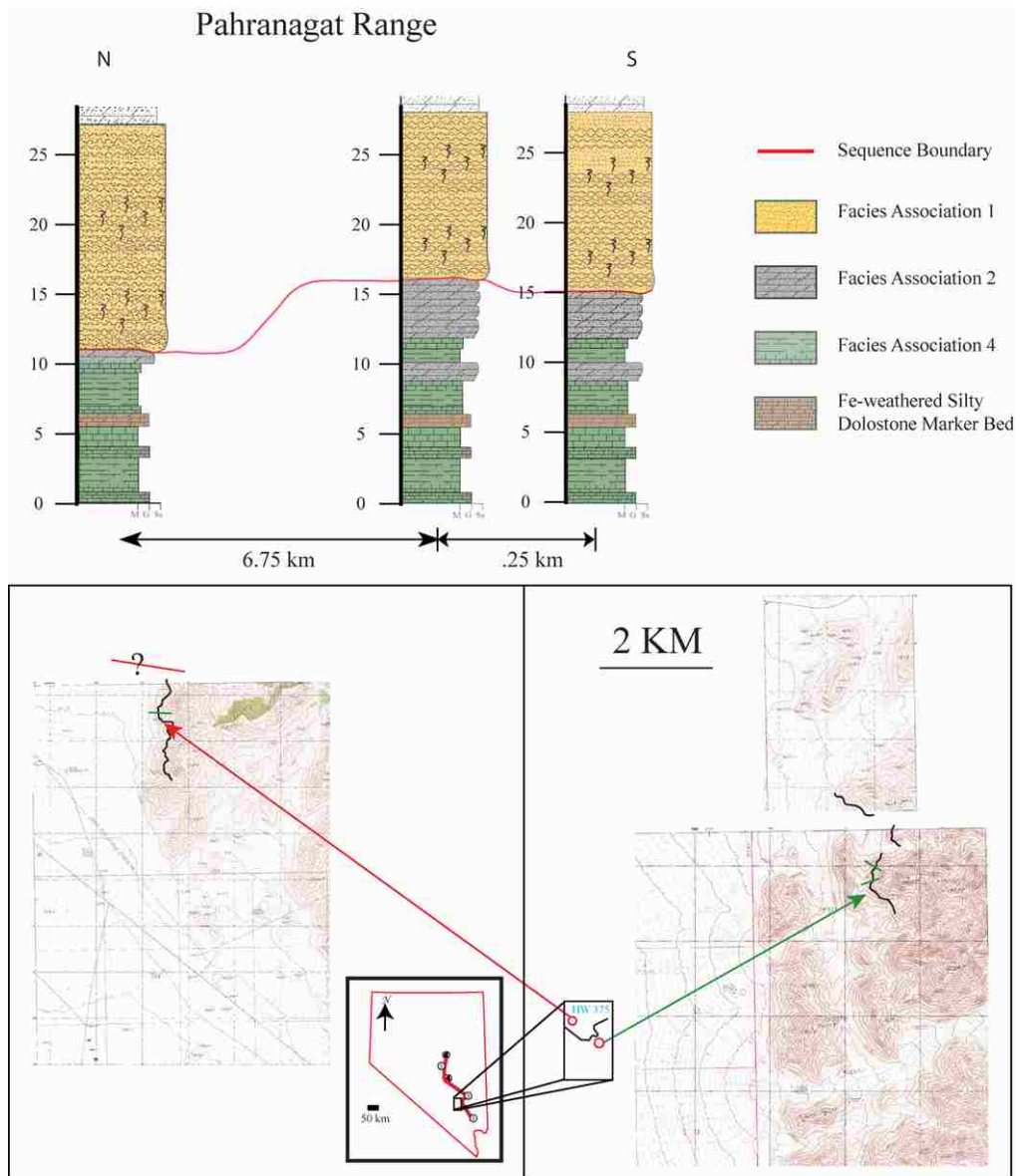
Figure 26. Erosional relief at sequence boundary. Erosion encompassed by unconformity at Eureka Quartzite-Antelope Valley Limestone at Pahranagat Range.

TABLES

Table 1

Table 1.
Whiterock Series fossil sub-zone assemblages compiled from Great Basin ranges. (From Ross et al., 1991).

	Corals	Trilobites	Graptolites	Brachiopods
Lichenaria-Oepikina Zone (Zone O)	• *Lichenaria* spp. • *Eofletcheria* sp.		• *Hustedograptus* *teretiusculus* Zone	• *Oepikina* sp. • *Macrocoelia* sp.
Upper Anomalorthis Zone (Zones M and N) Lower		• *Pseudoolenoides acicaudus* • *Bathyurus extans* • *Pseudomera barrandei* • *Basilicus mckeei* • *Pseudoolenoides dilectus* • *Pseudomera barrandei*		• *Desmosrthis* *nevadensis* • *Anomalorthis* *lonensis* • *Anomalorthis* *oklahomensis* • *Anomalorthis* *fascicostellatus* • *Anomalorthis* *lonensis* • *Anomalorthis* *utahensis*
Orthidiella Zone (Zone L of Ross, 1951)		• *Ectenonotus westoni*	• *Isograptus victoriae*	• *Orthidiella* sp. • *Liricamera* sp. • *Orthidium* spp.

Table 2

Stratigraphic Unit	Facies Association	Lithofacies	Bedding features	Sedimentary Structures	Trace and Body Fossils	Facies Interpretation
Eureka Quartzite	**Foreshore-shoreface siliciclastics**	I. Cross-bedded Quartz Arenite	• Mostly medium to thick (10-70 cm) beds with intervals of massive beds; comprising 30-80 m thick interval	• Low-angle planar and trough cross-bedding, ripple cross laminations, vertical and horizontal burrows	• *Skolithos*-, and *Calianassa*-type burrows	Upper shoreface to foreshore; possibly barrier island in the uppermost part
		II. Bioturbated lithic arenite	• Thin to medium (5-30 cm) sandstone beds interbedded with thin (1-12 cm) siltstone beds; comprising 4-15 m thick interval	• Planar and trough cross bedding, ripple cross laminations, rare identifiable vertical burrows	• Few discernable, *Skolithos*	Upper shoreface
Copenhagen Formation equivalents	**Tidal flat carbonate-siliciclastics**	III. Dolomitic siltstone and lime mudstone	• Thinly bedded (5-10 cm) dolomitic siltstone and lime mudstone	• Flaser bedding	• Moderate bioturbation, rare bioclasts	Upper intertidal to supratidal
		IV. Fenestral dolostone	• Thin (1-2 cm) beds between dolomitic siltstone and lime mudstone	• Parallel lamination, fenestral fabrics	• Weak bioturbation	Upper intertidal
Copenhagen Formation	**Restricted subtidal shale and carbonates**	V. Parallel-laminated shale and argillaceous	• Millimeter-thick fissile laminae; alternate shale and argillaceous limestone	• Parallel laminations	• Brachiopods, crinoids, trilobites, and gastropods	Deep subtidal in a restricted basin, below fair-weather wave base
		VI. Lime mudstone and wackestone	• Thinly (5-15 cm) bedded flat beds, laterally continuous	• Parallel laminations	• Brachiopods, crinoids, trilobites, and gastropods	Deep subtidal in a restricted basin, possibly below fair-weather wave base
Upper Antelope Valley Limestone	**Peritidal carbonates**	VII. Peloidal wackestone	• Thin (1-3 cm) wavy or flat beds; forming 0.3-1.5 m thick units	• Wavy beds, , dissolution cavities and brecciation at the top of the units	• Vertical burrows and skeletal fragments	Upper intertidal to supratidal

Stratigraphic Unit	Facies Association	Lithofacies	Bedding features	Sedimentary Structures	Trace and Body Fossils	Facies Interpretation
Upper Antelope Valley Limestone	Peritidal carbonates	VIII. Mudcracked lime mudstone	• Thin to medium (10-20 cm) units; erosional surface at the top	• Mudcracks, fenestrae,	• Sparse bioturbation	• Supratidal, subaerial exposure
		IX. Bioclastic packstone and grainstone	• Thin to medium (5-25 cm) beds, erosional bases	• Ripple-cross lamination and planar cross beds, erosional bases	• Brachiopod, crinoids, and gastropod fragments	• Shallow subtidal above fair-weather wave base
		X. Intraclastic conglomerate	• 20-35 cm thick beds with erosional bases	• Erosional bases, massive and occasionally faint cross beds	• Large gastropod and brachiopod fragments	• Shallow subtidal above fair-weather wave base
		XI. Bioturbated/nodular mudstone	• Thinly bedded (1-4 cm), laterally persistent beds; forming a few meter thick intervals	• Parallel and wavy laminations	• *Calianassa*-type burrows; skeletal fragments	Lower intertidal or protected, low-energy lagoon
		XII. Bioturbated-nodular wackestone	• Thin (1-4 cm)wavy beds separated by silty laminae	• Wavy bedding, intensely burrowed	• *Calianassa*-type burrows; skeletal fragments	Lower intertidal or protected, low-energy lagoon
	Oncolitic-oolitic sand shoals	XIII. Cross-bedded, oolitic grainstone	• 10-30 cm thick beds, laterally transitional to oncolitic packstones Medium (2-10 cm)	• Planar cross bedding, erosional bases	• Few fossils visible, *Palliseria* fragments	Subtidal sand shoals
		XIV. Oncolitic packstone	Lenticular beds, laterally transitional to oolitic grainstone	• Planar cross bedding, erosional bases; microbial laminae	• *Girvanella*-type oncoids; "bioherm-like" buildups	• Subtidal sand shoals

70

APPENDIX I

Isotopic results

Pahranagat Range

*Stratal Height	Sample ID	Color	Lithology	$\delta^{13}C$ (‰, VPDB)	$\delta^{18}O$(‰, VPDB)
-65.0	PR-50	Gray	Wackestone	-2.454	-6.846
-63.5	PR-51	Gray	Wackestone	-2.405	-6.978
-62.5	PR-54	Gray	Lime Mudstone	-1.847	-6.678
-61.5	PR-55	Gray	Lime Mudstone	-2.2	-6.702
-60.5	PR-56	Gray	Wackestone	-1.911	-6.912
-59.5	PR-57	Gray	Grainstone	-2.483	-6.782
-58.0	PR-58	Gray	Grainstone	-2.367	-6.392
-57.0	PR-59	Gray	Lime Mudstone	-3.058	-6.313
-56.0	PR-60	Gray	Wackestone	-1.298	-6.435
-55.0	PR-61	Gray	Wackestone	-2.807	-6.716
-53.5	PR-62	Gray	Lime Mudstone	-4.226	-6.819
-52.5	PR-63	Gray	Lime Mudstone	-3.091	-6.91
-51.0	PR-64	Gray	Wackestone	-2.9	-6.922
-50.5	PR-65	Gray	Lime Mudstone	-3.488	-6.492
-49.5	PR-66	Gray	Wackestone	-4.032	-6.429
-48.5	PR-67	Gray	Wackestone	-4.848	-6.944
-47.5	PR-68	Gray	Wackestone	-4.307	-6.544
-46.5	PR-70	Gray	Wackestone	-2.389	-6.371
-45.5	PR-71	Gray	Wackestone	-3.025	-6.735
-44.1	PR-72	Gray	Grainstone	-3.826	-6.342
-44.0	PR-72B	Gray	Wackestone	-2.755	-6.55
-43.0	PR-75	Gray	Lime Mudstone	-1.561	-7.123
-41.5	PR-76	Gray	Lime Mudstone	-1.9	-5.833
-40.0	PR-77	Gray	Lime Mudstone	-1.649	-7.088
-39.5	PR-78	Gray	Lime Mudstone	-1.774	-6.795
-38.5	PR-79	Gray	Lime Mudstone	-2.19	-6.65
-37.5	PR-80	Gray	Wackestone	-2.083	-6.894
-36.0	PR-81	Gray	Lime Mudstone	-2.384	-7.381
-35.0	PR-83	Gray	Packstone	-3.654	-7.003
-34.0	PR-84	Gray	Lime Mudstone	-1.989	-7.069
-32.5	PR-87	Gray	Lime Mudstone	-2.324	-6.963
-31.5	PR-88	Gray	Wackestone	-3.224	-7.551
-30.5	PR-90	Gray	Wackestone	-2.306	-6.83
-29.5	PR-91	Gray	Lime Mudstone	-1.514	-6.474
-28.5	PR-92	Gray	Wackestone	-5.268	-8.05
-27.5	PR-93	Gray	Wackestone	-2.142	-6.867
-26.0	PR-94	Gray	Lime Mudstone	-1.694	-6.845
-25.0	PR-95	Gray	Packstone	-2.195	-7
-24.5	PR-96	Gray	Lime Mudstone	-1.848	-6.691
-23.5	PR-97	Gray	Lime Mudstone	-2.532	-7.061
-22.0	PR-98	Gray	Lime Mudstone	-2.119	-6.852
-21.0	PR-99	Gray	Wackestone	-1.49	-7.085

-20.0	PR-100	Gray	Wackestone	-4.006	-7.477
-19.5	PR-101	Gray	Lime Mudstone	-2.962	-6.986
-18.0	PR-102	Gray	Wackestone	-4.104	-7.045
-17.0	PR-103	Gray	Wackestone	-3.141	-7.144
-16.5	PR-104	Gray	Wackestone	-3.64	-6.999
-15.5	PR-105	Gray	Wackestone	-3.954	-7.291
-14.0	PR-106	Gray	Wackestone	-4.481	-7.292
-13.0	PR-107	Gray	Wackestone	-2.317	-7.208
-11.5	PR-108	Gray	Wackestone	-2.645	-7.518
-10.0	PR-109	Gray	Wackestone	-2.816	-7.494
-9.0	PR-110	Gray	Wackestone	-2.272	-5.427
-7.5	PR-111	Gray	Wackestone	-2.194	-8.838
-6.5	PR-112	Gray	Wackestone	-0.799	-4.449
-5.0	PR-113	Gray	Wackestone	-0.972	-3.066
-4.0	PR-114	Light gray-tan	Silty dolostone	-0.949	-2.008
-3.0	PR-115	Light gray-tan	Silty dolostone	-1.354	-1.348
-1.5	PR-117	Light gray-tan	Silty dolostone	-1.245	-2.028
-0.5	PR-118	Light gray-tan	Silty dolostone	-1.693	-6.654

Hot Creek Canyon

*Stratal height	Sample ID	Color	Lithology	$\delta^{13}C$ (‰, VPDB)	$\delta^{18}O$(‰, VPDB)
-43.0	HC-1	Gray	Lime Mudstone	1.034	-3.521
-42.0	HC-2	Gray	Lime Mudstone	2.538	-2.601
-41.0	HC-3	Gray	Lime Mudstone	2.639	-2.919
-40.0	HC-4	Gray	Lime Mudstone	2.15	-3.475
-39.0	HC-5	Gray	Lime Mudstone	1.909	-3.252
-38.0	HC-6	Gray	Lime Mudstone	-1.005	-6.459
-37.0	HC-7	Gray	Lime Mudstone	0.953	-3.154
-36.0	HC-8	Gray	Lime Mudstone	1.191	-2.465
-35.0	HC-9	Gray	Lime Mudstone	1.015	-2.563
-34.0	HC-10	Gray	Lime Mudstone	0.413	-3.794
-33.0	HC-11	Gray	Lime Mudstone	0.331	-2.862
-32.0	HC-12	Gray	Lime Mudstone	0.641	-6.745
-31.0	HC-14	Gray	Lime Mudstone	0.306	-10.27
-30.0	HC-15	Gray	Lime Mudstone	0.325	-9.1
-29.0	HC-16	Gray	Lime Mudstone	-1.55	-8.493
-28.0	HC-17	Gray	Lime Mudstone	-1.551	-6.458
-27.0	HC-18	Gray	Lime Mudstone	-1.338	-9.019
-26.0	HC-19	Gray	Lime Mudstone	-1.714	-7.804
-25.0	HC-20	Gray	Lime Mudstone	-1.58	-7.626
-24.0	HC-21	Gray	Lime Mudstone	-1.398	-7.531
-23.0	HC-22	Gray	Lime Mudstone	-2.111	-8.516
-22.0	HC-23	Light tan	Silty dolostone	-1.581	-6.839
-21.0	HC-24	Light tan	Silty dolostone	-4.383	-11.508

				δ¹³C (‰, VPDB)	δ¹⁸O(‰, VPDB)
-20.0	HC-25	Light tan	Silty dolostone	-1.306	-9.355
-19.0	HC-26	Light tan	Silty dolostone	-4.529	-5.503
-18.0	HC-27	Light tan	Silty dolostone	-3.329	-11.842
-17.0	HC-28	Gray	Lime Mudstone	-1.017	-4.759
-16.0	HC-30	Light tan	Silty dolostone	-1.439	-4.96
-15.0	HC-31	Light tan	Silty dolostone	-1.331	-5.287
-14.0	HC-32	Gray	Lime Mudstone	-1.048	-5.33
-13.0	HC-34	Gray	Lime Mudstone	-1.006	-4.422
-12.0	HC-35	Gray	Lime Mudstone	-0.929	-3.943
-11.0	HC-36	Gray	Lime Mudstone	-0.555	-4.811
-10.0	HC-37	Light tan	Silty dolostone	-0.572	-2.892
-9.0	HC-38	Gray	Lime Mudstone	-0.432	-3.494
-8.0	HC-39	Gray	Lime Mudstone	-0.422	-4.18
-7.0	HC-40	Gray	Lime Mudstone	-0.312	-4.087
-6.0	HC-41	Gray	Lime Mudstone	-0.543	-3.975
-5.0	HC-42	Light tan	Silty dolostone	-0.525	-3.763
-4.0	HC-43	Gray	Lime Mudstone	-0.746	-4.782
-3.0	HC-44	Gray	Lime Mudstone	-1.09	-5.436
-2.0	HC-45	Gray	Lime Mudstone	-0.966	-2.806
-1.0	HC-46	Gray	Lime Mudstone	-0.814	-4.555
+0.5	HC-47	Gray	Lime Mudstone	-0.62	-5.832
+1.5	HC-48	Gray	Lime Mudstone	-1.24	-2.338
+2.5	HC-49	Gray	Lime Mudstone	-1.17	-4.115
+3.5	HC-50	Gray	Lime Mudstone	-1.225	-2.244
+4.5	HC-51	Gray	Lime Mudstone	-1.452	-3.587
+5.5	HC-52	Gray	Lime Mudstone	-1.543	-3.826

Lone Mountain

*Stratal height	Sample ID	Color	Lithology	δ¹³C (‰, VPDB)	δ¹⁸O(‰, VPDB)
-35.5	LM-001	Gray	Wackestone	0.568	-3.68
-34.5	LM-002	Gray	Wackestone	0.82	-5.286
-33.0	LM-003	Gray	Wackestone	0.92	-3.96
-32.0	LM-004	Gray	Silty wackestone	1.266	-4.001
-31.0	LM-005	Gray	Silty wackestone	0.901	-4.706
-30.0	LM-006	Gray	Silty wackestone	0.902	-4.237
-29.5	LM-007	Gray	Silty wackestone	0.397	-4.161
-28.5	LM-008	Gray	Wackestone	0.502	-2.593
-27.5	LM-009	Gray	Wackestone	0.644	-3.165
-26.5	LM-010	Gray	Wackestone	0.453	-2.57
-25.5	LM-011	Gray	Silty wackestone	0.73	-6.144
-22.0	LM-014	Gray	Silty wackestone	1.001	-5.975
-21.0	LM-015	Light tan	Silty dolostone	0.704	-5.053
-20.0	LM-016	Light gray-tan	Silty dolostone	0.804	-5.559
-19.0	LM-017	Light gray-white	Silty-sandy dolostone	0.825	-4.296
-18.0	LM-018	Light gray-tan	Silty dolostone	-0.047	-5.337

-17.0	LM-019	Light gray-tan	Silty dolostone	-0.894	-2.461
-16.0	LM-020	Gray	Wackestone	-0.735	-4.052
-15.0	LM-021	Gray	Wackestone	-1.071	-4.942
-13.5	LM-022	Light gray-tan	Silty dolostone	-0.84	-5.032
-12.0	LM-023	Light gray-tan	Silty dolostone	-1.253	-4.742
-11.0	LM-024	Light gray-tan	Silty dolostone	-1.095	-5.447
-9.5	LM-025	Light gray-tan	Silty dolostone	-1.239	-4.822
-8.0	LM-026	Gray	Wackestone	-1.25	-3.074
-6.5	LM-027	Gray	Wackestone	-2.387	-6.27
-5.0	LM-028	Gray	Wackestone	-4.502	-6.279
-4.0	LM-029	Gray	Wackestone	-5.113	-7.149
-2.0	LM-030	Gray	Wackestone	-4.414	-7.305

*Stratal height is measured as a negative or positive distance from the lithologic contact interpreted as the sequence boundary between the Antelope Valley Limestone and Eureka Quartzite.

APPENDIX II

Location of measured sections

Arrow Canyon Range

White River Narrows (Hiko)

White River Narrows

37°42'52" N
115°11'18"W

150

100

50

0

M G Ss

Facies Association 1

Facies Association 2

Facies Association 4

Facies Association 5

50 km

0.5 KM
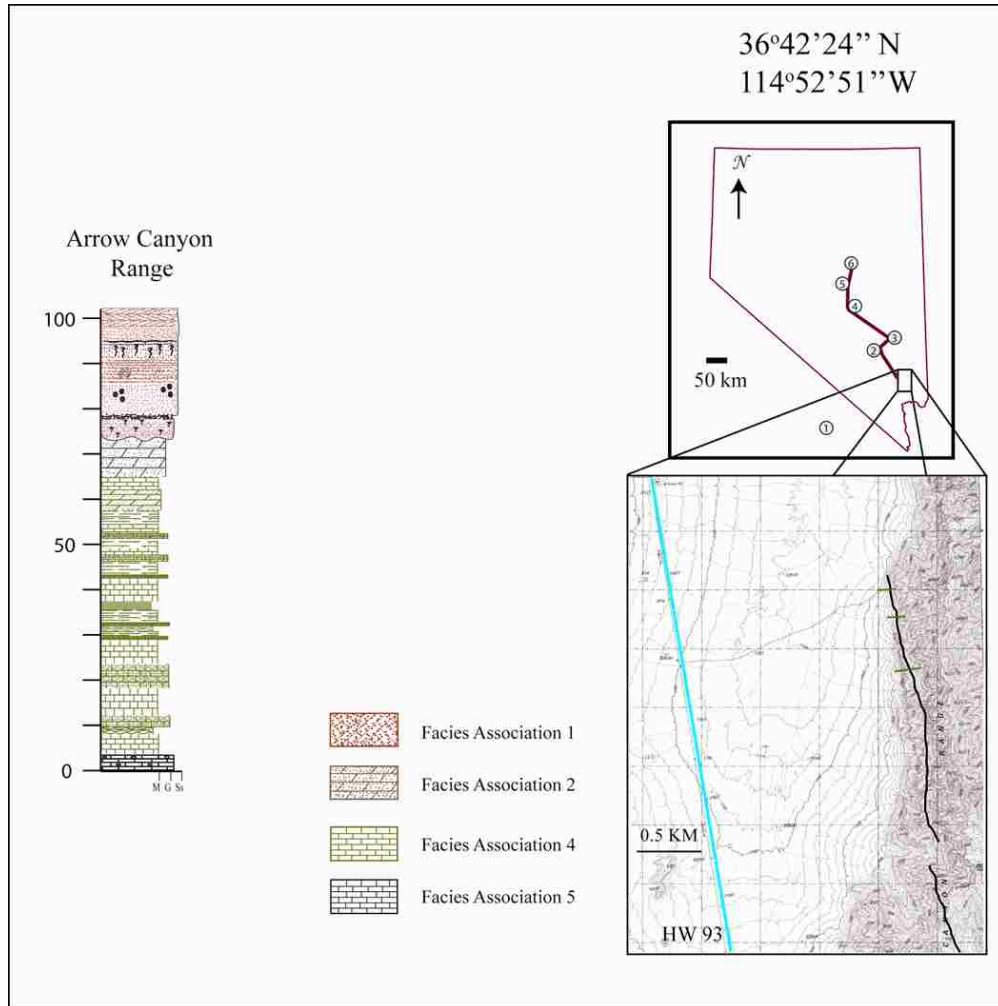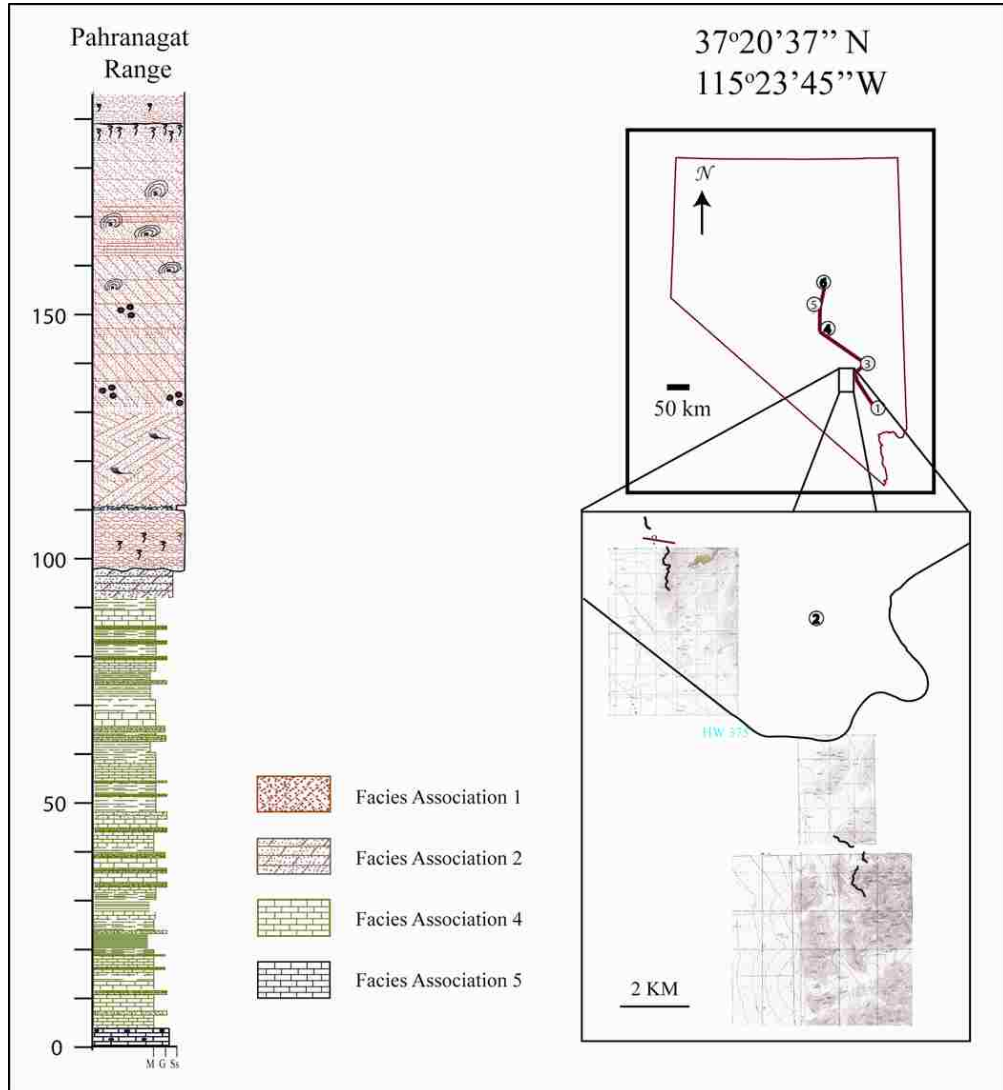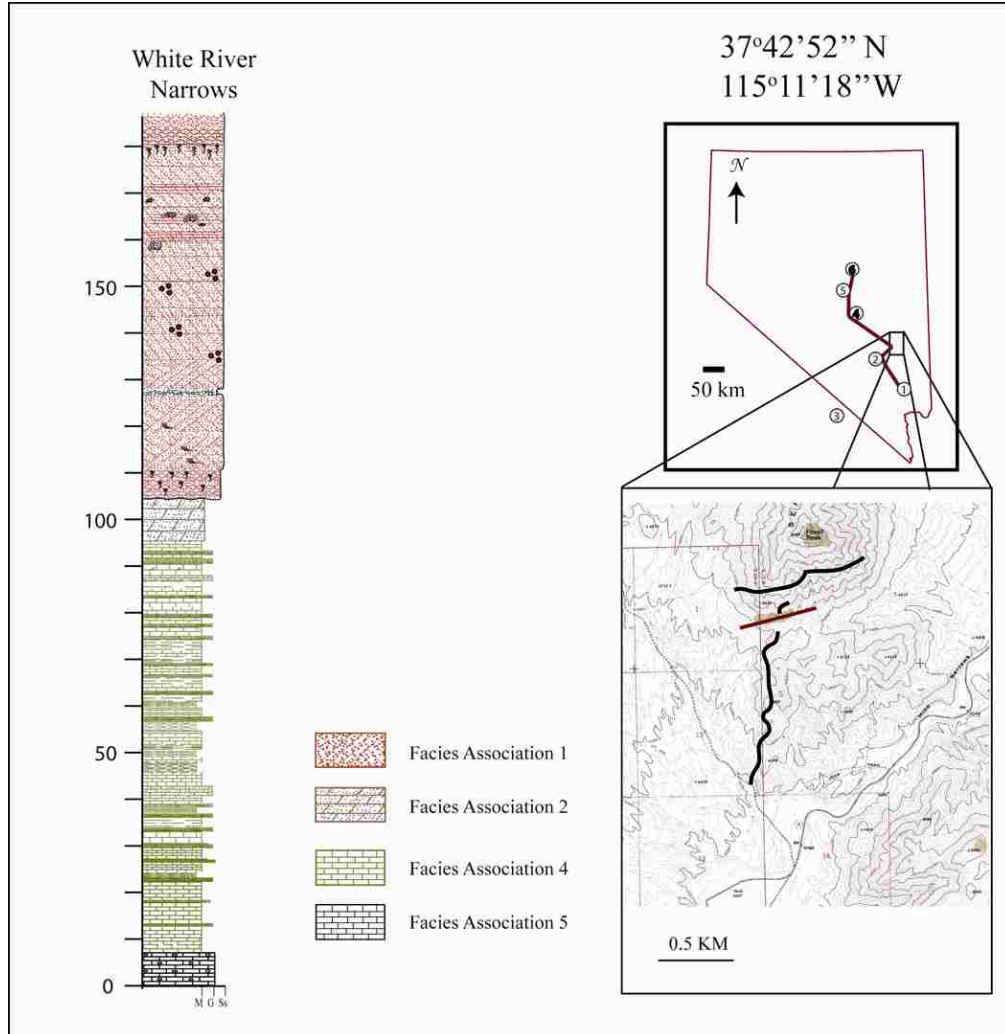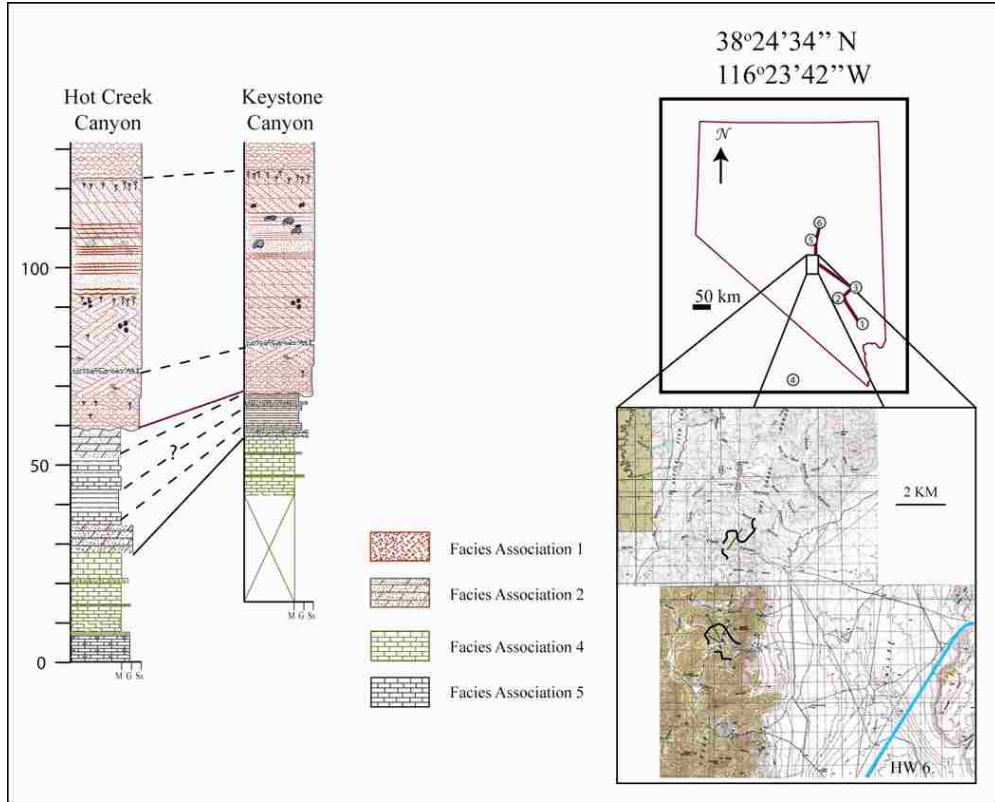
Copenhagen Canyon (Antelope Valley)

Lone Mountain

39°35'45" N
116°15'40"W

50 km

1 KM

HW 50

Facies Association 1

Facies Association 2

Facies Association 4

Facies Association 5

M G Ss
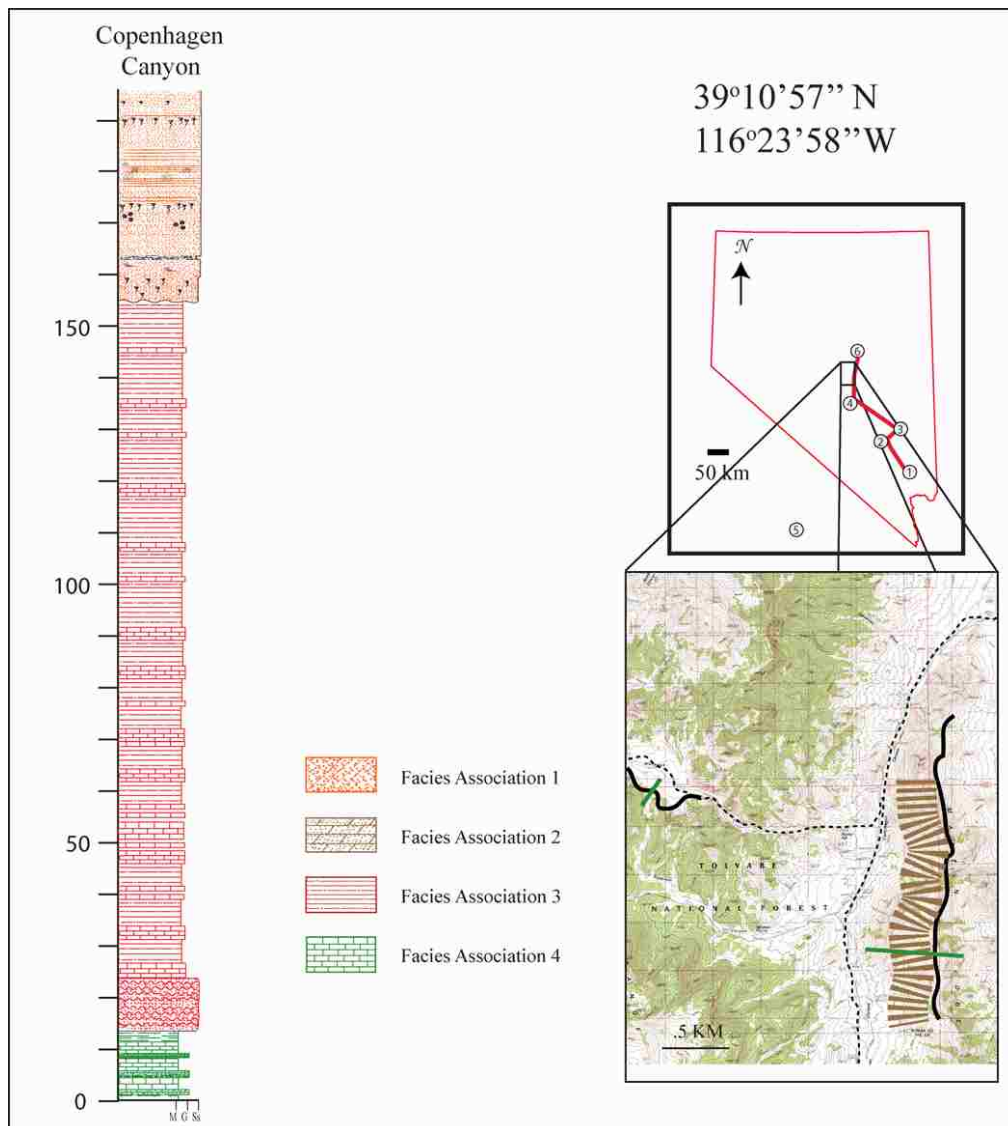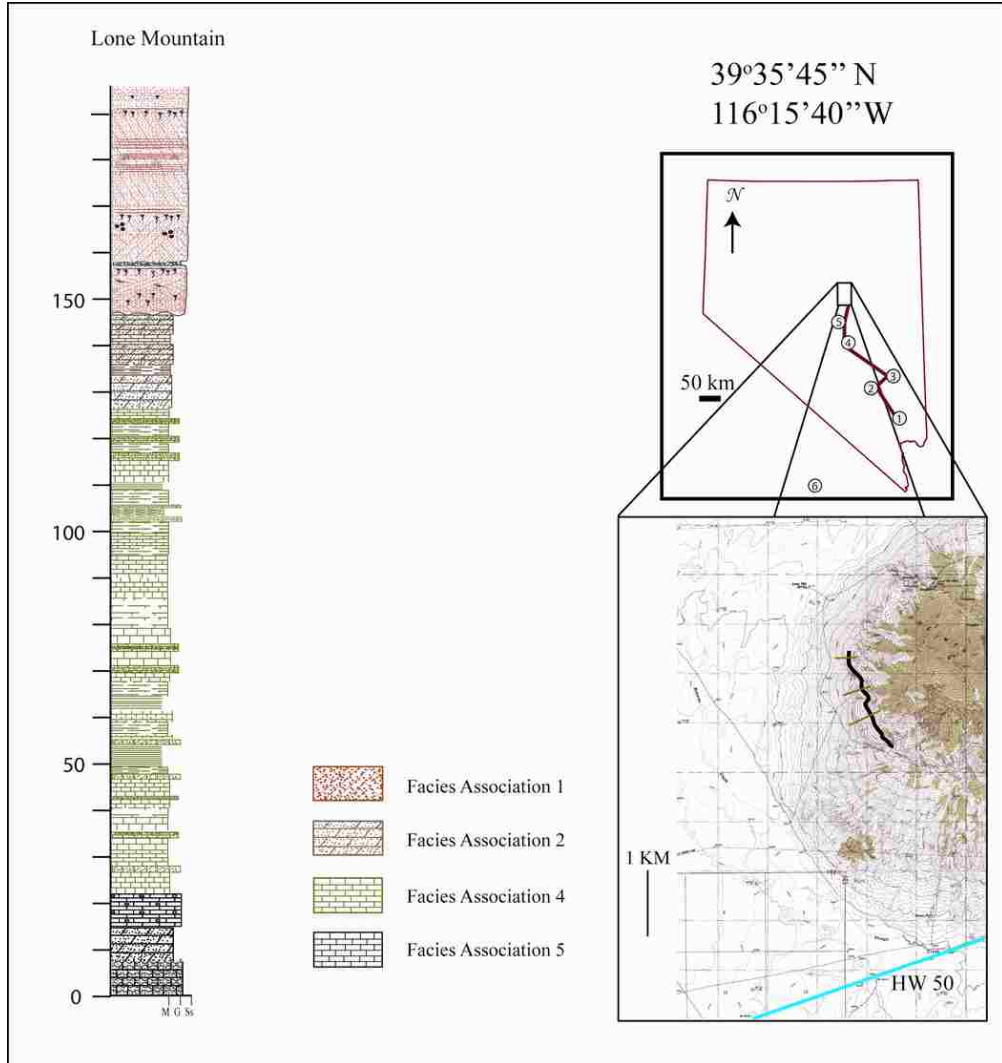
Facies reconstruction and sedimentary structure key

BIBLIOGRAPHY

Ainsaar, L., Meidla, T., Martma, T., 1999, Evidence for a widespread carbon isotopic event associated with late Middle Ordovician sedimentological and faunal changes in Estonia: Geological Magazine, v. 136, pp. 49– 62.

Ainsaar, L., Meidla, T., Martma, T., 2004, The Middle Caradoc facies and faunal turnover in the Late Ordovician Baltoscandian paleobasin: Palaeogeography, Palaeoclimatology, Palaeoecology, v. 210, pp. 119-133.

Allan, J.R., Matthews, R.K., 1982, Isotope signatures associated with early meteoric diagenesis: Sedimentology, v. 29, p. 797-817.

Armin, R., A. Mayer, L, 1983, Subsidence analysis of the Cordilleran miogeocline: Implications for timing of late Proterozoic rifting and amount of extension, v. 11, p. 702-705.

Azmy, K., Veizer, J., Bassett, M.G., Copper, P., 1998, Oxygen and carbon isotopic composition of Silurian brachiopods: Implications for coeval seawater and glaciations: Geological Society of America, Bulletin, v. 110, p. 1499–1512.

Barnes, C.R., 1992, The uppermost series of the Ordovician System: *In* Webby B.D. and Laurie J.R. eds. Global Perspectives on Ordovician Geology. AA Balkema, Rotterdam p. 185-192.

Bergström, S.M., 1995, The search for global biostratigraphic reference levels in the Ordovician: regional correlation potential of the base of the North American Whiterockian Series: *In* Cooper, J.D., Droser, M.L., and Finney, S.C., eds., Ordovician Odyssey; Short Papers, 7th International Symposium on the Ordovician System, Society of Economic Paleontologists and Mineralogists, Pacific Section, Book 77, p. 149-152.

Berry, W.B.N., Ripperdan, R.L., Finney, S.C., 2002, Late Ordovician extinction: A Laurentian view: *in* Koeberl, C., and MacLeod, K.G., eds., Catasptrophic Events and Mass Extinctions: Impacts and Beyond: Boulder, Colorado, Geological Society of America Special Paper 356, p. 463-471.

Berner, R.A., 1994, GEOCARB II: A revised model of atmospheric CO2 over Phanerozoic time: American Journal of Science, v. 294, p. 56–91.

Berner, R.A., Kothavala, Z., 2003, GEOCARB III: A revised model of atmospheric CO_2 over Phanerozoic time: American Journal of Science, v. 301, p. 182-204.
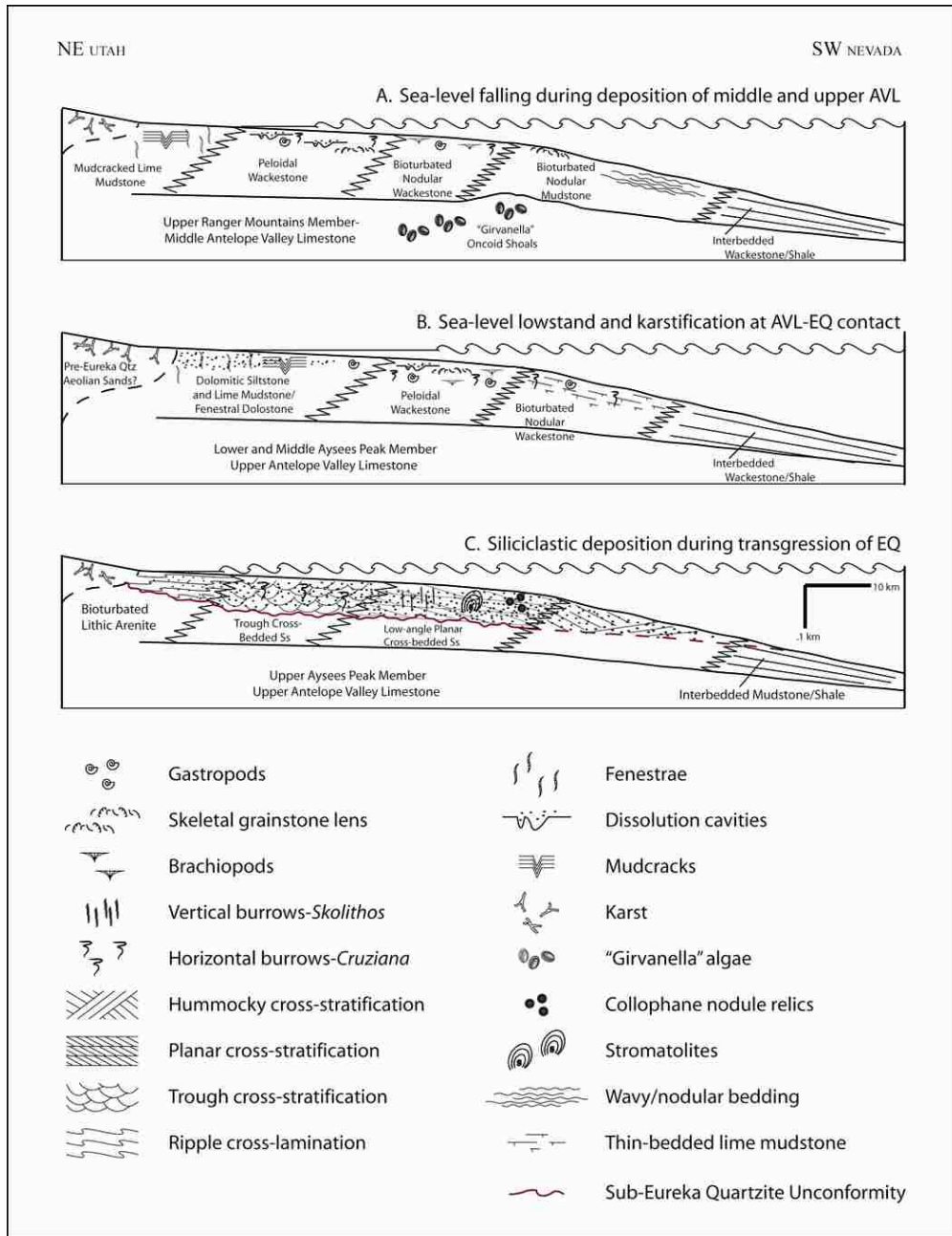
Bond, G.C., Kominz, M.A., 1988, Evolution of thought on passive continental margins from the origin of geosynclinal theory (~1860) to the present: Geological Society of America Bulletin, v. 100, p. 1909-1933

Bond, G.C., N. Christie-Blick, M.A. Kominz, W.J. Devlin, 1985, An early Cambrian rift to post-rift transition in the Cordillera of western North America: Nature, v. 316, p. 742-745

Bond, G.C., M.A. Kominz, 1984, Construction of tectonic subsidence curves for the early Paleozoic miogeocline, Southern Canadian Rocky Mountains: Implications for subsidence mechanisms, age of breakup and crustal thinning: Geological Society of America Bulletin, v. 95, p. 155-173.

Bond, G.C., M.A. Kominz, W.J. Devlin, 1983, Thermal subsidence and eustasy in the Lower Paleozoic miogeocline of western North America: Nature v. 306, p. 775-779.

Brenchley, P.J., Marshall, J. D., Hints, L., N˜olvak, J. 1997, New isotopic data solving an old biostratigraphic problem: the age of the upper Ordovician brachiopod Holorhynchus giganteus: Journal of the Geological Society, London, v. 154, p. 335–342.

Brenchley, P.J., Marshall, J.D., Carden, G.A.F., Robertson, D.B.R., Long, D.B.F., Meidla, T., Hints, L., Anderson, T.F., 1994, Bathymetric and isotopic evidence for a short-lived Late Ordovician glaciation in a greenhouse period: Geology, v. 22, p. 295–298.

Brenchley, P.J., Carden, G.A., Hints, L., Kaljo, D., Marshall, J.D., Martma, T., Meidla T., Nõlvak, J, 2003, High-resolution stable isotope stratigraphy of Upper Ordovician sequences: Constraints on the timing of bioevents and environmental changes associated with mass extinction and glaciation: Geological Society of America Bulletin, v. 115(1), p. 89-104.

Brown Jr., L.F., Fisher, W.L., 1977, Seismic stratigraphic interpretation of depositional systems: examples from Brazilian rift and pull-apart basins. *in*: Payton, C.E. ed., Seismic Stratigraphy-Applications to Hydrocarbon Exploration: American Association of Petroleum Geologists Memoir, v. 26, p. 213–248.

Byers, F.M., Barnes, H., Poole, F.G., Ross Jr., R.J., 1961, Revised subdivision of the Ordovician System at the Nevada Test Site and vicinity, Nevada: United States Geological Survey Professional Paper, v. 424-C, p. 106-110.

Catuneanu, O., Willis, A.J., Miall, A.D., 1998, Temporal significance of sequence boundaries: Sedimentary Geology, v. 121, p. 157–178.

Catuneanu, O., 2002, Sequence stratigraphy of clastic systems: concepts, merits, and pitfalls: Journal of African Earth Sciences, v. 35, no. 1, p. 1–43.

Catuneanu, O., Abreu, V., Bhattacharya, J.P., Blum, M.D., Dalrymple, R.W., Eriksson, P.G., Fielding, C.R., Fisher, W.L., Galloway, W.E., Gibling, M.R., Giles, K.A., Holbrook, J.M., Jordan, R., Kendall, C.G.St.C., Macurda, B., Martinsen, O.J., Miall, A.D., Neal, J.E., Nummedal, D., Pomar, L., Posamentier, H.W., Pratt, B.R., Sarg, J.F., Shanley, K.W., Steel, K.W., Strasser, A., Tucker, M.E., Winker, C., 2009, Towards the standardization of sequence stratigraphy: Earth-Science Reviews, v. 92, p. 1-33.

Chamberlin, T.L., 1975, Stratigraphy of the Ordovician Ely Springs Dolomite in the southeastern Great Basin, Utah and Nevada: unpublished Ph.D. dissertation, University of Illinois, Urbana-Camplain, pg. 202.

Christie-Blick, N., Grotzinger, J.P., von der Borch, C.C., 1988, Sequence stratigraphy in Proterozoic successions: Geology, v. 16, p. 100-104.

Christie-Blick, N., Driscoll, N.W., 1995, Sequence stratigraphy: Annual Reviews Earth Planetary Science, v. 23, p. 451-478.

Cooper, J.D., 1956, Chazyan and related brachiopods: Smithsonian Miscellaneous Collections, v. 127, pp. 1024.

Cooper, J.D., Keller, M.K., 2001, Paleokarst in the Ordovician of the southern Great Basin, USA: implications for sea-level history: Sedimentology, v. 48, p. 855-873.

Cotkin, S.J., 1989, The Callahan Event: expression of Ordovician-Silurian tectonism in northern California: Geological Society of America Abstracts with Programs, v. 21, no. 5, p. 69.

Cotkin, S.J. 1992, Ordovician-Silurian tectonism in northern California: the Callahan Event: Geology, v. 20, p. 821-824.

Crowell, J.C., 1999, Pre-Mesozoic ice ages: Their bearing on understanding the climate system: Geological Society of America Memoir 192, 106 p.

Crowley, T.J., Baum, S.K., 1995, Reconciling Late Ordovician (440 Ma) glaciation with very high CO_2 levels: Journal of Geophysical Research, v. 100, p. 1093–1101.

Dickinson, W.R., 2004, Evolution of the North American Cordillera: Annual Review of Earth and Planetary Science: v. 32, p. 13-45.

Dickinson, W.R., 2006, Geotectonic evolution of the Great Basin: Geosphere, v. 2, no. 7, p. 353-368.

Dilliard, K.A., M.C. Pope, M. Coniglio, S.T. Hasiotis, B.S. Lieberman, 2007, Stable isotope geochemistry of the lower Cambrian Sekwi Formation, Northwest Territories, Canada: Implications for ocean chemistry and secular curve generation: Palaeogeography, Palaeoclimatology, Palaeoecology, v. 256, p. 174-194.

Druschke, P.A, Jiang, G., Anderson, T.E., Hanson, A.D., 2008, Stromatolites in the Late Ordovician Eureka Quartzite: implications for microbial growth and preservation in siliciclastic settings: Sedimentology, v. , p.1-17.

Ethington, R.L., Schumacher, D., 1969, Conodonts of the Copenhagen Formation (Middle Ordovician) in central Nevada: Journal of Paleontology, V. 43, no. 2, P. 440-484.

Finney, S.C., Berry, W.B.N., Cooper, J.D., Ripperdan, R.L., Sewwt, W.C., Jacobson, S.R., Soufiane, A., Achab, A., Noble, P.J., 1999, Late Ordovician mass extinction: a new perspective from stratigraphic sections in central Nevada: Geology, v. 27, p. 215-218.

Finney, S.C., Ethington, R.L., 2000, Global Ordovician Series boundaries and global event biohorizons, Monitor Range and Roberts Mountains, Nevada *in* Lageson, D.R., Peters, S.G., Lahren, M.M. eds. Great Basin and Sierra Nevada: Boulder, Colorado, Geological Society of America Field Guide 2, p. 301-318.

Finney, S.C., Noble, P., Cluer, J.K., 2000, Lower Plaeozoic stratigraphy and structure of central Nevada: comparisons and contrasts between the lower and upper plates of the Roberts Mountains thrust: *in* Lageson, D.R., Peters, S.G., Lahren, M.M., eds., Great Basin and Sierra Nevada: Boulder, Colorado, Geological Society of America Field Giude 2, p. 279-300.

Fisher, D. W., 1957, Mohawkian (Middle Ordovician) Biostratigraphy of the Wells Outlier, Hamilton County, New York. New York State Museum Bulletin, v. 359, pp. 33

Fortey, R.A., Bassett, M.G., Harper, D.A.T., Hughes, R.A., Ingham, J.K., Molyneux, S.G., Owen, A.W., Owens, R.M., Rushton, A.W.A., and Sheldon, P.R., 1991, Progress and problems in the selection of stratotypes for the bases of series in the Ordovician System of the historical type area in the U.K.: *In* Barnes, C.R., and Williams, S.H., eds., Advances in Ordovician Geology; Geological Survey of Canada, Paper 90-9, p. 5-25.

Fortey, R.A., Harper, D.A.T., Ingham, J.K., Owen, A.W., and Rushton, A.W.A., 1995, A revision of Ordovician series and stages from the historical type area: Geological Magazine, v. 132, p. 15-30.

Fortey, R.A., Droser, M.L., 1999, Trilobites from the base of the type Whiterockian (Middle OrdovicianI in Nevada, Journal of Paleontology, v. 73 (2), p 182-201.

Frakes, L.A., Francis, J.E., Syktus, J.I., 1992, Climate Modes of the Phanerozoic: The History of the Earth's Climate Over the Past 600 Million Years. Cambridge Univ. Press, 274 p.

Friedman, I., Hall, W.E., 1963, Fractionation of O^{18}/O^{16} between coexisting calcite and dolomite: Journal of Geology, v. 71, p. 238-243.

Goldstein, R.H., Franseen, E.K., Mills, M.S., 1990, Diagenesis associated with subaerial exposure of Miocene strata, southeastern Spain: implications for sea-level change and preservation of low-temperature fluid inclusions in calcite cement: Geochimica et Cosmochimica Acta, v. 54, p. 699-704.

Hamoumi, N. 1999, Upper Ordovician glaciation spreading and its sedimentary record in Moroccan North Gondwana margin: *in* Quo Vadis Ordovician., eds. P. Kraft and O. Fatka, pp. 11–14. Acta Universitatis Carolinae, Geologica 43(1/2).

Handford, C.R., Loucks, R.G., 2001, Carbonate depositional sequences and systems tracts-responses of carbonate platforms to relative sea-level changes: Ch. 1. ARCO Exploration and Production Technology, p. 3-41.

Hatch, J.R., Jacobson, S.R., Witzke, B.J., Risatti, J.B., Anders, D.E., Watney, W.L., Newell, K.D., and Vuletich, A.K., 1987, Possible late Middle Ordovician organic carbon isotope excursion: Evidence from Ordovician oils and hydrocarbon source rocks, mid-continent and east-central United States: American Association of Petroleum Geologists Bulletin, v. 71, p. 1342-1354.

Hollander, D.J., McKenzie, J.A., 1991, CO_2 control on carbon-isotope fractionation during aqueous photosynthesis: A paleo- pCO_2 barometer: Geology, p. 929-932.

Hughes, T.J., Denton, G.H., Anderson, B.E., Schilling, D., Fastook, J.L., Lingle, C.S., 1981, The last great ice sheets: A global view, *in* G. H. Denton and T. J. Hughes, editors, The Last Great Ice Sheets: New York, Wiley Interscience, pages 263-318

Immenhauser, A., Schlager, W., Burns, S.J., Scott, R.W., Geel, T., Lehmann, J., Van Der Gaast, S., Bolder-Schrijver, L.J.A., 1999, Late Aptian to Late Albian Sea-level fluctuations constrained by geochemical and biological evidence (Nahr Umr Formation, Oman), Journal of Sedimentary Research, v. 69, p. 434-446.

Jiang, G., Christie-Blick, N., Kaufman, A.J., Banerjee, D.M., and Rai, V., 2002, Sequence stratigraphy of the Neoproterozoic Infra Krol Formation and Krol Group, Lesser Himalaya, India: Journal of Sedimentary Research, v. 72, p. 524-542.

Jiang, G., Kaufman, A.J., Christie-Blick, N., Zhang, S., and Wu, H., 2007, Carbon isotope variability across the Ediacaran Yangtze platform in South China: Implications for a large surface-to-deep ocean $\delta^{13}C$ gradient: Earth and Planetary Science Letters, v. 261, p. 303-320.

Jiang, G.Q., Zhang, S.H., Shi, X.Y., and Wang, X.Q., 2008, Chemocline instability and isotope variations of the Ediacaran Doushantuo basin in South China: Science in China Series D-Earth Sciences, v. 51, p. 1560-1569.

Joachimski, M.M., 1994, Subaerial exposure and deposition of shallowing upward sequences: evidence from stable isotopes of Purbeckian peritidal carbonates (basal Cretaceous), Swiss and French Jura Mountains: Sedimentology, v. 41, p. 805-824.

Joachimski, M.M., Pancost, R.D., Freeman, K.H., Ostertag-Henning, C., Buggisch, W., 2002, Carbon isotope geochemistry of the Frasnian–Famennian transition: Palaeogeography, Palaeoclimatology, Palaeoecology, v. 181, p. 91–109.

Kapp, U.S., Stearn, C.W., 1975, Stromatopooids of the Chazy Group (Middle Ordovician, Lake Champlain, Vermont, and New York: Society of Economic Paleontologista and Mineralogists, v. 49(1), p. 163-186.

Kaufman, A.J., and Knoll, A.H., 1995, Neoproterozoic variations in the C-isotopic composition of seawater; stratigraphic and biogeochemical implications: Precambrian Research, v. 73, p. 27-49.

Kaya, A., Friedman, G.M., 1997, Sedimentation and facies analysis of the Girvanella-constituted oncolitic shoals and associated lithofacies in the Middle Ordovician Antelope Valley Limestone, central Nevada, USA: Carbonates and Evaporites, v. 12, no.1, p. 134-156.

Ketner, K.B., 1986, Eureka Quartzite in Mexico? Tectonic Implications: Geology, v. 14, p. 1027-1030.

Ketner, K.B., 1977, Deposition and deformation of Lower Paleozoic Western Facies rocks, northern Nevada, *in* Paleozoic Paleogeography of the Western United States, eds., J.H. Stewart, C.H. Stevens, A.E. Fritsche: Pacific Section of the Society of Economic Paleontologists and Mineralogists, Los Angeles, p. 251-258.

Kump, L.R., Arthur, M.A., Patzkowsky, M.E., Gibbs, M.T., Pinkus, D.S., and Sheehan, P.M., 1999, A weathering hypothesis for glaciation at high atmospheric pCO2 during the Late Ordovician: Palaeogeography, Palaeoclimatology, Palaeoecology, v. 152, p. 173–187.

Kirk, E., 1933, The Eureka Quartzite of the Great Basin region: American Journal of Science, v. 26, p. 27-44.

Knoll, A.H., Hayes, J.M., Kaufman, A.J., Swett, K., Lambert, I.B., 1986, Secular variation in carbon isotope ratios from Upper Proterozoic successions of Svalbard and East Greenland: Nature, v. 321, p. 832-383.

Kump, L.R., and Arthur, M.A., 1999, Interpreting carbon-isotope excursions: carbonates and organic matter: Chemical Geology, v. 161, p. 181-198.

Langenheim Jr. R.J., Carss, B.W., Kennerly, J.B., Waines, R.H., 1962, Paleozoic section in Arrow Canyon Range, Clark County, Nevada: American Association of Petroleum Geologists Bulletin, v. 46, p. 592-609.

Levy, M., Christie-Blick, N., 1991, Tectonic subsidence of the Early Paleozoic passive continental margin in eastern California and southern Nevada: Geological Society of America Bulletin, v. 103, p. 190-1606.

Li, X., Droser, M.L., 1999, Lower and Middle Ordovician shell beds from the Basin and Range province of the western United States (California, Nevada, and Utah): Palaios, v. 14, p. 215-233.

Ludvigson, G.A., Jacobson, S.R., Witzke, B.J., and González, L.A., 1996, Carbonate component chemostratigraphy and depositional history of the Ordovician Decorah Formation, Upper Mississippi Valley, in Witzke, B.J., Ludvigson, G.A., and Day, J., eds., Paleozoic Sequence Stratigraphy: Views from the North American Craton: Geological Society of America, Special Paper 306, p. 67-86.

Ludvigson, G.A., Witzke, B.J., Gonzalez, L.A., Carpenter, S.J., Schneider, C.L., Hasiuk, F., 2004, Late Ordovician (Turinian–Chatfieldian) carbon isotope excursions and their stratigraphic and paleoceanographic significance: Palaeogeography, Palaeoclimatology, Palaoecology, v. 210, p. 187–214.

Manspeizer, W., Cousminer, H.L, 1988, Late Triassic-Early Jurassic synrift basins of the U.S. Atlantic margin *in* R. E. Sheridan and J. A. Grow, eds. The Atlantic continental margin, U. S: The geology of North America: Geological Society of America, v, I-2, 197- 216

Marshall, J. D., Middleton, P. D., 1990, Changes in marine isotopic composition and the Late Ordovician glaciation: Geological Society of London, v. 147, p. 1–4.

Miall, A.D., 1991, Stratigraphic sequences and their chronostratigraphic correlation: Journal of Sedimentary Petrology, v. 61, p. 497–505.

Mii, H., Grossman, E.L., Yancey, T.E., 1999, Carboniferous isotope stratigraphies of North America: Implications for Carboniferous paleoceanography and Mississippian glaciation: Geological Society of America Bulletin, v. 111, p. 960–973.

Miller, M.F., 1977, Middle and Upper Ordovician biogenic structures and paleoenvironments, southern Nevada: Journal of Sedimentary Petrology, v. 43, n. 3, p. 1328-1338.

Moldovanyi, E.P., Lohmann, K.C., 1984, Isotopic and petrographic record of phreatic diagenesis: Lower Cretaceous Sligo and Cupido Formations, Journal of Sedimentary Petrology, v. 58, p. 688-705.

Montanez, I.P., and Osleger, D.A., 1996, Contrasting sequence boundary zones developed within cyclic carbonates of the Bonanza King Formation, Middle to Late Cambrian, southern Great Basin: Special Paper - Geological Society of America, v. 306, p. 7-21.

Nolan, T.B., Merriam, C.W., Williams, J.S., 1956, The stratigraphic section in the vicinity of Eureka, Nevada: United States Geological Survey Professional Paper 276, pp. 77.

O'Neil, J.R., Epstein, S, 1966, Oxygen isotope fractionation in the system dolomite-calcite-carbon dioxide: Science, v. 152, p 198-201.

Osleger, D.A., and Montanez, I.P., 1996, Cross-platform architecture of a sequence boundary in mixed siliciclastic-carbonate lithofacies, Middle Cambrian, southern Great Basin, USA: Sedimentology, v. 43, p. 197-217.

Panchuk, K.M., Holmden, C.E., Leslie, S.A., 2006, Local controls on carbon cycling in the Ordovician Midcontinent region of North America, with implications for carbon isotope secular curves: Journal of Sedimentary Research, v. 76, p. 200-211.

Parsons, S.M., 1996, Sequence stratigraphy and biostratigraphy of the lower member of the Deep Spring Formation: Implications for the Neoproterozoic-Cambrian boundary in the Basin and Range province, western United States [MS thesis]: Las Vegas, University of Nevada, p.181.

Patterson, W.P., Walter, L.M., 1994, Depletion of ^{13}C in seawater CO_2 on modern carbonate platforms: significance for the carbon isotopic record of carbonates: Geology, v. 22, p. 885-888.

Patzkowsky, M.E., Slupik, L.M., Arthur, M.A., Pancost, R.D., Freeman, K.H., 1997, Late Middle Ordovician environmental change and extinction: harbinger of the Late Ordovician or continuation of Cambrian patterns?: Geology, v. 25, p. 911–914.

Pope, M.C., Steffen, J.B., 2003, Widespread, prolonged late Middle to Late Ordovician upwelling in North America: a proxy record of glaciation?: Geology, v. 31, p. 63–66.

Pope, M.C., and Read, J.F., 1998, Ordovician metre-scale cycles: Implications for Ordovician climate and eustatic fluctuations in the central Appalachian Basin, USA: Palaeoclimatology, Palaeogeography, Palaeoecology, v. 138, p. 27-42.

Pope, M.C., and Read, J.F., 1997, High-frequency cyclicity of the Lexington Limestone (Middle Ordovician), a cool-water carbonate clastic ramp in an active foreland basin. In: Cool-Water Carbonates, eds., N.P. James and J.P. Clarke, SEPM Special Publication, v.56, p. 411-429.

Posamentier, H.W., Jervey, M.T., Vail, P.R., 1988, Eustatic controls on clastic Sa deposition: a conceptual framework, In: Wilgus, C.K., Hastings, B.S., Kendall, C.G.St.C., Posamentier, H.W., Ross, C.A., Van Wagoner, J.C. eds., Sea Level Changes - An Integrated Approach: Society of Economic Paleontologists and Mineralogists Special Publication, v. 42., p. 110–124.

Rankey, E.C., Bachtel, S.L., 1998, Subaerial exposure surfaces in carbonate strata: their recognition and significance. in: Cox, D.M. ed., Upper Pennsylvanian and Wolfcampian mixed siliciclastic systems, Sacramento Mountains, New Mexico : outcrop models for subsurface plays and reservoir development : 1998 annual field trip guidebook, p. 115-123.

Rees, M.N., 1986, A fault-controlled trough through a carbonate platform, the Middle Cambrian House Range Embayment: Geological Society of America Bulletin, v. 97, p. 1054-1069.

Ripperdan, R.L., Magaritz, M., Nicoll, R.S., Shergold, J.H., 1992, Simultaneous changes in carbon isotopes, sea-level and conodont biozones within the Cambrian–Ordovician boundary interval at Black Mountain, Australia: Geology, v. 20, p. 1039–1042.

Ross, Jr. R.J., James, N.P., Hintze, L.F., Poole, F.G., 1989, Architecture and evolution of of a Whiterockian (early Middle Ordovician) carbonate platform, Basin Ranges of western U.S.A: Society of Economic Paleontologists and Mineralogists Special Publication, no. 44, p. 167-185.

Ross, Jr., R. S., Ethington, R. L., Mitchell, C.E., 1991, Stratotype of Ordovician Whiterock Series: Society for Sedimentary Geology Research Reports, p. 156-173.

Ross, Jr., R.S., Shaw, F.C., 1970, Distribution of the Middle Ordovician Copenhagen Formation and its trilobites in Nevada: U. S. Geological Survey Professional Paper 749, 33 p., 8 pls.

Ross, Jr., RS., 1970, Ordovician brachiopods, trilobites, and stratigraphy in eastern and central Nevada: U.S. Geological Survey Professional Paper 639, 103 p., 22 pls.

Ross, Jr., RS., 1967, Some middle Ordovician brachiopods and trilobites from the Basin Ranges, western United States: U.S. Geological Survey Professional Paper 523-D, pp. 43, 10 pls.

Ross, Jr., RS., 1964, Middle and lower Ordovician formations in southernmost Nevada and adjacent California: U.S. Geological Survey Bulletin, v. 1180-C, 101 p.

Royer, D.L. 2006, CO_2-forced climate thresholds during the Phanerozoic: Geochimica et Cosmochimica Acta, v. 70, p. 5665-5675.

Royer, D.L., Berner, R.A., Montanez, I.P., Tabor, N.J., Beerling, D.J., 2004, CO_2 as a primary driver of Phanerozoic climate: GSA Today, v. 14, p. 4-10.

Railsback, L.B., Holland, S.M., Hunter, D.M., Jordan, E.M., Diaz, J.R., Crowe, D.E., 2003, Controls on geochemical expression of subaerial exposure in Ordovician limestones from the Nashville Dome, Tennessee, USA: Journal of Sedimentary Research, v. 73, p. 790-805.

Saltzman, M.R., Ripperdan, R.L., Brasier, M.D., Lohman, K.C., Robison, R.A., Chang, W.T., Peng, S., Ergaliev, E.K., Runnegar, B., 2000, A global carbon isotope excursion (SPICE) during the Late Cambrian: relation to trilobite extinctions, organic-matter burial and sea-level: Palaeogeography, Palaeoclimatology, Palaeoecology, V. 162, p. 211-223.

Saltzman, M.R., 2002, Carbon and oxygen isotope stratigraphy of the Lower Mississippian (Kinderhookian–early Osagean), western United States: Implications for seawater chemistry and glaciation: Geological Society of America, Bulletin, v. 114, p. 96–108.

Saltzman, M.R., Runnegar, B., Lohmann, K.C., 1998, Carbon-isotope stratigraphy of the Pterocephaliid Biomere in the eastern Great Basin: Record of a global oceanographic event during the Late Cambrian: Geological Society of America, Bulletin, v. 110, p. 285–297.

Saltzman, M.R., Young, S.A., 2005, Long-lived glaciation in the Late Ordovician? Isotopic and sequence-stratigraphic evidence from western Laurentia: Geology, v. 33, p. 109– 112.

Sarg, J.F., 1988, Carbonate sequence stratigraphy. *In*: Wilgus, C.K., Hastings, B.S., Kendall, C.G.St.C., Posamentier, H.W., Ross, C.A., VanWagoner, J.C. eds., Sea Level   Changes - An Integrated Approach: Society of Economic Paleontologists and Mineralogists Special Publication, v. 42., p. 155–181.

Scholle, P.A., Ulmer-Scholle, D.S., 2003, A color guide to the petrography of carbonate rocks, AAPG Memoir 77: Tulsa, American Association of Petroleum Geologists, p. 1-474.

Shields, G.A., Carden, G.A.F., Veizer, J., Meidla, T., Rong, J., Li, R., 2005, Sr, C, and O isotope geochemistry of Ordovician brachiopods: a major isotopic event around the Middle-Late Ordovician transition: Geochimica et Cosmochimica, v. 67, p. 2005-226.

Simo, J.A., Emerson, N.R, Byers, C.W., Ludvigson, G.A., 2003, Anatomy of an embayment in an Ordovician epeiric sea, Upper Mississippi Valley, USA: Geology, v. 31, no. 6, p. 545–548

Sloss, L.L., 1963, Sequences in the cratonic interior of North America. Geological Society of America Bulletin, v. 74, p. 93–114.

Stewart, J.T., Suczek, C.A., 1977, Cambrian and latest Precambrian paleogeography and tectonics in the western United States, *in* Paleozoic Paleogeography of the Western Inited States, eds., J.H. Stewart, C.H. Stevens, A.E. Fritsche: Pacific Section of the Society of Economic Paleontologists and Mineralogists, Los Angeles, p. 7-17.

Swart, P.K., 2008. Global synchronous changes in the carbon isotopic composition of carbonate sediments unrelated to changes in the global carbon cycle: Proceedings of the Natural Academy f Sciences, v. 105, p. 13741-13745.

Thieling, B. P., Railsback, B.L., Holland, S.M., Crowe, D.E., 2007, Heterogeneity in geochemical expression of subaerial exposure in limestones, and its implications for sampling to detect exposure surfaces: Journal of Sedimentary Research, v. 77, p. 159-169.

Tobin, K.J., Bergstrom, S.M., De La Garza, P., 2005, A Mid-Caradocian (453Ma) drawdown in atmospheric pCO$_2$ without ice sheet development?: Palaeogeography, Palaeoclimatology, Palaeoecology, v. 226, p. 187-204.

Tucker, M., 1988, Techniques in Sedimentology: Oxford, p. 1-394.

Tucker, M.E., Wright, V.P., 1990, Carbonate sedimentology, Oxford Publishing, p. 482.

Vail, P.R., Mitchum Jr., R.M., Thompson III, S., 1977, Seismic stratigraphy and global changes of sea level, part 3: relative changes of sea level from coastal onlap. *In*: Payton, C.E. ed., Seismic Stratigraphy-Applications to Hydrocarbon Exploration American Association of Petroleum Geologists Memoir, v. 26, p. 63–81.

Van Wagoner, J.C., Posamentier, H.W., Mitchum, R.M., Vail, P.R., Sarg, J.F., Loutit, T.S., Hardenbol, J., 1988, An overview of sequence stratigraphy and key definitions, *In*: Wilgus, C.K., Hastings, B.S., Kendall, C.G.St.C., Posamentier, H.W., Ross, C.A., Van Wagoner, J.C. eds., Sea Level Changes-An Integrated Approach. Society of Economic Paleontologists and Mineralogists Special Publication, v. 42, p. 39–45.

Van Wagoner, J.C., Mitchum, R.M., Campion, K.M., Rahmanian, V.D., 1990, Siliciclastic sequence stratigraphy in well logs, cores, and outcrops: Tulsa, Oklahoma, American Association of Petroleum Geologists Methods in Exploration Series, v. 7, p. 55.

Veizer, J., Hoefs, J., 1976, The nature of O^{18}/O^{16} and $C^{13}/C/^{12}$ secular trends in sedimentary carbonate rocks: Geochimica et Cosmochimica Acta, v. 40, p. 1387-1395.

Webb, G.W., 1958, Middle Ordovician stratigraphy in eastern Nevada and western Utah: Bulletin of the American Association of Petroleum Geologists, v. 42, no. 10, pp. 2335-2377.

Weissert, H., Lini, A., Föllmi, K., Kuhn, O., (1998) Correlation of Early Cretaceous carbon isotope stratigraphy and platform drowning events: a possible link? Palaeogeography, Palaeoecology, Palaeoclimatology, 137 (3-4): 189-203.

Young, S.A., Saltzman, M.R., Bergstrom, S.M. 2005, Upper Ordovician (Mohawkian) carbon isotope ($\delta^{13}C$) stratigraphy in eastern and central North America: Regional expression of a perturbation of the global carbon cycle: Palaeogeography, Palaeoclimatology, Palaeoecology, v. 222, p. 53–76.

Zimmerman, M. K., Cooper, J. D., 1999, Sequence Stratigraphy of the Middle Ordovician Eureka Quartzite, Southeastern California and Southern Nevada, USA: Acta Universitatis Carolinae – Geologica, v. 43 (1/2), p. 147 –150.

VITA

Graduate College
University of Nevada, Las Vegas

Apostolos Paul Kosmidis

Local Address:
    2770 Sherwood Ln, 2-A
    Juneau, AK 99801

Home Address:
    804 S. Ellis Ave
    Newtown Square, PA 19073

Degrees:
    Bachelor of Science, Geology, 2005
    Temple University

Special Honors and Awards:
     Bernada French Award

Publications:

    Kosmidis, P., Jiang, G., Druschke, P. 2007, The Unconformity at the Basal
Eureka Quartzite in Nevada and California; Implications for Sea-level Change and the
Initiation of Late Ordovician Glaciation, Geological Society of America Abstracts with
Programs, Vol. 40, No. 1, p. 43.

    Terry, D.O., Jr., and Kosmidis, P.G., 2004, An Oligocene springfed carbonate
lake in the middle of a volcaniclastic eolianite, BadlandsNational Park, South Dakota,
Geological Society of America Abstracts with Programs, V. 36, no. 5, p. 35.

    Kosmidis, P.G., and Terry, D.O., Jr. 2004, Sedimentology and Taphonomy of the
Poleslide Member, Brule Formation, Badlands National Park, South Dakota: Geological
Society of America Abstracts with Programs, Northeast/Southeast Combined Meeting, V.
36, no. 2, p. 38.

    Kosmidis, P.G., and Schaefer, A.N., and Tremain, E.S., and Maxson, J.,
2002. Textural Criteria for Paleo-environmental Interpretation of Palustrine Facies of the
Cretaceous Cedar Mountain Formation in Dinosaur National Monument, Utah and
Colorado, USA: Geological Society of America Abstracts with Programs, V. 34, no. 3, p.
27.

Dissertation/Thesis Title: Sequence and chemostratigraphic study across the basal Eureka
Quartzite unconformity in the Great Basin, Nevada: implications for the origin of
the Late Ordovician carbon isotope excursion.

Thesis Examination Committee:
Chairperson, Ganqing Jiang, Ph. D.
Committee Member, Andrew R. Hanson, Ph. D.
Committee Member, Wanda J. Taylor, Ph. D.
Graduate Faculty Representative, Clark S. Kincaid, Pd. D.